Call: HORIZON-HLTH-2023-STAYHLTH-01
Topic: HORIZON-HLTH-2023-STAYHLTH-01-01
Funding Scheme: HORIZON Research and Innovation Actions (RIA)

Grant Agreement no: 101136376

Smart Implants for Life Enrichment

Deliverable No. 4.2

Sensors and Actuators Implementation

Contractual Submission Date: 30/06/2026

Actual Submission Date: 02/07/2026

Responsible partner: P18 - UNIBS: Università degli Studi di Brescia

Grant agreement no.	101136376
Project full title	SmILE – Smart Implants for Life Enrichment

Deliverable number	D4.2
Deliverable title	Sensors and Actuators Implementation
Type[1]	R
Dissemination level[2]	PU
Work package number	4
Work package leader	P11 – IMEC
Author(s)	Mauro Serpelloni (P18 – UNIBS) Jorge Schroeter (P19 – UKSH) Maarten Cauwe (P11 – IMEC) Frieder Kohler (P5 – BOSCH) Karl Blynow (P23 - UROS) Cristina Martínez Oliver and Giulio Rosati (P8 – EUT) Carmelo Pirritano (P21 – ZeMA) Mathias Muench and Lea Meißner and Tobias Barth (P2 - BGKH) Eva María Garrido García (P8 – CIBER) + Inputs from several WP4 and WP5 participants
Reviewer(s)	Mauro Serpelloni (P18 – UNIBS) Maarten Cauwe (P11 – IMEC) Giulio Rosati (P8 – EUT) Carmelo Pirritano (P21 – ZeMA) Michael Utz (P3 – AESC)
Keywords	Sensors, Actuators, strain, impedance, wear, temperature, pH, acoustic sensors, Inertial Measurement Unit, Drug release

Funded by the European Union under the Horizon Europe grant agreement No. 101136376 (project SmILE), and from the Swiss State Secretariat for Education, Research and Innovation (SERI). Views and opinions expressed are however those of the author(s) only and do not necessarily reflect those of the European Union nor European Health and Digital Executive Agency (HaDEA). Neither the European Union nor HaDEA can be held responsible for them.

Document History

Version	Date	Description

[1] **Type**: Use one of the following codes (in consistence with the Description of the Action):

R: Document, report (excluding the periodic and final reports)
DEM: Demonstrator, pilot, prototype, plan designs
DEC: Websites, patents filing, press & media actions, videos, etc.

[2] **Dissemination level**: Use one of the following codes (in consistence with the Description of the Action)

PU: Public, fully open, e.g. web
SEN: Sensitive, limited under conditions of the Grant Agreement

Funded by:

Schweizerische Eidgenossenschaft
Confédération suisse
Confederazione Svizzera
Confederaziun svizra

Funded by the European Union

The SmILE project has received funding from the European Union's Horizon Europe programme and the Swiss State Secretariat for Education, Research and Innovation (SERI).

V1	30/05/2026	First Draft
V2	16/06/2026	First Revision
V3	30/06/2026	Final Version
V4	02/07/2026	Final Version accepted by all the partners

Table of Contents

Funded by:

Schweizerische Eidgenossenschaft
Confédération suisse
Confederazione Svizzera
Confederaziun svizra

Funded by the European Union

The SmILE project has received funding from the European Union's Horizon Europe programme and the Swiss State Secretariat for Education, Research and Innovation (SERI).

Funded by:

Schweizerische Eidgenossenschaft
Confédération suisse
Confederazione Svizzera
Confederaziun svizra

Funded by the European Union

The SmILE project has received funding from the European Union's Horizon Europe programme and the Swiss State Secretariat for Education, Research and Innovation (SERI).

Funded by:

Schweizerische Eidgenossenschaft
Confédération suisse
Confederazione Svizzera
Confederaziun svizra

Funded by the European Union

The SmILE project has received funding from the European Union's Horizon Europe programme and the Swiss State Secretariat for Education, Research and Innovation (SERI).

List of Abbreviations

Term	Meaning
ADC	Analog-to-digital converter
AFE	Analog front-end
AJP	Aerosol Jet Printing
ASIC	Application-specific integrated circuit
DEX	Dexamethasone
DMM	Digital multimeter
DMF	N,N-Dimethylformamide
DMSO	Dimethyl sulfoxide
EDC	1-Ethyl-3-(3-
EIS	Electrical impedance spectroscopy
EL	Electro-labile
FITEP	Flexible, Implantable, Thin Electronic
GF	Gauge factor
HPLC	High-performance liquid
LNA	Low-noise amplifier
MEA	Microelectrode array
MWCNT	Multi-walled carbon nanotubes
NMR	Nuclear magnetic resonance
NVM	Non-volatile memory
PBS	Phosphate-buffered saline
PEDOT:PSS	Poly(3,4-
PEEK	Polyether ether ketone
PGA	Programmable gain amplifier
PI	Polyimide
SEM	Scanning electron microscopy
SPI	Serial peripheral interface
STC	Self-temperature compensation
TCGF	Temperature coefficient of gauge
TCR	Temperature coefficient of resistance
TLC	Thin-layer chromatography
TRL	Technology readiness level
UTM	Universal testing machine
WP	Work package
XPS	X-ray photoelectron spectroscopy

Funded by:

Schweizerische Eidgenossenschaft
Confédération suisse
Confederazione Svizzera
Confederaziun svizra

Funded by the European Union

The SmILE project has received funding from the European Union's Horizon Europe programme and the Swiss State Secretariat for Education, Research and Innovation (SERI).

Summary

Deliverable D4.2 documents the design, development, and initial implementation of the sensing and actuation technologies defined in Task 4.2, in alignment with the technical specifications established in D4.1. The objective of this deliverable is to demonstrate that the selected high-TRL components and the developed low-TRL solutions have been translated into concrete hardware implementations suitable for integration within the WP4 electronic system architecture.

The work focuses on the engineering realization of sensors and actuators tailored to the clinical use cases, including strain and deformation sensors, infection and environmental monitoring sensors (pH, temperature), structural and bone quality monitoring solutions (acoustic and impedance-based sensing), implant wear sensors, smart drug delivery systems, activity monitoring modules and actuators.

It is important to note that D4.2 addresses the implementation and technological maturation of individual components. Comprehensive functional validation under simulated physiological conditions and system-level verification are outside the scope of this deliverable and are addressed in Task 4.4 and Task 4.6.

This document has been divided into 8 parts, each corresponding to one of the project's subtasks. The structure is outlined below.

4.2.**1** - Strain sensors on implants High-TRL (commercial) and Low-TRL (Printed)

Strain sensing represents a core functionality across multiple use cases. High-TRL commercial strain gauges are adapted and implemented on implants, while innovative low-TRL printed strain gauges are designed and fabricated using advanced printed electronics technologies (e.g., Aerosol Jet Printing, Photonic Curing). These manufacturing approaches enable enhanced sensitivity, mechanical flexibility, and direct deposition on complex 3D implant surfaces using functional inks.

4.2.**2** - Inductive strain sensor (rotator cuff)

An inductive strain sensor is adapted for soft tissue monitoring in the rotator cuff, with specific optimization to anatomical and physiological constraints.

4.2.**3** - pH sensors (low-TRL), temperature sensors (High-TRL and Low-TRL), and acoustic piezoelectric sensors (low-TRL)

Low-TRL printed pH, temperature, and acoustic sensors have been developed and experimentally validated on flexible substrates. Current results demonstrate the feasibility of the proposed designs, although further optimization is required. Future work will focus on improving the long-term stability of the pH sensors, reducing noise and drift in the temperature sensors, and calibrating the acoustic sensors to enhance their sensitivity and repeatability.

4.2.**4** - Impedance spectroscopy for bone density

Impedance spectroscopy is investigated as a method for detecting changes in bone density. This includes electrode array design to enable reliable bioelectrical measurements.

4.2.**5** - Wear sensors for knee prosthesis

Two complementary wear sensing approaches have been investigated for knee endoprostheses. The first solution is based on scratch-sensitive sensors directly printed onto the polyethylene insert surface, enabling localized detection of surface degradation. The second approach considers the integration of force sensors within the tibial tray; when combined with motion sensors through sensor fusion algorithms, these devices allow indirect estimation of wear progression based on load distribution and kinematic patterns. Both concepts have been designed and assessed through preliminary mechanical bench testing to evaluate their feasibility and integration potential.

4.2.**6** - Smart Drug Delivery Systems

Funded by:

Schweizerische Eidgenossenschaft
Confédération suisse
Confederazione Svizzera
Confederaziun svizra

Funded by the European Union

The SmILE project has received funding from the European Union's Horizon Europe programme and the Swiss State Secretariat for Education, Research and Innovation (SERI).

A controlled drug delivery system based on electro- and thermo-responsive gated mesoporous silica particles is proposed. Suitable pharmaceutical molecules are selected according to clinical requirements, and functionalized particles are studied to enable externally triggered and controlled release mechanisms.

4.2.**7** - Smart Activity Monitoring and Data Processing

A dedicated smart sensing solution for activity monitoring is developed, based on a 6-axis inertial measurement unit (IMU) integrating gyroscope and accelerometer functionalities, an embedded microcontroller unit, and pre-installed sensor fusion algorithms. Low-power preprocessing algorithms are implemented to reduce energy consumption and data transmission requirements.

4.2.**8** - Smart Actuation

Smart actuator systems are implemented in active implants to enable growth stimulation and axis correction. Beyond actuation, these components exploit intrinsic self-sensing capabilities to monitor fracture gap stiffness from the first postoperative day, thereby providing early insight into healing progression.

Funded by:

Schweizerische Eidgenossenschaft
Confédération suisse
Confederazione Svizzera
Confederaziun svizra

Funded by
the European Union

The SmILE project has received funding from the European Union's Horizon Europe programme and the Swiss State Secretariat for Education, Research and Innovation (SERI).

1. Strain sensors on implants High-TRL (commercial) and Low-TRL (Printed)

1.1 Introduction

This deliverable summarizes the strain-sensing options evaluated for the SmILE implant and assistive-device use cases. The common design target is a low-power bridge-compatible sensor, mechanically adaptable to crutches, bone plates and prosthetic components, and electrically compatible with the conditioning front-end in the 5-10 kΩ range.

The high-TRL baseline is a 5 kΩ full-bridge metallic strain gauge based on modified Karma alloy. The S5229 and S5020 (Vishay Precision Group) full-bridge patterns provide similar electrical performance; the final choice is driven mainly by available bonding area, installation constraints and the substrate material, especially the STC value required for aluminium, titanium or cobalt-chrome structures. For torsional strain measurements, the full-bridge S5046 strain gauge pattern provides an optimal solution.

A semiconductor strain-gauge option was considered because of its high gauge factor, but it introduces significant thermal-compensation and bridge-matching requirements. It is therefore retained as a potential high-sensitivity option, not as the primary baseline.

Low-TRL strain-sensing activities focused on the screening and optimization of printed sensors on flexible PI and PEEK substrates. The work on PEDOT:PSS as sensor material was discontinued due to poor adhesion and low sensitivity, while PEDOT+rGO and stamped rGO showed preliminary promising results requiring further validation. Carbon black/MWCNT sensors emerged as the most promising printed solution, combining improved adhesion, tuneable resistance, good sensitivity, and low drift. The parallel configuration reached resistances compatible with the ASIC range, with mean values of 3.72 kΩ on PI and 5.84 kΩ on PEEK, and gauge factors of 4.1–4.3 on PI and 6.5–6.8 on PEEK under cyclic bending.

The current strategy is to use the commercial 5 kΩ full-bridge gauge as the near-term validated reference, while continuing the development of the printed carbon/MWCNT full-bridge sensor as the low-TRL innovation path, focusing on bridge balancing, silver-pad adhesion, encapsulation, and calibration against the commercial solution.

1.2 High-TRL commercial strain gauges

The selected strain-sensing element must support repeatable strain measurement on heterogeneous metallic structures while minimizing power consumption and thermal drift. The target applications include external load-bearing devices, such as crutches, and implantable or semi-implantable structures, such as bone plates and prosthetic components.

Strain gauges exploit the resistance variation induced by mechanical deformation: R = rho L/A and GF = (Delta R/R)/epsilon. In a full Wheatstone bridge, the normalized differential output is proportional to strain and, for a fully active bridge, can be approximated by Vout/Vexc ~= GF epsilon. A full-bridge layout maximizes sensitivity and reduces temperature-induced apparent strain because all active arms are bonded to the same substrate.

A 5 kΩ nominal bridge resistance was selected to match the ASIC-oriented conditioning strategy. For a fixed excitation voltage, bridge power scales as P = $Vexc^2$/R, so the 5 kΩ configuration reduces Joule heating, improves thermal stability and supports long-term or implantable monitoring scenarios. In the following table the candidate commercial full-bridge patterns are reported.

Funded by:

Schweizerische Eidgenossenschaft
Confédération suisse
Confederazione Svizzera
Confederaziun svizra

Funded by
the European Union

The SmILE project has received funding from the European Union's Horizon Europe programme and the Swiss State Secretariat for Education, Research and Innovation (SERI).

Candidate	Common features	Main advantage	Preferred use
S5229, 5 kΩ	Modified Karma alloy, polyimide backing, integrated full bridge	Smaller footprint and lower local stiffening	Small-diameter or space-constrained components
S5020, 5 kΩ	Same bridge class and ASIC-compatible resistance	Larger grid/bonding area and easier handling	Substrates with less stringent space constraints
S5046, 5 kΩ	Bridge, pattern for torsional strength, ASIC-compatible resistance	Small footprint	Small-diameter
Selection criterion	Electrical performance comparable	Driven by integration constraints	Finalize per geometry and installation process

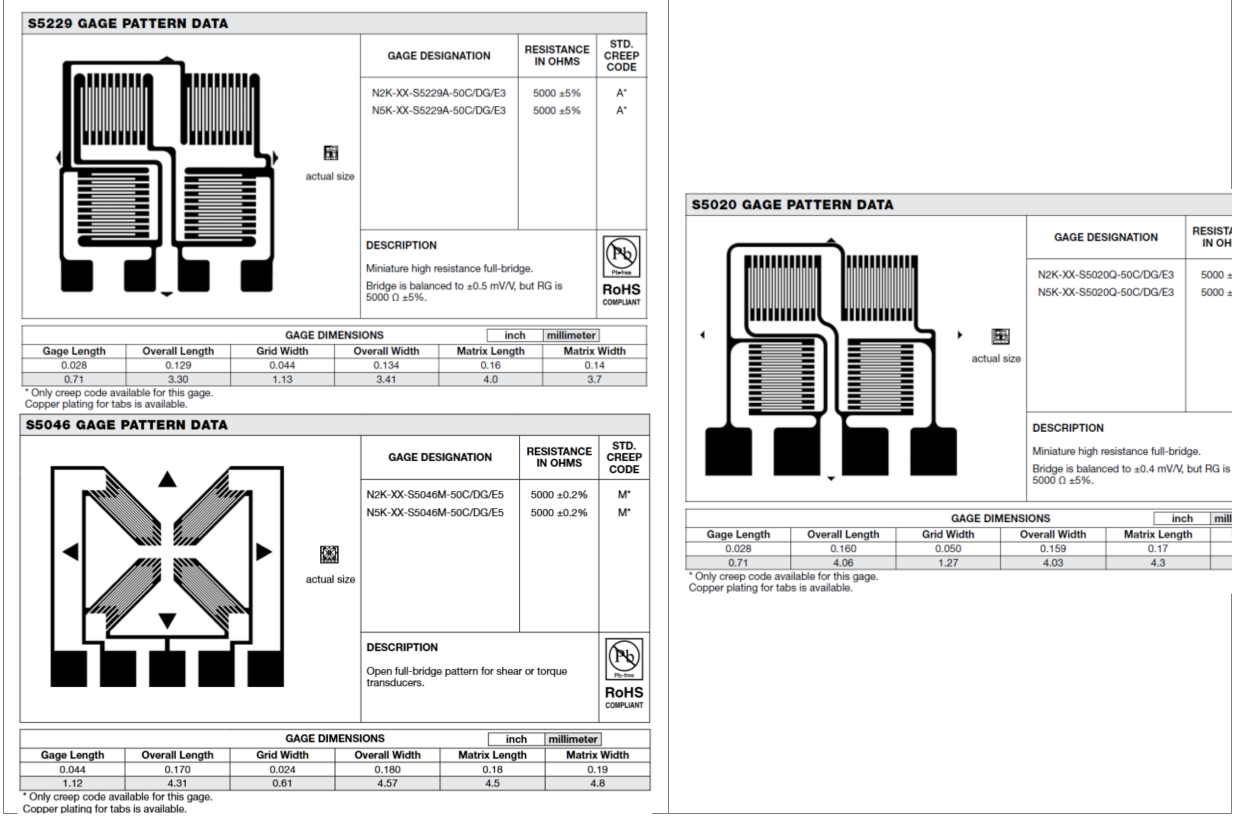

S5229 GAGE PATTERN DATA

actual size

GAGE DESIGNATION	RESISTANCE IN OHMS	STD. CREEP CODE
N2K-XX-S5229A-50C/DG/E3	5000 ±5%	A*
N5K-XX-S5229A-50C/DG/E3	5000 ±5%	A*

DESCRIPTION

Miniature high resistance full-bridge.

Bridge is balanced to ±0.5 mV/V, but RG is 5000 Ω ±5%.

RoHS COMPLIANT

GAGE DIMENSIONS (inch / millimeter)

Gage Length	Overall Length	Grid Width	Overall Width	Matrix Length	Matrix Width
0.028	0.129	0.044	0.134	0.16	0.14
0.71	3.30	1.13	3.41	4.0	3.7

* Only creep code available for this gage.
Copper plating for tabs is available.

S5046 GAGE PATTERN DATA

actual size

GAGE DESIGNATION	RESISTANCE IN OHMS	STD. CREEP CODE
N2K-XX-S5046M-50C/DG/E5	5000 ±0.2%	M*
N5K-XX-S5046M-50C/DG/E5	5000 ±0.2%	M*

DESCRIPTION

Open full-bridge pattern for shear or torque transducers.

RoHS COMPLIANT

GAGE DIMENSIONS (inch / millimeter)

Gage Length	Overall Length	Grid Width	Overall Width	Matrix Length	Matrix Width
0.044	0.170	0.024	0.180	0.18	0.19
1.12	4.31	0.61	4.57	4.5	4.8

* Only creep code available for this gage.
Copper plating for tabs is available.

S5020 GAGE PATTERN DATA

actual size

GAGE DESIGNATION	RESISTA IN OH
N2K-XX-S5020Q-50C/DG/E3	5000 ±
N5K-XX-S5020Q-50C/DG/E3	5000 ±

DESCRIPTION

Miniature high resistance full-bridge.

Bridge is balanced to ±0.4 mV/V, but RG is 5000 Ω ±5%.

GAGE DIMENSIONS (inch / mill)

Gage Length	Overall Length	Grid Width	Overall Width	Matrix Length
0.028	0.160	0.050	0.159	0.17
0.71	4.06	1.27	4.03	4.3

* Only creep code available for this gage.
Copper plating for tabs is available.

Figure 1. Commercial 5 kΩ Transducer-Class full-bridge strain-gauge patterns considered as high-TRL candidates.

The choice between N2K and N5K series is mainly associated with thermal robustness and long-term stability. N2K is adequate for room-temperature laboratory validation and external assistive devices. N5K provides a wider robustness margin for implantable or long-term monitoring cases where thermal excursions or drift may be more critical.

The STC value must be matched to the coefficient of thermal expansion of the substrate. STC 13 is appropriate for aluminium alloys, while STC 06 is more suitable for titanium and cobalt-chrome alloys. Although full-bridge symmetry reduces thermal output, correct STC matching remains beneficial for residual drift and long-term stability.

Funded by:

Schweizerische Eidgenossenschaft
Confédération suisse
Confederazione Svizzera
Confederaziun svizra

Funded by the European Union

The SmILE project has received funding from the European Union's Horizon Europe programme and the Swiss State Secretariat for Education, Research and Innovation (SERI).

Semiconductor strain sensors were also analyzed as part of the design activity. The table below presents an example of a semiconductor strain sensor identified during the process.

Parameter	Kulite S/UHP-5000-060	Implication for SmILE
Nominal resistance	5 kΩ	Compatible with the selected high-resistance front-end
Gauge factor	approx. +175	Very high sensitivity and lower amplification needs
Temperature behaviour	TCR +45%; TCGF -23%	Requires careful thermal compensation and calibration
Bridge integration	Single active element	Custom bridge assembly needed; matching risk increases
Assessment	Promising but complex	Potential high-sensitivity alternative, not baseline

The commercial 5 kΩ modified-Karma full bridge is the preferred high-TRL solution because it combines ASIC compatibility, low excitation current, thermal self-compensation and straightforward integration. Semiconductor gauges remain a candidate for future high-sensitivity studies, provided that temperature compensation and bridge matching are addressed.

1.2.6 Mechanical testing

The selected N2K-S5229 strain gauges were attached to Ti_6Al_4V bars (100 mm × 20 mm × 3 mm) using the M-Bond 610 glue (Luchsinger) and evaluated using three-point bending tests performed on an ESM1500 Mark-10 universal testing machine. The strain gauge output was measured using a Keysight 34460A digital multimeter, while a GW Instek GPP-3060L DC voltage supply provided the excitation voltage. Data acquisition and instrument control were implemented through a LabVIEW-based routine. The sensors were tested under various strain levels and were also subjected to cyclic bending at a strain amplitude of 0.5% for 1,000 cycles. In addition, the sensors were held under a constant strain for one hour to evaluate their stability and behavior under sustained loading conditions.
The sensor exhibited excellent strain transfer throughout the testing campaign. Following testing, the sensor remained firmly bonded to the substrate, with no visible signs of adhesive degradation, debonding, or stress-induced damage. During the one-hour constant-strain test, no detectable signal drift was observed, demonstrating good stability under sustained loading conditions. Furthermore, the sensor response remained highly linear across the entire strain range investigated. During the 1,000-cycle fatigue test, the sensor consistently measured the applied strain without any noticeable drift in either the baseline signal or the peak response, confirming its excellent repeatability and reliability under cyclic loading.

Funded by:

Schweizerische Eidgenossenschaft
Confédération suisse
Confederazione Svizzera
Confederaziun svizra

Funded by the European Union

The SmILE project has received funding from the European Union's Horizon Europe programme and the Swiss State Secretariat for Education, Research and Innovation (SERI).

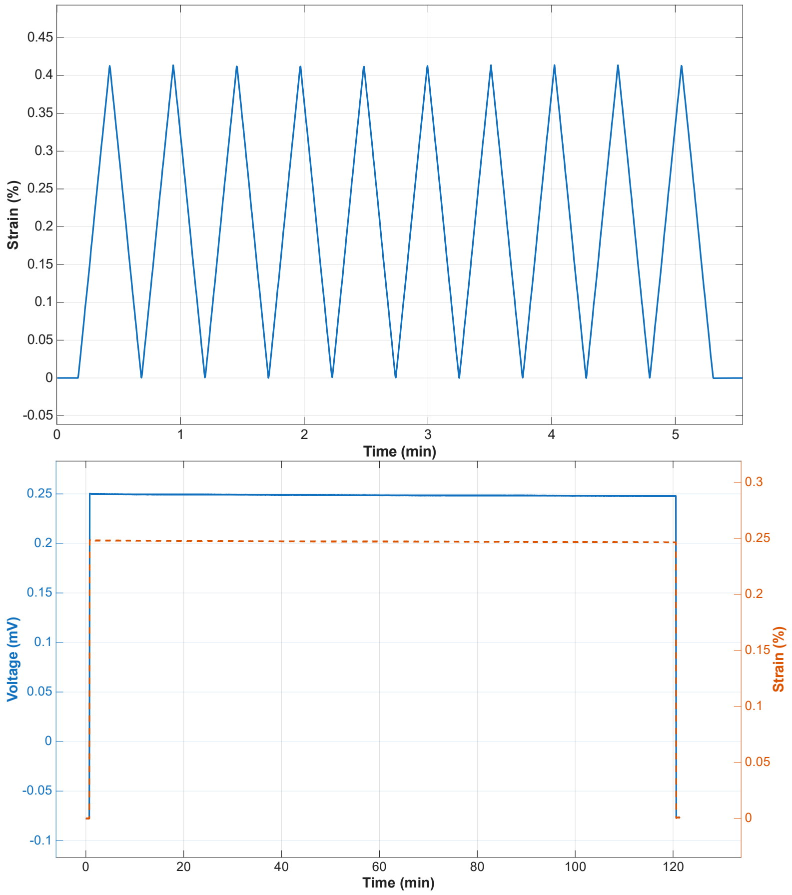

Figure 2. Representative plots of the cycle and constant strain behaviour of the bridge.

1.3 Low-TRL printed strain sensors: strategy and methods

Low-TRL strain sensors were designed, fabricated and tested using Aerosol Jet Printing. The objective was to obtain a small-footprint, additively manufactured strain-sensing device in full-bridge configuration with resistance in the 5-10 kΩ range, gauge factor above metallic strain gauges, good thermal stability and resolution suitable for low-strain metallic structures.

Item	Options evaluated	Rationale
Substrates	PI and PEEK sheets	PI benchmarks printed electronics; PEEK is relevant for biomedical structures
Sensing inks	PEDOT:PSS; carbon black + MWCNT	Conductive polymers/carbon inks allow higher resistance in compact layouts
Interconnect ink	Silver nanoparticle ink	Low-resistance traces and contact pads
Integration route	Printed-on-substrate, then bonded to metal	Compatible with crutches, titanium plates and prosthetic structures

In parallel, other additive manufacturing strategies have been tested for the development of low-TRL strain sensors at Eurecat. Both PEDOT and reduced graphene oxide have been employed testing screen-printing and stamping techniques as resumed in the following table. The fabrication methods employed are easily scalable.

Funded by:

Schweizerische Eidgenossenschaft
Confédération suisse
Confederazione Svizzera
Confederaziun svizra

Funded by the European Union

The SmILE project has received funding from the European Union's Horizon Europe programme and the Swiss State Secretariat for Education, Research and Innovation (SERI).

Item	Options evaluated	Rationale
Substrates	Polyimide (PI)	PI benchmarks printed electronics
Sensing inks	PEDOT; reduced graphene oxide (rGO) and PEDOT+0.1%rGO	Conductive polymers/carbon-based inks allow higher resistance in compact layouts (reduced currents implies longer battery life)
Layout and interconnect ink	Meander resistor (0.6 mm width); soldered crimps and wires	Typical strain gauge shape; Low-resistance contacts
Integration route	Printed on substrate, captured at the extremes for elongation test with custom setup	Evaluation of the stress-strain of the sensor alone without any structure bound to it.

1.3.1 Validation workflow

Validation combined morphological inspection, adhesion screening and electromechanical tests. Printed tracks were inspected by microscopy and, where feasible, profilometry. Adhesion was initially assessed with a manual tape peel-off test. Mechanical response was measured with an ESM1500 Mark-10 universal test machine and Keysight 34460A digital multi-meters controlled through a LabView acquisition routine.
To isolate sensor behaviour, tensile tests were performed directly on PI/PEEK strips. For application-relevant validation, printed sensors and commercial reference gauges were bonded side-by-side on Ti6Al4V strips (0.5 mm x 18 mm x 70 mm) and tested in three-point bending with 50 mm span. The commercialgauge gauge provided the reference strain for the printed sensor. The testing of the screen printed and stamped PEDOT and rGO sensors is still ongoing. Preliminary results have been obtained with a tensile custom setup system.

Figure 3. Electromechanical validation setup and three-point bending fixture used for titanium specimens.

1.4 Low-TRL results: material screening

1.4.1 PEDOT:PSS preliminary attempt

PEDOT:PSS sensors were printed on PI and PEEK as an early screening route. The geometry consisted of three meandered turns with 10 mm grid length and 3.4 mm grid width. Track width was

Funded by:

Schweizerische Eidgenossenschaft
Confédération suisse
Confederazione Svizzera
Confederaziun svizra

Funded by the European Union

The SmILE project has received funding from the European Union's Horizon Europe programme and the Swiss State Secretariat for Education, Research and Innovation (SERI).

approximately 520 µm on PEEK and 540 µm on PI, with deposition height in the 3-3.5 µm range. However, the tape peel-off test showed unacceptable adhesion and most samples did not provide a reliable resistance change under tensile loading. The observed sensitivity was below 1, so PEDOT:PSS was discontinued for the current target.

1.4.2 Screen-printed and stamped PEDOT and rGO sensors

Tensile tests on the PEDOT and rGO devices on PI have been performed in Eurecat with a custom setup based on stepper translational motors with a resolution of 0.1 mm. The results of the PEDOT so far have not been satisfying (more tests are needed) while for PEDOT+0.1%rGO and stamped pure rGO the first results are more promising as shown in the figure below. More testing is needed to clearly define the performance of these sensors and a better setup is currently under development.

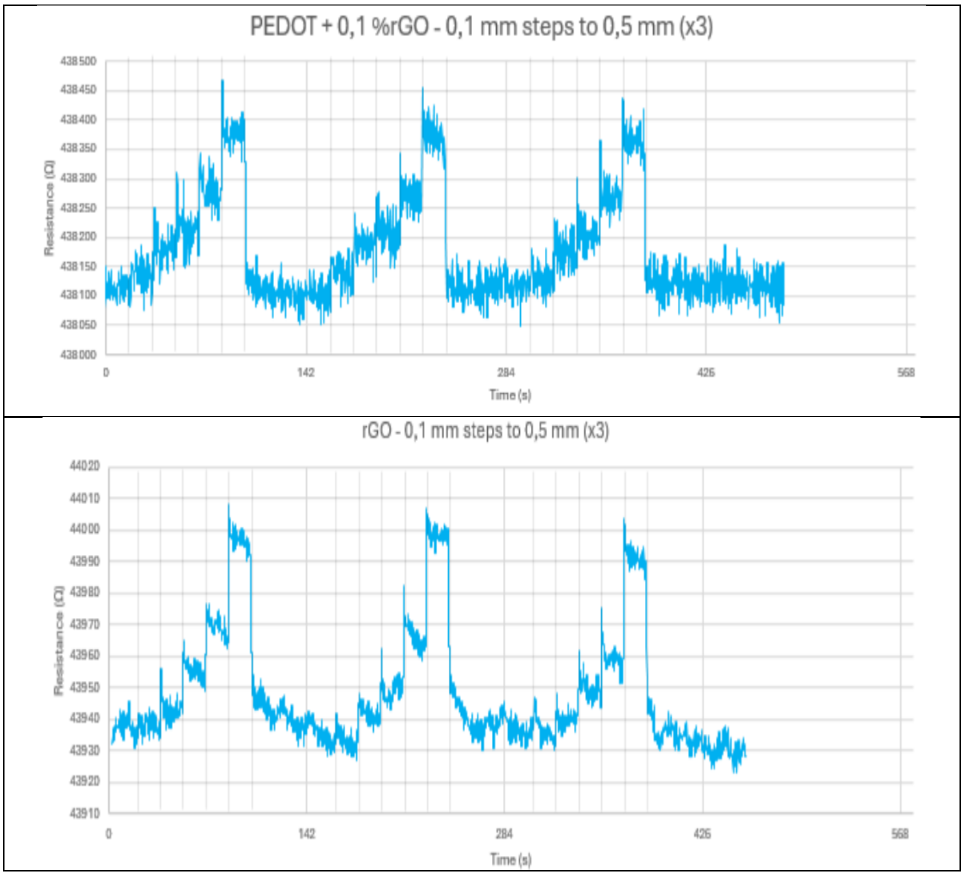

Figure 4. PEDOT+0.1% rGO and pure rGO meanders resistance variations with 3 cycles of 5 step elongation from 0 to 0.5 mm.

1.4.3 Carbon black + MWCNT first prototype

The first carbon/MWCNT prototypes used a serpentine pattern on PI and PEEK. Carbon black was deposited first to improve adhesion of the subsequent water-based MWCNT layer. Sensors were dried for approximately one hour at 130 °C. The resulting mean resistances were high: about 630 kΩ on PEEK and 350 kΩ on PI.

Adhesion improved compared with PEDOT:PSS. The peel-off test removed only a superficial MWCNT fraction while the printed tracks remained functional. Tensile testing showed a measurable piezoresistive response, with GF of 3.2-3.6 on PI and 2.8-3.2 on PEEK in the investigated range. A PI sensor bonded to titanium reached GF 4.6. This confirmed the suitability of carbon/MWCNT inks, but the resistance was too high for the ASIC target, so the layout was redesigned.

Funded by:

Schweizerische Eidgenossenschaft
Confédération suisse
Confederazione Svizzera
Confederaziun svizra

Funded by
the European Union

The SmILE project has received funding from the European Union's Horizon Europe programme and the Swiss State Secretariat for Education, Research and Innovation (SERI).

Route	Resistance / sensitivity	Adhesion	Decision
PEDOT:PSS	GF < 1; unreliable response	Poor; ink removed by tape	Discarded
Carbon/MWCNT serpentine	GF > 2 but R = 350-630 kΩ	Functional after peel-off	Keep ink, redesign geometry
Carbon/MWCNT on Ti	GF approx. 4.6 on one PI sensor	Promising after bonding	Move to lower-resistance layout

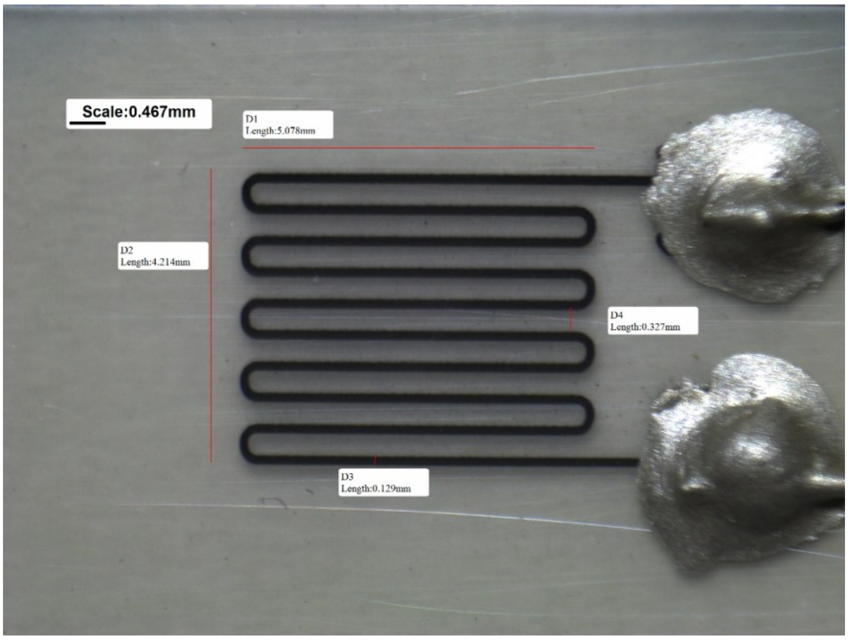

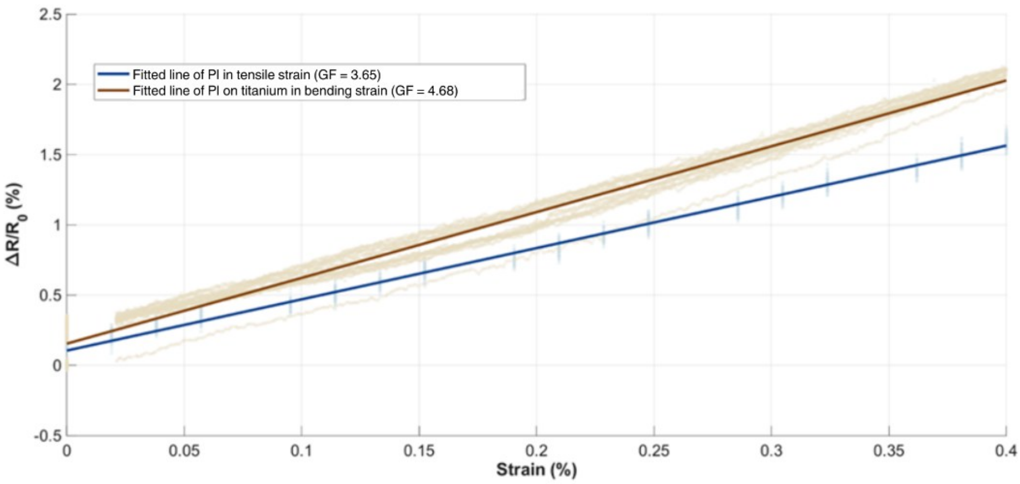

Figure 5. Early carbon/MWCNT prototype and representative electromechanical response.

1.4.4 Parallel carbon/MWCNT configuration

To reduce resistance, a parallel layout was introduced. Ten or more shorter sensing lines were connected in parallel and silver ink was added for short-circuiting and contact pads. The approach successfully shifted the resistance into the target range: the mean values were 3.72 kΩ on PI and 5.84

Funded by:

Schweizerische Eidgenossenschaft
Confédération suisse
Confederazione Svizzera
Confederaziun svizra

Funded by
the European Union

The SmILE project has received funding from the European Union's Horizon Europe programme and the Swiss State Secretariat for Education, Research and Innovation (SERI).

kΩ on PEEK. The sensing area was compact, with overall footprint 14.633 mm x 5.565 mm including pads and sensing length 4.279 mm.
The peel-off test showed the same general behaviour as the previous carbon/MWCNT samples: the carbon/MWCNT section remained functional with only minor resistance increase. The silver pads and narrow silver interconnects were the weakest point, with partial to severe detachment. Silver adhesion is therefore a key design risk for the next iteration.

Validation item	Observed result	Interpretation
Resistance	PI: 3.72 kΩ; PEEK: 5.84 kΩ	Geometry meets the ASIC-oriented range after tuning
C100 cyclic bending	PEEK GF 6.5-6.8; PI GF 4.1-4.3	Printed sensors exceed metallic GF target
Linearity	Approx. 0.03-0.5% strain	Reduced sensitivity below approx. 0.03%
Speed dependence	GF variation below 0.1 without trend	No relevant loading-rate effect observed
Hold tests	Drift below 0.1% over 10 min	Good stability under sustained strain

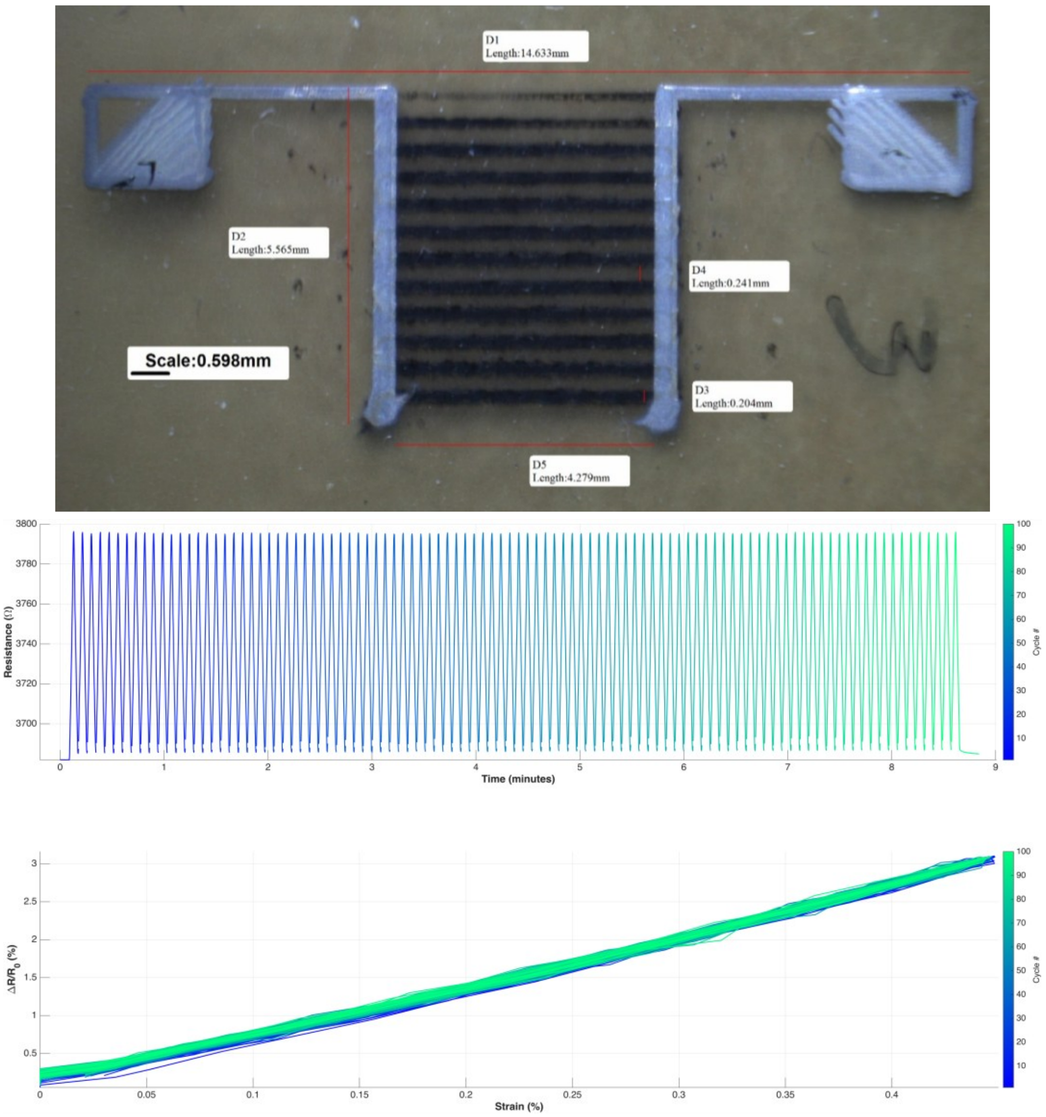

Figure 6. Parallel geometry and C100 cyclic response for a representative printed sensor.

Funded by:

Schweizerische Eidgenossenschaft
Confédération suisse
Confederazione Svizzera
Confederaziun svizra

Funded by
the European Union

The SmILE project has received funding from the European Union's Horizon Europe programme and the Swiss State Secretariat for Education, Research and Innovation (SERI).

1.4.5 Full-bridge printed sensor and comparative assessment

A full-bridge printed layout was fabricated using the same carbon/MWCNT sensing stack and silver interconnects. Two sensing elements were oriented along the longitudinal axis and two along the transverse axis. Each arm included 11 parallel strips so that selected strips can be removed to fine-tune bridge balance after printing. Two bridge ends were left open for individual resistance measurements and can be shorted before bridge-level testing.

The full-bridge sensor has an overall footprint of 11.640 mm x 7.310 mm including pads and a compact sensing area of 2.317 mm x 2.177 mm. Track width was approximately 73 µm with 156 µm spacing. Adhesion results were consistent with previous tests: carbon/MWCNT remained largely attached, while silver adhesion remained the main limitation. Bridge-level testing is the key pending validation step.

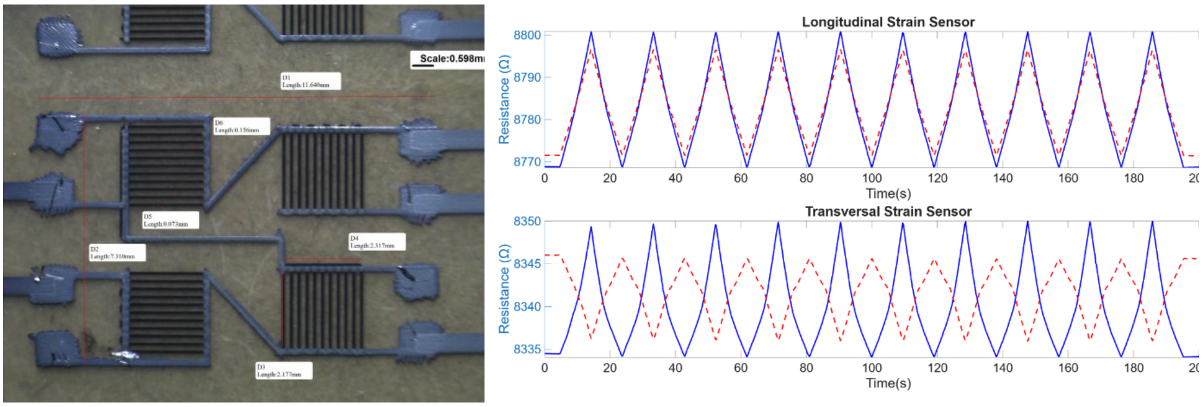

Figure 7. Printed full-bridge layout and representative behaviour of the directional strain sensed by the bridge

The printed bridge was evaluated under a 0.1% bending strain to investigate the behaviour of the transverse strain gauge. The longitudinal gauge showed the expected response, accurately tracking the applied strain with high linearity and a gauge factor comparable to that of the single printed sensor. In contrast, the transverse gauge exhibited an opposite response to that expected under compression, suggesting sensitivity to strain components in both directions. The measured signal appeared to be dominated by the larger longitudinal strain component despite the sensor orientation. Thermal characterization was performed through three temperature cycles between 30 °C and 44 °C. The sensors displayed NTC behaviour, with resistance decreasing as temperature increased. Temperature sensitivity was low, with a maximum resistance variation of approximately 0.3% over the 14 °C range (≈0.02%/°C), indicating minimal temperature-induced error in strain measurements under typical operating conditions.

Funded by:

Schweizerische Eidgenossenschaft
Confédération suisse
Confederazione Svizzera
Confederaziun svizra

Funded by the European Union

The SmILE project has received funding from the European Union's Horizon Europe programme and the Swiss State Secretariat for Education, Research and Innovation (SERI).

Option	Strengths	Limitations	Current role
Commercial full bridge	Low power, stable, integrated bridge, known installation route	Requires careful bonding and STC selection	High-TRL baseline
Semiconductor gauge	Very high GF and compact active area	Strong temperature dependence; custom bridge needed	Alternative for high sensitivity
Printed carbon/MWCNT parallel	GF 4.1-6.8, tunable resistance, low drift	Silver adhesion and low-strain threshold	Best low-TRL proof of concept
Printed full bridge	Compact bridge, balance tuning by strip removal	Poor directional strain selectivity	Next low-TRL validation

1.5 Conclusions and next steps

The current evidence supports a dual-track strategy. The commercial 5 kΩ modified-Karma full-bridgegauge gauge should be maintained as the high-TRL reference because it directly satisfies the low-power bridge architecture and offers intrinsic thermal compensation. Selection between S5229 and S5020 should be finalized case by case according to bonding area and mechanical integration constraints.

For the low-TRL route, carbon black/MWCNT printed sensors are the most promising candidate. PEEK showed the highest gauge factor in cyclic bending, while PI remains a viable benchmark substrate. The parallel geometry demonstrated that resistance can be tuned into the conditioning range without losing sensitivity. The full-bridge geometry has now been fabricated and must be validated under the same titanium-bending protocol.

Screen-printed PEDOT+0.1%rGO sensors showed promising preliminary results in Eurecat and will be studied more in depth on better tensile and 3 point bending setups so to obtain a full characterization of the sensors for use in the real-use cases.

Use the commercial 5 kΩ full-bridgegauge gauge for near-term validation and integration benchmarking. Continue the printed carbon/MWCNT full-bridge route as the low-TRL innovation path, focusing on bridge balancing, silver-pad adhesion, encapsulation and calibration against the commercial reference.

Funded by:

Schweizerische Eidgenossenschaft
Confédération suisse
Confederazione Svizzera
Confederaziun svizra

Funded by the European Union

The SmILE project has received funding from the European Union's Horizon Europe programme and the Swiss State Secretariat for Education, Research and Innovation (SERI).

2. Inductive strain sensor (rotator cuff)

2.1 Introduction

The sensors must consist of highly flexible strain gauges that are suitable for monitoring the strain of soft tissue structures in vivo. The idea was to assess the strain of the tissue via an implanted, flexible sensor that can detect elongation at high ranges that are unavailable with conventional, resistive strain gauges. Technically, a coil that is wound from enamelled copper wire and embedded in biocompatible silicone that changes inductance when the length is changed.
The clinical considerations were taken into account before designing the sensor after discussing with the orthopedic surgeon from UKSH regarding the potential implantation scenarios. According to the clinical feedback, the available space for placing these sensors in ligament and tendon is highly limited, with a placement area of approximately 5 mm x 5 mm. The thickness should be less than 1 mm. This spatial constraint is pertinent in regions such as rotator cuff, where the surrounding anatomical structures restrict the implant size. As a consequence of this, the design of sensor geometry will be designed to comply with this dimensional requirement while maintaining mechanical flexibility and sensing functionality.

2.2 Inductive Strain Sensor

Operating principle:
The inductive sensor coil was connected to an external resonant circuit, where change in coil geometry under applied strain resulted in measurable shifts in resonance frequency. The inductance L of the coil was calculated from the measured resonance frequency f using the standard LC resonance relationship:

$$f = \frac{1}{2\pi\sqrt{LC}}$$

Equation 1: Formula for calculating frequency from Inductance and Capacitance
Where C represents the known capacitance of the resonant circuit. By continuously recording the frequency changes during mechanical expansion and deformation of the sensor coil, corresponding changes in inductance were derived and correlated with the applied strain.

2.3 Coil Winding Machine

A coil winding machine (**Errore. L'origine riferimento non è stata trovata.**) has been built to produce double layer coils with an outer diameter of approximately 1mm and 5 mm length. It is also used in the manufacture of bifilar-wound transmission lines. In addition to the cylindrical geometry, both

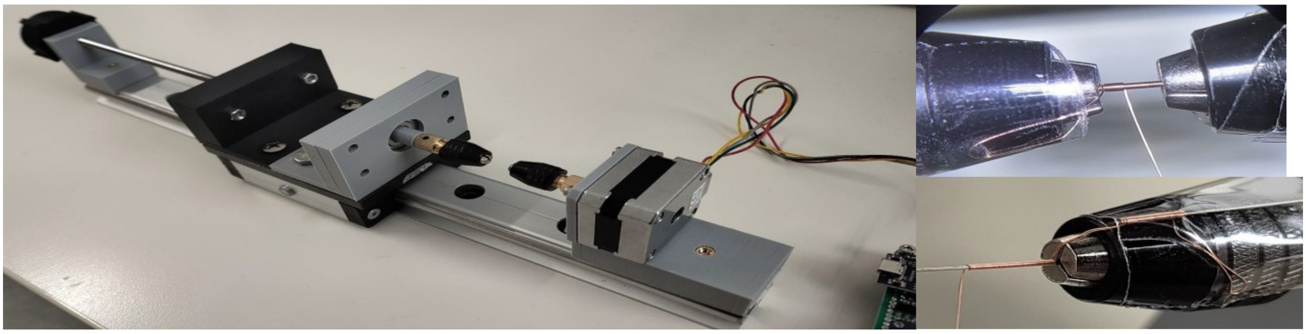

Figure 8. Coil winding machine to produce cylindrical Sensors and transmission lines.
circular and oval sensor coils were manufactured. 3D-printed Molds were created in which the sensors were embedded in silicone.

Funded by:
Schweizerische Eidgenossenschaft
Confédération suisse
Confederazione Svizzera
Confederaziun svizra
Funded by the European Union
The SmILE project has received funding from the European Union's Horizon Europe programme and the Swiss State Secretariat for Education, Research and Innovation (SERI).

2.4 Frequency Measurement Device

A specialized measurement setup was built to characterize the inductive response of the fabricated sensor. In this measurement setup, LDC1101 inductance to digital converter (Texas Instruments) was interfaced with ESP32-based, Arduino-compatible microcontroller (Waveshare ESP32-S3 Zero) to enable data acquisition and communication with a host computer. The LDC1101 allows the precise measurement of inductance and resonance frequency and supports flexible configuration for inductive sensing applications. The ESP32 microcontroller provides adequate computational performance, integrated peripherals and reliable SPI communication for real-time measurements of control and data transmission. A custom firmware was developed and implemented on the ESP32 to configure LDC1101 via SPI communication, that acquires inductance and resonance frequency data and transmits the measurements to the host computer.

2.5 Construction of a test setup for static strain measurements

A test bench for static strain measurements was constructed to evaluate the various sensor designs. The sensor samples were mounted over a mechanical loading platform that enables controlled uniaxial displacement. This was done using the bent needles from the syringes and glued over the linear stage where the sensor can be placed to measure the inductance. One end of the sensor was fixed, while the opposite end was connected to a movable linear stage equipped with a displacement scale. Strain was applied to the fabricated sensor placed over the linear scale by incrementally moving the stage by predefined displaces of 0.5mm, 1.5mm, and 2.0mm. These displacement values were selected depending on physiological considerations, as ligament and tendon tissues typically experience strains of up to approximately 10% under normal loading conditions. These applied displacements therefore relate to strain levels within the elastic deformation range of both the silicone substrate and the targeted biological tissue

2.6 Designed 3 different Sensor geometries with different modifications for fixation

The clinical considerations were taken in account before designing the sensor after discussing with the orthopedic surgeon from UKSH regarding the potential implantation scenarios, the size, thickness and possible fixation methods. In addition to the cylindrical sensor geometry described in the proposal, both a circular variant and an oval variant were designed. Both the circular and oval sensors were manufactured with 5 turns and 20 turns, respectively.

The following attachment methods have been identified to allow the sensor to be sewn onto the torn tendon:

1. Silicone surfaces are provided
2. Holes for the sutures are provided in the silicone
3. Sutures are embedded in the silicone casing

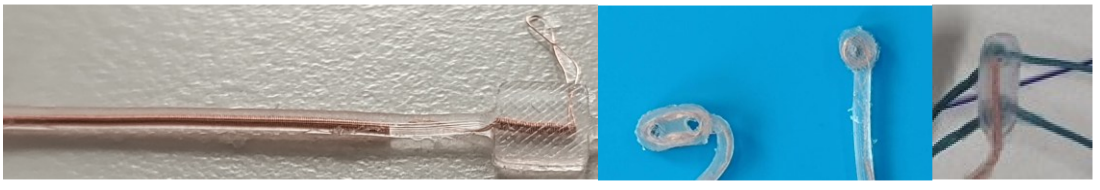

Figure 9. Fixation methods: Cylindrical sensor with silicon patches, oval and circular sensors with suture holes, cylindical sensor with embedded sutures.

Funded by:

Schweizerische Eidgenossenschaft
Confédération suisse
Confederazione Svizzera
Confederaziun svizra

Funded by the European Union

The SmILE project has received funding from the European Union's Horizon Europe programme and the Swiss State Secretariat for Education, Research and Innovation (SERI).

To date, a total of 18 different versions of the strain sensor have been designed, and approximately 35 sensors have been manufactured.

2.7 Results

2.7.1 Sensitivity

The sensitivity of the cylindrical sensors, as well as the circular and oval sensors (each with 5 turns), is low but sufficient. For the circular and oval sensors, sensitivity can be increased by adding more turns. However, this makes the sensors stiffer, which may prevent them from detecting small changes in strain. (Figure)
In the cylindrical version, changing the number of turns is not possible due to the design.

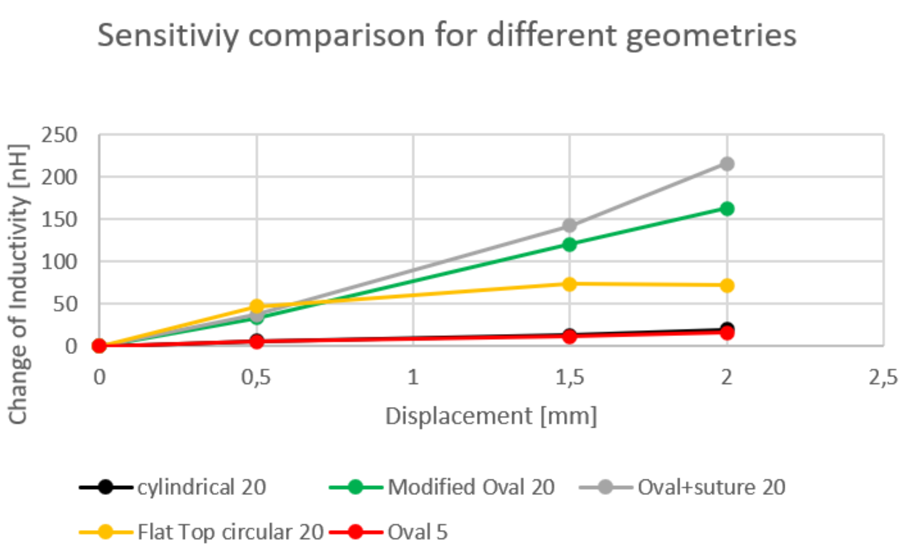

Figure 10. Sensitivity comparison of different sensor versions

The sensors were encapsulated in silicone with Shore hardnesses of 10, 25, and 33. The comparison shows that, in the case of the Shore 10 silicone variant, a change in length is not fully transferred to a deformation of the sensor. (Figure)

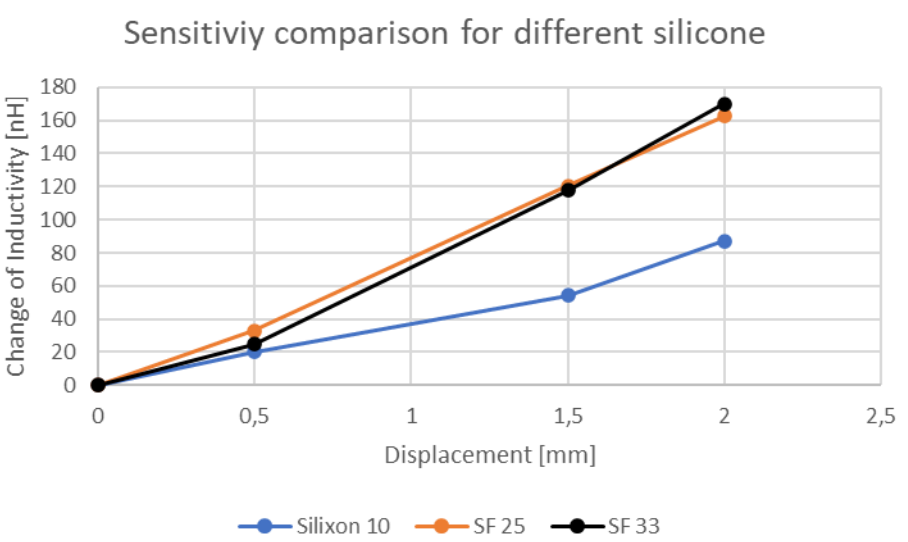

Figure 11. The influence of silicone Shore hardness on sensor sensitivity.

Funded by:
Schweizerische Eidgenossenschaft
Confédération suisse
Confederazione Svizzera
Confederaziun svizra
Funded by the European Union
The SmILE project has received funding from the European Union's Horizon Europe programme and the Swiss State Secretariat for Education, Research and Innovation (SERI).

2.8 Conclusion and next steps

The inductive sensors that have been manufactured can, in principle, measure relatively large deformations in soft tissue. The circular sensor geometry will not be pursued further at this time. Embedding the sensors in silicone is reliably possible using the molds manufactured for this purpose. A more sophisticated test setup is being constructed to perform cyclic deformation tests. The mounting methods will be optimized in two respects. First, it must be ensured that even the smallest strain results in a change in inductance; second, the ease of use for surgeons must also be considered.

During the reporting period, two academic theses were completed, and another was started:
Bachelor Thesis: Entwicklung eines semiautomatischen Verfahrens zur Fertigung von implantierbaren, hochflexiblen Sensoren für die Dehnungsmessung an Sehnen. (06/2025)
Masterthesis: Design and Evaluation of Implantable, Highly Flexible Inductive Sensors for Measuring Tendon Strain. (03/2026)
Masterthesis: Optimierung der Dauerfestigkeit und Sensitivität von Implantierbaren, induktiven Sensoren für die Dehnungsmessung an Sehnen. (started)

Funded by:

Schweizerische Eidgenossenschaft
Confédération suisse
Confederazione Svizzera
Confederaziun svizra

Funded by
the European Union

The SmILE project has received funding from the European Union's Horizon Europe programme and the Swiss State Secretariat for Education, Research and Innovation (SERI).

3. Printed pH, temperature, and acoustic sensors

3.1 Introduction

This deliverable summarizes the pH, temperature, and acoustic sensing options evaluated for the SmILE implants and assistive-device use cases. The design targets are low-power bridge-compatible sensors, mechanically adaptable to crutches, bone plates and prosthetic components, and electrically compatible with the conditioning front-end in the 5-10 kΩ range.
The pH and temperature sensors' function is to monitor the appearance of an infection around the implant area, while the acoustic emission sensor functions as implant loosening detection.
The pH sensors are designed to be completely printed, avoiding the need of any 3D component, and to be as small as possible. A prototype of these devices has been tested in a microfluidic channel so to be able to automatize the flow of the testing solution in a laboratory environment.
The temperature sensors have been studied with completely printed configurations based on non-metallic materials, so to increase the resistance of the devices and allow for a lower current usage and increasing the lifetime of the battery of the system that will be implanted.
The acoustic emission sensors are also fully printed with non-metallic materials, reacting to force/pressure changes with the generation of a potential. The frequency of the sensor's response is proportional to the vibration sensed. In the following we detail the sensors' working principle, structure and characterizations performed so far, describing as well the next steps planned for their development, which are resumed in the last paragraph.

3.2 The pH sensors

For potentiometric measurements, such as pH and selective ions, a two-electrode configuration is used: an indicator electrode, functionalized for the detection of the analyte of interest, and a reference electrode that guarantees a stable potential.

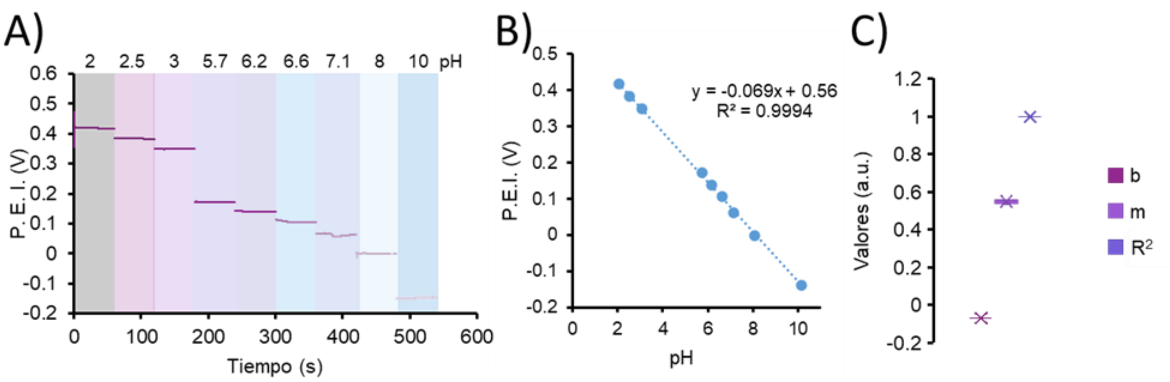

Figure 12. A) Temporal variation of the potential of the pH indicator electrode (P. E. I) for the different pH values studied. B) Calibration line of the potential of the indicator electrode as a function of the pH of the solution. C) Main linearity parameters used in the characterization of pH sensors, including the Nernstian slope (m), the standard potential (b) and the linear coefficient of determination (R^2).

In the case of pH measurement, the electrochemical system is configured by assembling two electrodes: an indicator electrode and a reference electrode. The indicator electrode is based on a conductive carbon layer screen-printed on the flexible substrate, subsequently coated with a nanometric layer of iridium oxide deposited by electrodeposition. This material has been selected for its high potentiometric sensitivity, chemical stability and quasi-Nernstian response in a wide pH range.

As for the reference electrode, it is manufactured by printing a silver/silver chloride (Ag/AgCl) ink, which provides a stable and reproducible potential during measurements. This electrode is specifically

Funded by:
Schweizerische Eidgenossenschaft
Confédération suisse
Confederazione Svizzera
Confederaziun svizra
Funded by the European Union
The SmILE project has received funding from the European Union's Horizon Europe programme and the Swiss State Secretariat for Education, Research and Innovation (SERI).

positioned in the area corresponding to the salt bridge of the microfluidic system, where a 3 M KCl solution is maintained. During the experiments, the flow of the reference channel remains practically zero, while the sample circulates continuously through the main channel. This configuration allows the reference potential to be stabilized and contamination between the sample and the saline solution to be minimized. Both electrodes have been printed on a device integrating a microfluidic channel so to be able to rapidly change the testing solution on top of them without interrupting the measurements and of emulating the low volume of sample expected in proximity with the electrodes in a real scenario.

For the introduction of the samples, a system of peristaltic pumps, capable of providing a continuous flow of approximately 300 µL/min. This flow rate was optimized experimentally to guarantee the stabilization of the electrochemical signal in intervals of less than one minute, thus allowing a fast and stable acquisition of the data. To simplify the experimental setup, both the input and the output of the microfluidic system were connected to the same container containing the analyte to be studied. In parallel, a commercial reference pH-meter was integrated into this container to simultaneously obtain the real pH value of the solution and the open circuit potential (OCP) generated by the Lab-on-a-Chip device.

The electrochemical acquisition was performed using a commercial PalmSens potentiostat, selected for its high stability and sensitivity, as well as to reduce possible parasitic potentials or electronic noise associated with electronic systems developed ad hoc and not optimized for this type of application. The experimental procedure consisted of the preparation of a 0.24 M dipotassium phosphate (K_2HPO_4) buffer solution initially adjusted to pH 2 by the addition of HCl. Once this solution was integrated into the microfluidic system, known volumes of 1 M NaOH were added sequentially, generating controlled increases in pH. During this process, the pH values obtained with the commercial pH meter and the open circuit potentials of the LoC device were simultaneously recorded, thus establishing a direct correlation between both measurements. As shown in Figure 12A, measurements were obtained in a pH range of approximately 2 to 10. In this range, the potential of the indicator electrode varied from about 450 mV to values close to 180 mV.

These absolute values depend both on the specific characteristics of each sensor and on the initial potential established at acidic pH. The evaluation of the linearity of the sensor was carried out based on the Nernst equation, which describes the relationship between the electrochemical potential and the activity of the hydrogen ions present in the solution:

$$E = E^0 - \frac{RT}{nF} \ln\left(a_{H^+}\right)$$

Under standard conditions, this relationship theoretically corresponds to a sensitivity of 59 mV/pH. However, in printed electrochemical sensors it is common to observe a certain dispersion in this value due to variations associated with the manufacturing processes, the surface morphology and the properties of the functional materials. Based on previous experiences, sensitivities between approximately 45 and 80 mV/pH are considered acceptable. The analysis of one of the integrated sensors shows a clearly Nernstian behaviour, with an experimental slope of 69 mV/pH, a value that is within the established range and that confirms the correct functionality of the system (Figure 12B). In addition, the response presents an excellent linearity, characterized by a coefficient of determination very close to unity. The joint characterization of the three analysed sensors shows an average slope of 69 ± 1 mV/pH, a standard potential of 550 ± 10 mV and an average coefficient of determination of R^2=0.9999±0.0003 (Figure 12C). These results demonstrate a high reproducibility between devices, as well as an excellent electrochemical stability of the integrated system.

The next steps for this sensor go in two directions: the first is to analyse the stability of the sensor over prolonged periods of time and in more complex solutions emulating the situation the sensor should

Funded by:

Schweizerische Eidgenossenschaft
Confédération suisse
Confederazione Svizzera
Confederaziun svizra

Funded by the European Union

The SmILE project has received funding from the European Union's Horizon Europe programme and the Swiss State Secretariat for Education, Research and Innovation (SERI).

face inside the body. The second direction is to analyse the possibility to use part of the prosthetic (opportunely modified with specific surface treatments) as the working electrode of the system and to see if this prolongs the device life and stability in complex solutions. In particular, the fixation screws of the prosthetics have been defined as an interesting target for this study, which is currently in progress.

3.3 The temperature sensors

With the aim to reduce the power consumption of the sensor, standard metallic materials have been avoided since their high conductivity imply relatively high currents. PEDOT conductive polymer and graphene have been evaluated for this purpose, analysing the response of a meander layout with the same geometrical characteristics but different fabrication methods.

The following table lists the analysed cases:

Material	**Fabrication**	**Layout**	**Length**	**Width**	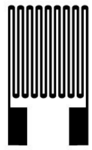
PEDOT	Screen-print	meander	130 mm	600 µm	
Graphene	Stamping	meander	130 mm	600 µm	
PEDOT+0.1% rGO	Screen-print	meander	130 mm	600 µm	

The devices have been fabricated on Kapton substrate and covered by a transparent dielectric by screen printing, leaving only square pads uncovered and connected to a multichannel (12 channels) setup to measure their resistance over time. The devices have been kept in a climatic chamber undergoing temperature cycles at a fixed humidity (50%) after an initial thermal treatment.

The calibration of the devices has been performed in the 30-50ºC nominal range with steps of 5ºC in both directions for at least 9 cycles (about 150 hours in total). Both the materials employed respond to temperature increase decreasing their resistance (a well-known effect which differs from the typical behaviour of metals, going in the opposite direction). The parameters evaluated to characterize the response of the different configurations tested are listed in the following table.

Parameter	**Definition**	**Calculation**
Linearity	Degree of proportionality of the measured signal variation to the temperature one	R2 of the linear fitting of the 5 data points tested both in ascending and descending mode
Sensitivity	Level of variation of the measured signal with respect to 1ºC temperature variation in the linear range	Slope of the linear fit in the tested range
Drift	Variation of the measured signal over each cycle not due to temperature variation	Percentage variation of the resistance percentual variation accumulated for each cycle
Resolution	Minimum measurable temperature variation	Temperature variation causing a signal variation bigger than 3 times the standard deviation of the "blank" signal (blank condition defined as the 30ºC stable condition)
Resolution after filtration	As above but after the filtration of the signal.	As above but after the filtration of the signal with a mobile average filter with a window width of 10 samples

Funded by:

Schweizerische Eidgenossenschaft
Confédération suisse
Confederazione Svizzera
Confederaziun svizra

Funded by the European Union

The SmILE project has received funding from the European Union's Horizon Europe programme and the Swiss State Secretariat for Education, Research and Innovation (SERI).

Figure 13 shows an example of one temperature cycle, highlighting the response of a commercial thermocouple (used as reference in the climatic chamber), and the unfiltered signal measured by the devices in the periods of time with a stable temperature.
In the analysed temperature range, noise is heavily affecting the measurements. Nevertheless, the calibration curve calculated from the sensors’ response (averaging the data points in each interval of time with a stable temperature) showed a very good linearity and a relatively low drift.

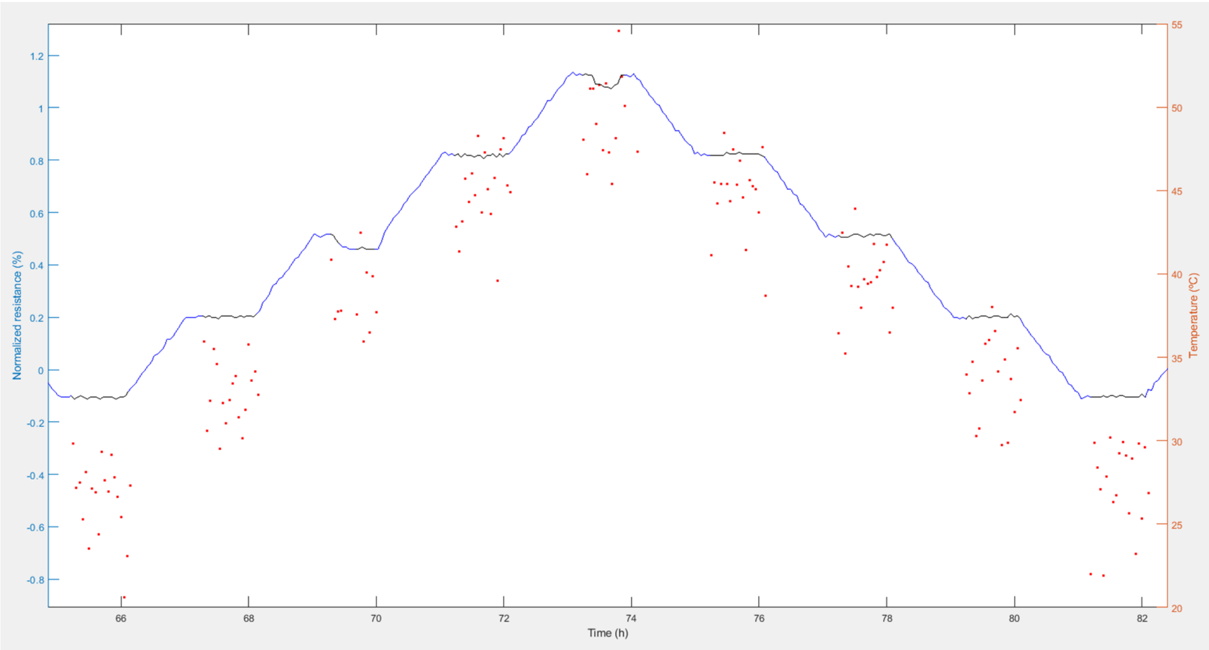

Figure 13. Example of the unfiltered calibration measurements obtained from the testing of the rGO meander resistor. The blue curve represents the thermocouple data (reference temperature data), the black intervals are the portions of the thermocouple data which have been defined as stable by our data analysis software, and the red dots are the rGO sensor data (normalized) used for the calculation of the calibration curve.

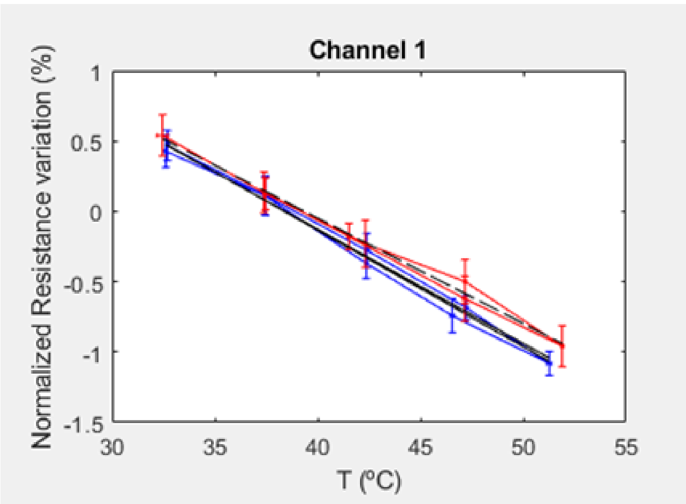

Figure 14. Example of calibration curve. The blue points represent the average signal calculated at each stabilized temperature with their respective standard deviations, for the first cycle. The red points represent the same for the last (the 9th) cycle. The points are duplicated because both the ascending and descending curves have been used for the calculations. The dashed lines represent the linear fittings of the blue and red points, respectively.

Funded by:

Schweizerische Eidgenossenschaft
Confédération suisse
Confederazione Svizzera
Confederaziun svizra

Funded by the European Union

The SmILE project has received funding from the European Union’s Horizon Europe programme and the Swiss State Secretariat for Education, Research and Innovation (SERI).

Configuration	Sensitivity	Drift	Drift after filtration	Resolution	Resolution after filtration
PEDOT meander	-0.280%/ºC	0.46%/cycle	0.60%/cycle	2.28ºC	0.47ºC
PEDOT +0.1%rGO meander	-0.156%/ºC	0.02%/cycle	0.005%/cycle	3.05ºC	0.82ºC
rGO meander	-0.075%/ºC	0.01%/cycle	0.006%/cycle	5.64ºC	2.11ºC

The drift obtained with graphene devices have been very good despite their low sensitivity compared with the PEDOT ones. The obtained resolutions after filtration improved significatively but are still not satisfying. Considering their dependence by the noise in the measurements, one of the next steps (currently under development) is the use of a new setup with shielded wires and commercially available connectors so to avoid any soldering on the printed devices and also a faster setup (and testing) time. Furthermore, the next steps will involve also the study of different layouts and more refined data collection setups to minimize the noise of the measurements, which heavily affects the resolution, probably the most important performance factor parameter in the intended application of the sensor.

3.4 The acoustic emission sensors

Acoustic emission (AE) sensors can detect high-frequency stress waves generated by damage mechanisms such as friction, micro-crack initiation, and crack propagation, providing an early warning before visible damage appears. AE measurements complement temperature and strain sensing because they indicate when and where damage is progressing, while the other sensors quantify applied loads and environmental conditions. Conventional AE transducers offer higher sensitivity and broader bandwidth than printed polymer-film sensors, which may exhibit a lower signal-to-noise ratio (SNR) and a narrower high-frequency response. However, printed sensors provide clear advantages in terms of embeddability, sensor density, and spatial coverage, while also reducing wiring complexity and coupling-related issues.

The sensors were fabricated using an organic conductive material based on PEDOT. This material provides sufficient conductivity to obtain a homogeneous charge distribution across the device, while maintaining adequate stability and solvent compatibility to prevent short-circuiting of the piezoelectric layer. The piezoelectric copolymer, polyvinylidene fluoride–trifluoroethylene (PVDF-TrFE, 75:25), was sandwiched between two PEDOT contacts. After fabrication, piezoelectric sensors require poling to activate their piezoelectric properties. For PVDF-based polymers, the material must be in its ferroelectric β-phase to exhibit piezoelectric behaviour. This requires heating the material above its Curie temperature to increase dipole mobility, followed by the application of a high DC electric field during cooling. This process aligns the dipoles into a stable piezoelectric configuration.

Printed piezoelectric sensors can be adapted to diverse settings and used in multiple configurations. During fabrication, the sensors can be directly crimped or connected to wires through printed silver tracks, allowing them to be subsequently integrated into parts or mounted onto their surfaces. Their versatility enables them either to be embedded within composite structures or attached to their surfaces, allowing vibration detection in the target object. Characterising sensors embedded in composite structures enables a controlled evaluation of their performance under representative mechanical loads, while isolating variables related to material behaviour and sensor response.

Funded by:

Schweizerische Eidgenossenschaft
Confédération suisse
Confederazione Svizzera
Confederaziun svizra

Funded by the European Union

The SmILE project has received funding from the European Union's Horizon Europe programme and the Swiss State Secretariat for Education, Research and Innovation (SERI).

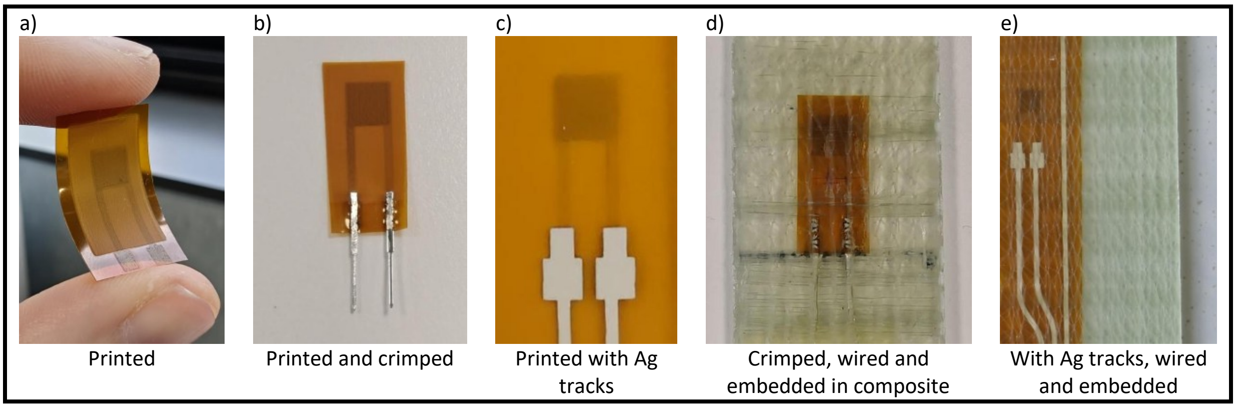

Figure 15. Different configurations of the printed piezoelectric sensors on Kapton. a) Fully printed piezoelectric sensor, b) printed and crimped sensor, c) printed with Ag tracks added, d) printed, crimped, wired, and embedded in composite, and e) printed with Ag tracks added, crimped, wired and embedded in composite.

The sensors were characterised through vibration testing. First, an individual crimped sensor was evaluated using a hold-and-release test. Its response when attached to the surface of a composite part was then compared with that of a second sensor, which was connected to wires through printed silver tracks and embedded within the composite part.

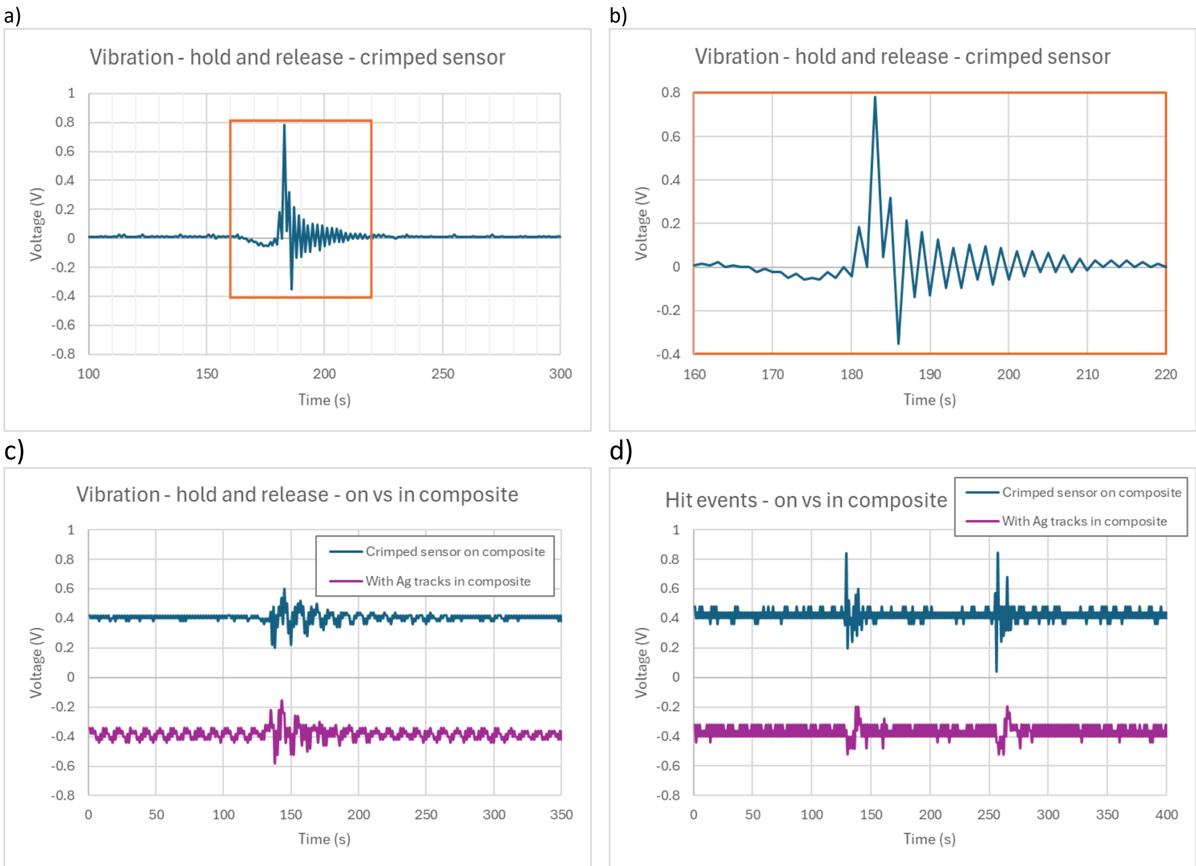

Figure 16. Voltage response of the piezoelectric sensors under different conditions. a) and b) Hold-and-release test on a crimped sensor, b) being a scaled up version of a). c) and d) Tests performed on an embedded sensor with Ag tracks compared to a crimped sensor attached to the surface of the composite, on top of the embedded sensor, c) being a hold-and-release test and d) being hit events test, performed on the composite structure.

Funded by:

Schweizerische Eidgenossenschaft
Confédération suisse
Confederazione Svizzera
Confederaziun svizra

Funded by the European Union

The SmILE project has received funding from the European Union's Horizon Europe programme and the Swiss State Secretariat for Education, Research and Innovation (SERI).

As the hit events occur the compression of the sensor produce a voltage peak followed by a series of smaller peaks due to the transmission of the vibrations. A complete amplitude and frequency characterization need a different setup based either on sound waves or controllable pressure piston so to be able to calibrate the sensor with respect to the response of a commercially available accelerometer.

3.5 Conclusions and next steps

The printed sensors developed so far in the project for pH sensing, temperature monitoring and acoustic sensing are based only on printed configurations on flexible substrate and take advantage of non-metallic materials to comply with the specifications required by the ASIC under development and the power available for the platform.

The layout tested in this first phase of the project has been selected for laboratory validation, taking into account the geometrical characteristics of the target prosthetic devices (in this case, primarily the osteosynthesis plate, since at least the first two devices are designed to be mounted on the prosthetic surface that is not in contact with the bone).

The characterization of the devices has proved that they are working relatively well but also that their performance still needs to be improved before moving to the real use-case so to comply with all the desired specifications.

The next steps for the pH sensor are the study of its response stability over time without recalibration in complex media emulating the ones with which is expected to come in contact inside the body. In parallel with this study, the development of a different configuration has started. In this case, the surface of one of the fixation screws of the plate will be modified so to be used directly for the pH sensing, accompanied by a printed reference electrode around it. This configuration might be more functional and might grant a longer operation time, as requested by the clinical partners.

For the temperature sensor the next step will be the exploration of new layouts and the reduction of the noise in the measurements thanks to a better electronic setup, which is expected to improve drastically the resolution of the temperature measurements. The drift of the new sensor will be analysed as well.

For the acoustic sensors, the next step will be the precise calibration of the devices. Two characterisation setups are planned: one based on controlled impacts and another based on sound waves. The first setup consists of a piston actuated by controlled air pressure, which will apply impacts directly onto the sensor surface at different force levels. The second setup is based on a speaker cone with a top surface on which the sensor can be mounted. This system will transmit vibrations at different controlled frequencies, allowing the sensor's ability to detect sound waves to be characterised.

Funded by:

Schweizerische Eidgenossenschaft
Confédération suisse
Confederazione Svizzera
Confederaziun svizra

Funded by the European Union

The SmILE project has received funding from the European Union's Horizon Europe programme and the Swiss State Secretariat for Education, Research and Innovation (SERI).

4 Impedance spectroscopy for bone density

4.1 Introduction

This part defines the impedance spectroscopy sensing module to be integrated on a titanium bone plate for monitoring bone regeneration and density-related changes. This part regards the design decisions, material down-selection, prototype evidence and open actions required before full functional validation. The baseline sensing architecture is a tetrapolar impedance spectroscopy configuration: the two outer electrodes inject a controlled AC current into the bone region, while the two inner electrodes sense the differential voltage. This configuration reduces the influence of electrode-tissue interface impedance and improves sensitivity to tissue properties in the fracture or regeneration region

The electrode layout has been defined for integration within the bone plate, featuring four longitudinal sensing electrodes electrically insulated from the Grade 5 titanium substrate through dedicated dielectric layers and interconnected by encapsulated vias. This configuration provides a robust basis for reliable signal routing while preserving the structural integrity of the implant.
Material screening identified polyimide and EPO-TEK MED systems as suitable insulating candidates. In particular, MED-301 and MED-353 provided homogeneous coating, dry insulation resistance above 100 MΩ, and good adhesion on titanium substrates. Among the conductive materials evaluated, gold, PEDOT and H20E showed satisfactory morphology, whereas platinum exhibited cracking under the preliminary curing conditions, indicating the need for further process optimisation.
Although H20E achieved the lowest electrical resistance, the potential exposure of silver-filled materials to physiological fluids makes noble-metal surfaces, such as gold, the preferred option for sensing electrodes. Functional bioimpedance testing will be reported in the next validation deliverable, while the present report focuses on the electrode design, material and process feasibility, and preliminary coupon-level validation.

4.2 Impedance measurement principle

The impedance sensing approach is based on multi-frequency electrical impedance spectroscopy. A known alternating current is injected through the tissue and the resulting differential voltage is measured.

Both impedance magnitude and phase are relevant, because bone is heterogeneous and frequency-dependent: mineralized matrix, extracellular fluids, porosity and cellular structures contribute differently across the spectrum. The selected operating window remains in the kHz to low-MHz range, using microampere-level injection currents to maintain safety margins and avoid unintended tissue stimulation.

The expected evolution of the impedance response during fracture healing (and bone density change) can be summarized as follows:

• Early healing phases are expected to show lower impedance due to higher fluid content and lower mineralization.

• As regeneration progresses, mineralization and fracture-gap stiffening should increase the resistive contribution and modify the impedance spectrum.

• Lower frequency ranges are primarily sensitive to extracellular ionic conduction; higher frequencies reduce electrode polarization effects and emphasize capacitive components.

4.2.1 Interface with the WP4 readout chain

The impedance electrodes will be connected to a dedicated AFE. The readout must provide a stable current source, high-input-impedance differential voltage sensing, low-noise amplification and sufficient dynamic range to capture the expected variation in bone impedance throughout the healing

Funded by:

Schweizerische Eidgenossenschaft
Confédération suisse
Confederazione Svizzera
Confederaziun svizra

Funded by
the European Union

The SmILE project has received funding from the European Union's Horizon Europe programme and the Swiss State Secretariat for Education, Research and Innovation (SERI).

process. The bone-electrode system can be approximated by tissue resistance, distributed capacitance and residual electrode polarization impedance. Even though tetrapolar sensing strongly reduces electrode interface effects, equivalent-circuit fitting may be required to extract robust tissue-related parameters from the measured impedance spectra.

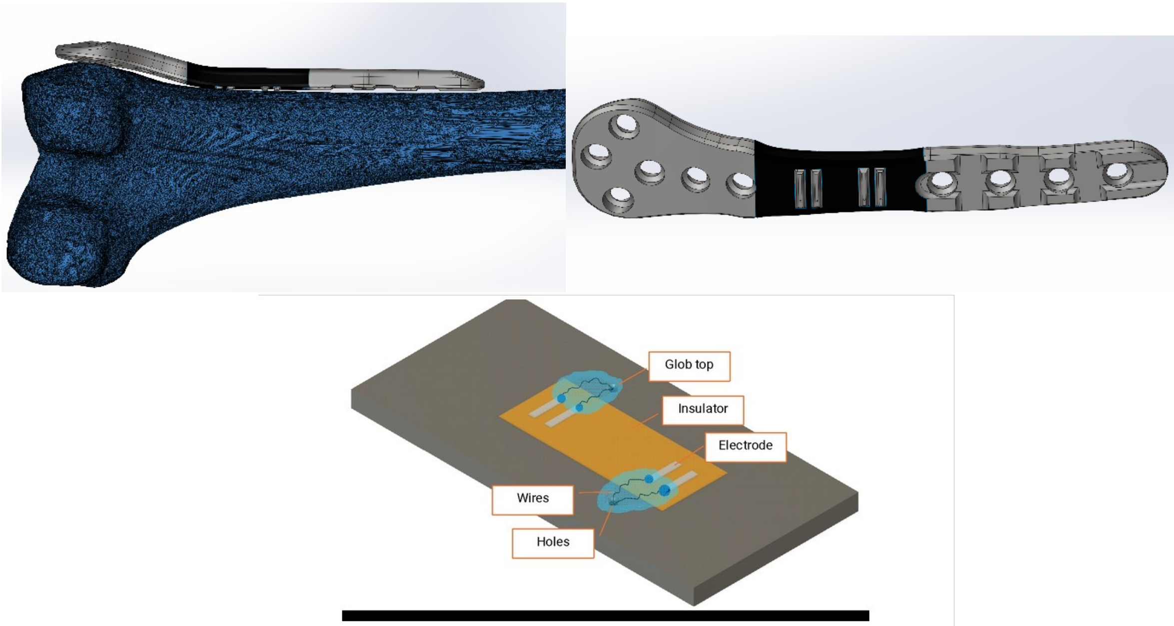

Electrode, insulation and wiring concept

Figure 17. Target use case and electrode/interconnection concept for bone plate integration.

4.3 Electrode architecture for the bone plate

Four electrodes are arranged linearly along the longitudinal axis of the plate. The outer pair injects current, while the inner pair senses voltage. The measurement volume is mainly governed by the spacing of the voltage electrodes and should encompass the fracture gap or regeneration region. The electrode dimension and spacing will be tailored to the dimensions of the bone plate.

Funded by:

Schweizerische Eidgenossenschaft
Confédération suisse
Confederazione Svizzera
Confederaziun svizra

Funded by
the European Union

The SmILE project has received funding from the European Union's Horizon Europe programme and the Swiss State Secretariat for Education, Research and Innovation (SERI).

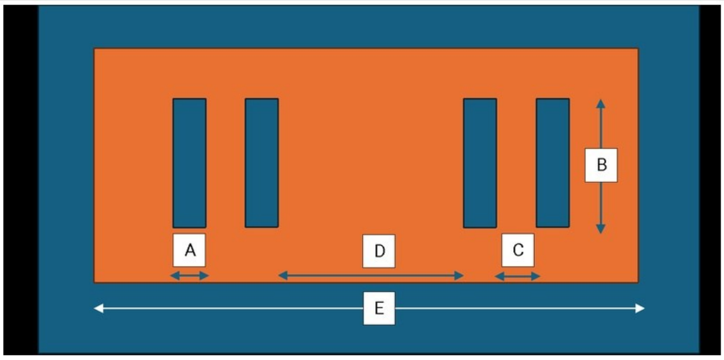

Tetrapolar electrode layout

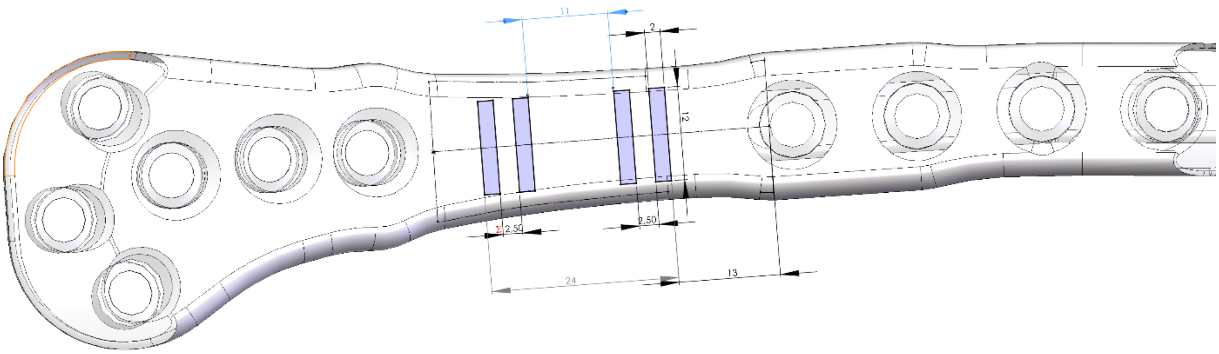

Figure 18. Baseline tetrapolar layout and indicative dimensional envelope.

4.3.1 Indicative geometry

In the following table the key design parameters and implementation constraints of the proposed sensor are summarized.

Design item	Target / range	Implementation note
Electrode width (A)	2-5 mm	Defines local contact area and current density.
Electrode length (B)	8-12 mm	Provides sufficient contact length without excessive footprint.
Inner voltage spacing (C)	2.5-5 mm	Sets the primary sensitive region for bone regeneration monitoring.
Outer current spacing (D)	> C	Ensures current distribution through the region of interest.
Substrate isolation	Required	Titanium plate is conductive; a continuous dielectric layer is mandatory.
Interconnection route	Vias/wires + encapsulation	Electronics can be placed on the opposite side of the plate.

For the next prototype, several design constraints will be maintained to ensure reliable operation in the intended environment. First, the dielectric layer must remain continuous, free of pinholes, and stable during prolonged soaking in physiological media, as any defect could compromise the electrical

Funded by:

Schweizerische Eidgenossenschaft
Confédération suisse
Confederazione Svizzera
Confederaziun svizra

Funded by
the European Union

The SmILE project has received funding from the European Union's Horizon Europe programme and the Swiss State Secretariat for Education, Research and Innovation (SERI).

insulation and sensor performance. The conductive electrode surface must also provide sufficient corrosion resistance and biocompatibility over the expected exposure time.
Particular attention will be given to the protection of interconnections and vias, which require robust encapsulation to prevent leakage paths, moisture ingress, and mechanical damage during loading. Finally, while the electrode dimensions may be adapted according to the specific use case and integration requirements, the four-terminal measurement principle will be retained as the baseline configuration for the next development stage.

4.4 Material and process down-selection

The material stack has two critical functions: electrical isolation from the titanium plate and stable electrochemical contact with the tissue. Selection is therefore driven by insulation of reliability, adhesion to titanium, process compatibility, long-term wet stability and biocompatibility of any exposed surface. Use noble-metal or titanium/gold exposed surfaces for sensing electrodes where possible. Use silver-filled conductive epoxy primarily for low-resistance interconnections, provided it is covered or encapsulated. Continue wet aging, adhesion and biocompatibility checks before freezing the stack.

4.4.1 Insulating materials

The candidate dielectric materials and their main characteristics, together with the key validation aspects, are summarized in the following table.

Candidate	Main value	Critical checks
Polyimide / PI2611 route	High dielectric performance, chemical resistance, proven use in microelectronics.	Requires complete curing and imidization at about 250-300 °C; thickness must be built without bubbles or voids.
EPO-TEK MED-302-3M	Low water absorption, low-temperature cure and medical-device relevance.	Promising candidate for printed-electronics insulation; wet aging and adhesion on treated titanium must be verified.
EPO-TEK MED-301 / MED-301-2	Low viscosity, good wetting and long working time.	Useful for smooth planar insulation and prototypes; already tested at coupon level.
EPO-TEK MED-353ND / variants	Higher mechanical robustness and high glass-transition temperature.	Good candidate where mechanical stability is prioritized; cure conditions must remain compatible with the full stack.
Parylene control route	Conformal coating option for capacitive/control samples.	To be prepared for comparison and long-term barrier assessment.

4.4.2 Conductive materials

The candidate conductive materials, their potential applications, and the main validation challenges are summarized in the following table.

Funded by:

Schweizerische Eidgenossenschaft
Confédération suisse
Confederazione Svizzera
Confederaziun svizra

Funded by the European Union

The SmILE project has received funding from the European Union's Horizon Europe programme and the Swiss State Secretariat for Education, Research and Innovation (SERI).

Candidate	Potential role	Key limitation / action
Gold	Stable noble metal, compatible with exposed electrode concepts.	Requires adequate sintering and verification of ink additives/removal.
Platinum	Electrochemically stable and biocompatible in principle.	Preliminary films cracked; printing/sintering recipe needs optimization.
PEDOT:PSS	Low interface impedance and printable at moderate temperature.	Long-term swelling, drift and biocompatibility of additives such as DMSO/PVP must be verified.
H20E / H20S conductive epoxy	Very low resistance and practical for interconnects.	Silver-filled material should not remain directly exposed to body fluids; encapsulation or metal covering is required.

4.5 Preliminary validation plan

Before full functional bioimpedance validation, the electrode-insulator-substrate assembly must pass material-level and sensor-level checks. The goal is to identify early failure mechanisms before integration with the AFE and encapsulated implant demonstrator.

Test block	Method	Acceptance purpose
Electrical insulation	Resistance/leakage between each electrode and titanium substrate, initially dry and then in PBS at 37 °C.	Detect pinholes, moisture ingress and parasitic current paths.
Electrochemical response	Impedance magnitude/phase in controlled saline over the selected frequency range.	Establish electrode-electrolyte baseline and short-term repeatability.
Accelerated aging	Soaking in PBS at physiological and, where appropriate, elevated temperature; periodic EIS and visual inspection.	Capture drift, corrosion, swelling, delamination and material degradation.
Mechanical reliability	Adhesion and cyclic loading on titanium coupons; electrical checks before, during and after deformation.	Verify that strain and handling do not crack the stack or cause electrical discontinuities.

Funded by:

Schweizerische Eidgenossenschaft
Confédération suisse
Confederazione Svizzera
Confederaziun svizra

Funded by the European Union

The SmILE project has received funding from the European Union's Horizon Europe programme and the Swiss State Secretariat for Education, Research and Innovation (SERI).

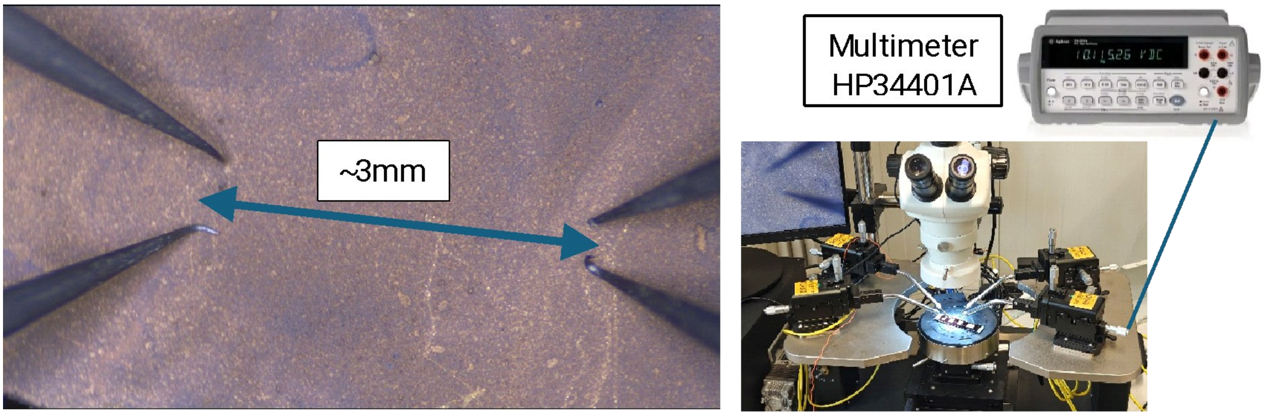

Figure 19. Representative laboratory setup for electrical characterization with micro-positioned contacts.

4.6 Preliminary prototypes: insulating layers on titanium

Grade 5 titanium bars were used as representative coupons for bone plate integration. The first screening compared MED-301 and MED-353 insulating coatings deposited and cured according to the respective datasheets. MED-301 and MED-353 are suitable for the next prototype phase. The decisive tests remain wet insulation stability, cyclic mechanical loading and compatibility with the selected conductive electrode/interconnect deposition process.

Item	Result
Substrate preparation	Titanium Grade 5 bars cleaned before coating.
Materials tested	Five samples coated with MED-301 and five samples coated with MED-353.
Curing	MED-301: 45 °C for 16 h. MED-353: 150 °C for 1.5 h.
Morphology	Optical microscopy showed homogeneous, continuous layers with no macroscopic cracks or delamination.
Dry insulation	All measured locations exceeded the 100 MOhm instrument limit between coating and titanium substrate.
Adhesion	Cross-incision plus tape peel-off showed no visible detachment for either material.
Thermal stress	After 250 °C for about 1.5 h, repeated peel-off tests still showed no visible cracking or detachment.

Funded by:

Schweizerische Eidgenossenschaft
Confédération suisse
Confederazione Svizzera
Confederaziun svizra

Funded by the European Union

The SmILE project has received funding from the European Union's Horizon Europe programme and the Swiss State Secretariat for Education, Research and Innovation (SERI).

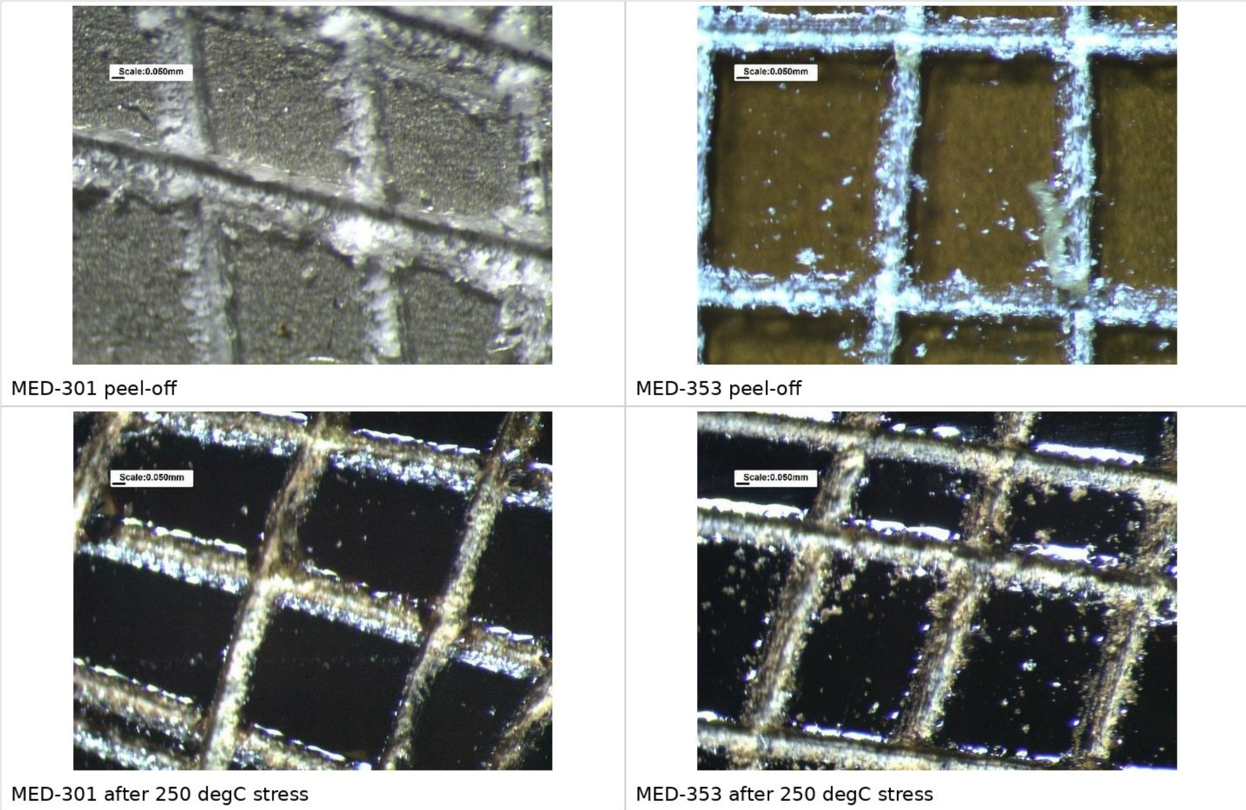

Figure 20. Representative peel-off and thermal-stress observations on MED-301 and MED-353 coated titanium.

4.7 Conductive layer compatibility on insulated titanium

After validating insulating coatings, conductive materials were deposited on MED-301 and MED-353 coated titanium. The goal was to screen morphology, adhesion, thickness and resistance before defining the electrode/interconnect stack.

• PEDOT:PSS was tested in pure form and with DMSO/PVP additives; drying was performed under a fume hood.

• H20E conductive epoxy was thermally cured at 150 °C for about 1.5 h.

• Gold and platinum inks were treated at 150 °C for about 1.5 h; metallic films required subsequent photonic sintering to improve consolidation.

• Gold, PEDOT:PSS and H20E showed continuous deposits; platinum showed cracking, more pronounced on MED-353.

H20E provides the lowest resistance and is attractive for interconnections, but the silver filler raises long-term exposure concerns. Gold remains the more conservative exposed-electrode option. Platinum is not rejected in principle, but the printing/sintering recipe must be improved to avoid cracking.

Funded by:

Schweizerische Eidgenossenschaft
Confédération suisse
Confederazione Svizzera
Confederaziun svizra

Funded by the European Union

The SmILE project has received funding from the European Union's Horizon Europe programme and the Swiss State Secretariat for Education, Research and Innovation (SERI).

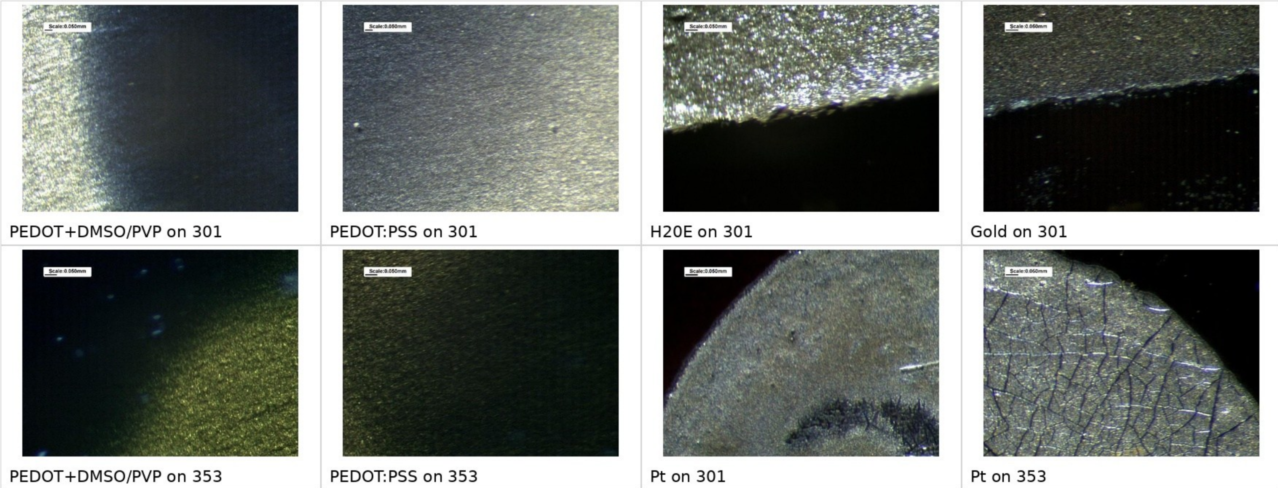

Figure 21. Conductive coatings on MED-301 and MED-353 insulating substrates.

Table X summarizes the measured electrical resistance of the candidate conductive materials deposited on the investigated dielectric substrates.

Substrate	**Pt**	**Au**	**PEDOT:PSS**	**PEDOT + DMSO/PVP**	**H20E**
MED-301	12-25 ohm	55-65 ohm	40 Mohm	19-21 ohm	2.2 ohm
MED-353	Inf.	36-42 ohm	38 Mohm	36-96 ohm	1.9 ohm

The representative thicknesses obtained for the different printed conductive layers are summarized in the following table. These values provide an indication of the deposition characteristics achieved with the adopted fabrication process.

Layer	**Representative thickness**
Gold	~6 um
H20E	~20 um
Platinum	~4-5 um
PEDOT:PSS	>1 um
PEDOT + DMSO/PVP	~6 um

4.8 Polyimide insulation and process integration strategy

A polyimide route was also investigated to create a thin, stable dielectric layer on titanium. The process uses surface activation and silane chemistry to improve adhesion before polyamic-acid deposition and imidization. Increasing PI thickness in a single step can generate bubbles or voids due to solvent entrapment. Thickness should therefore be built by sequential thin-layer deposition and curing, while monitoring residual stress and total process time.

Funded by:

Schweizerische Eidgenossenschaft
Confédération suisse
Confederazione Svizzera
Confederaziun svizra

Funded by the European Union

The SmILE project has received funding from the European Union's Horizon Europe programme and the Swiss State Secretariat for Education, Research and Innovation (SERI).

Step	Condensed process
Cleaning	Ethanol and distilled-water ultrasonic cleaning, followed by drying.
Surface activation	RF plasma in air: 75 W, 2 min, approx. 20 sccm, to increase surface reactivity.
Adhesion promoter	GLYMO-based silane solution in ethanol/water, approx. 1% v/v silane, 15 min immersion.
Silane consolidation	Ethanol rinse, drying and thermal treatment at approx. 100 °C for 10 min.
PI deposition	Polyimide precursor deposited and imidized with a ramp from 120 °C to 250 °C over approx. 5 h; process repeated twice.
Initial result	Insulation exceeded the instrument limit; thickness approx. 5 um; peel-off showed strong adhesion.

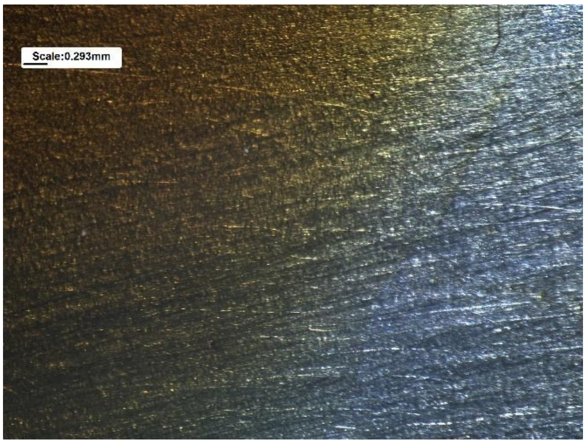

Polymide Layer on titanium

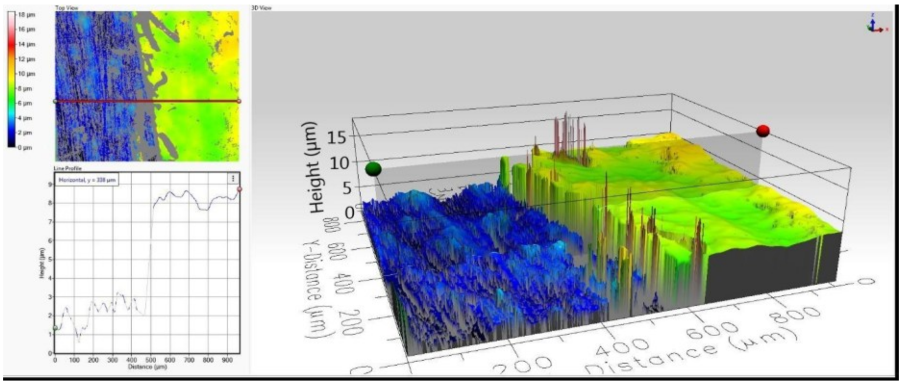

Representative profilometry result

Figure 22. Polyimide deposition result and profilometry example.

4.9 Epotek 301-2 Insulation and Gold Leaf Deposition

Epotek 301-2 was deposited on titanium following a strict protocol reported in the table below. The protocol is necessary because the epoxy resin has an epoxy group that bonds with the epoxy group of the GLYMO silane, while the silane forms a covalent bond with the titanium. This increases the surface energy and, consequently, the adhesion strength between the titanium and the epoxy resin. After deposition, before the resin cured, 200 nm thick gold leaves were added to define the 4 electrodes for

Funded by:

Schweizerische Eidgenossenschaft
Confédération suisse
Confederazione Svizzera
Confederaziun svizra

Funded by the European Union

The SmILE project has received funding from the European Union's Horizon Europe programme and the Swiss State Secretariat for Education, Research and Innovation (SERI).

bioimpedance measurements. The curing was then performed in an oven for 3 hours at 80 °C. Since thermal shocks were found to cause material shrinkage, the oven temperature was increased using a ramp of 3°C/min to ensure gradual heating. These results are preliminary and further investigations are ongoing to optimize the deposition process and validate the electrode performance.

Step	**Condensed process**
Titanium treatment	Titanium sandblasted with 200 µm corundum particles to improve adhesion.
Cleaning	Ethanol and distilled-water ultrasonic cleaning, followed by drying.
Surface activation	RF plasma in air: 75 W, 2 min, approx. 20 sccm, to increase surface reactivity.
Adhesion promoter	GLYMO-based silane solution in ethanol approx. 1% v/v silane, 30 min immersion.
Silane consolidation	Ethanol rinse, drying and thermal treatment at approx. 110 °C for 60 min.
301-2 deposition	Epoxy deposition using a squeegee ; gold leaf added before polymerization
Curing	3 hours at 80 °C
Initial result	35 µm thickness of Epotek 301-2, resulting in high impedance values consistent with an insulating material.

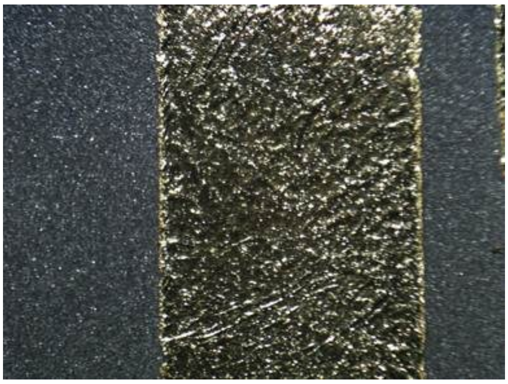
(a)

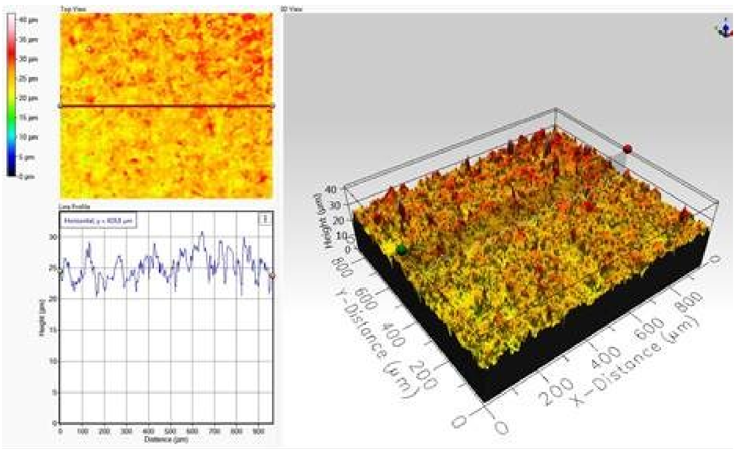

(b)

Figure 23. (a) 301-2 and gold leaf deposition result. (b) Sand-blasted titanium

Funded by:

Schweizerische Eidgenossenschaft
Confédération suisse
Confederazione Svizzera
Confederaziun svizra

Funded by
the European Union

The SmILE project has received funding from the European Union's Horizon Europe programme and the Swiss State Secretariat for Education, Research and Innovation (SERI).

4.10 Thin-film, flexible microelectrode arrays

As an alternative to printed electrodes, thin-film microelectrode arrays (MEAs) can be manufactured separately and attached to the bone plate in the desired location(s). The MEAs from imec are constructed using biocompatible polyimide (PI) as flexible, insulating material and noble metals such as gold or platinum for the interconnections. The electrode material is determined by the requirements of the application, mainly the electrode impedance and charge injection capacity. In addition to gold and platinum, iridium oxide (IrO_2) can be applied to the electrode surface to improve recording and stimulation performance. Impedance spectroscopy for bone density only requires monitoring of the impedance and as such, gold electrodes are deemed sufficient. To improve the lifetime of the MEAs inside the body, ultra-thin ceramic layers (Al_2O_3 and HfO_2) are added using atomic layer deposition (ALD). These provide excellent barrier properties without impacting the functionality and flexibility of the MEAs. The design of the MEAs, including number of electrodes, size of the electrodes, interconnections (routing) and shape of the MEA can be chosen freely. Limitations are the patterning capabilities (down to 10 µm) and the size of the glass carrier substrates (up to 10 cm x 10 cm).
The manufacturing starts by depositing the Polyimide on a rigid carrier using spin coating. Typical PI thickness is 5 µm and multiple layers can be deposited on top of each other to increase thickness and/or mechanical strength. The Au interconnections are deposited by sputtering and patterned using a photolithography and wet-etch process. Above and below the Au layer, a triple stack of $HfO_2/Al_2O_3/HfO_2$ ALD is deposited. On top of the ALD-Au-ALD sandwich, polyimide is again spin coated to provide isolated openings for the electrodes. These openings are realized using a dry-etch process, exposing the Au electrode underneath. When large electrode surfaces are needed, an additional Au layer and via interconnections can be realized. The shape of the MEAs is cut out by laser, after which the flexible MEAs are released from the glass carrier.

4.11 Conclusions and next steps

The impedance spectroscopy module has progressed from measurement concept to a defined tetrapolar layout and a first material/process screening on titanium substrates. The current baseline is technically viable, but final selection of the stack must depend on wet insulation stability, exposed-electrode biocompatibility and mechanical reliability under implant-relevant deformation.

Area	Current conclusion	Next decision/action
Architecture	Tetrapolar four-electrode spectroscopy is retained as the baseline.	Freeze the layout variants for fracture-gap and plate-geometry constraints.
Insulation	MED-301, MED-353 and PI all showed promising initial adhesion/insulation.	Run PBS aging, leakage monitoring and cyclic deformation tests.
Conductors	Gold is the conservative exposed-electrode candidate; H20E is strong for interconnects; Pt requires recipe tuning; PEDOT:PSS needs stability/biocompatibility evidence.	Avoid direct exposure of silver-filled materials unless encapsulated or covered by a stable electrode surface.
Manufacturing	Direct deposition and printed-carrier routes remain open.	Compare process yield, roughness tolerance, curing budget and assembly reliability.
Validation path	Bioimpedance functional tests are intentionally deferred.	Report correlation with bone-related changes in the subsequent validation deliverable.

Funded by:
Schweizerische Eidgenossenschaft
Confédération suisse
Confederazione Svizzera
Confederaziun svizra
Funded by the European Union
The SmILE project has received funding from the European Union's Horizon Europe programme and the Swiss State Secretariat for Education, Research and Innovation (SERI).

The next activities will focus on establishing a reproducible fabrication process for the electrode platform by depositing EPO-TEK insulating layers together with gold or H20E conductive tracks using screen printing or dispensing techniques. Four-electrode prototypes will then be manufactured for mechanical and electrical validation, including peel-off, wet aging, cyclic deformation and leakage tests, alongside parylene-coated capacitive control samples. Additional work will clarify the implantability of the polyimide-based process and PEDOT formulations, particularly when conductivity enhancers such as DMSO are employed. Functional bioimpedance characterization and correlation with bone-related changes will be carried out in Task 4.4, while final verification of the fully integrated and encapsulated device is planned for Task 4.6.

Funded by:

Schweizerische Eidgenossenschaft
Confédération suisse
Confederazione Svizzera
Confederaziun svizra

Funded by
the European Union

The SmILE project has received funding from the European Union's Horizon Europe programme and the Swiss State Secretariat for Education, Research and Innovation (SERI).

5 Wear sensors for knee prosthesis

5.1 Introduction

Two complementary strategies are considered for monitoring wear of the polyethylene insert in total knee prostheses. The first strategy is direct: conductive traces are printed on the UHMWPE insert and progressive abrasion modifies or interrupts the conductive path. The second strategy is indirect: force-sensing elements and an IMU monitor the loading and kinematic conditions that drive wear, enabling wear-related indicators to be inferred during operation.

Direct scratch-sensor prototypes were produced using AJP and conductive materials including silver inks, PEDOT:PSS, platinum and conductive epoxy. Abrasion tests confirmed the expected progressive degradation of printed traces, but also highlighted adhesion and process-uniformity challenges. Plasma cleaning alone did not sufficiently improve PEDOT:PSS adhesion, whereas a thin TPU primer combined with H20E conductive paste gave the best preliminary peel-off behaviour. The H20E layer remained attached and was compressed rather than removed, but the deposited strips were still irregular and thick, approximately 40-50 um.

The indirect route combines a force-sensing layer at the polyethylene insert/tibial tray interface with IMU measurements. It can provide total axial load, medial-lateral load balance, condylar lift-off, anterior-posterior contact migration through CoP tracking, impact loading and cycle-to-cycle load symmetry. High-TRL Tekscan FSRs were identified, while preliminary tests with Ohmite FSR05 sensors demonstrated calibration, pressure estimation and CoP computation on a TKA assembly.

The preferred next steps are to refine direct-sensor deposition and adhesion; validate FSR encapsulation and fixation under cyclic loading; confirm ASIC front-end compatibility, channel availability and sampling rate; and perform longer durability tests representative of daily gait loading.

5.2 Scope and sensing strategy

Wear monitoring for total knee prostheses is addressed at the polyethylene insert, which is the mechanically weakest element between the femoral component and the tibial tray. The inlay experiences repeated compression, sliding, rolling and gliding under gait and daily activities; over time these mechanisms can remove material, change contact mechanics and contribute to implant degradation.

The deliverable therefore compares two sensing routes. The first route attempts to make wear directly observable by printing a conductive pattern on the insert surface. The second route measures the mechanical conditions that are known to drive wear and uses those measurements as indirect indicators of the wear state.

Route	Measurement principle	Main value	Main implementation risk
Direct printed scratch sensor	Conductive traces are printed on UHMWPE. Abrasion changes resistance or breaks continuity.	Directly coupled to surface material loss; conceptually simple indicator of local wear.	Requires strong adhesion, biocompatible exposed materials, controlled thickness and survivability under articulation.
Indirect force + IMU route	FSRs under the insert and IMU data record load distribution and kinematics.	Captures clinically relevant load and motion variables before catastrophic surface failure; compatible with modelling.	Requires robust calibration, encapsulation, ASIC channel allocation and long-term stability under cyclic load.

Funded by:
Schweizerische Eidgenossenschaft
Confédération suisse
Confederazione Svizzera
Confederaziun svizra
Funded by the European Union
The SmILE project has received funding from the European Union's Horizon Europe programme and the Swiss State Secretariat for Education, Research and Innovation (SERI).

The two sensing approaches should be regarded as complementary rather than mutually exclusive. The direct scratch sensor can provide localized evidence of surface degradation and wear progression, whereas the combination of force sensing and inertial measurements supplies the mechanical context required to interpret the conditions leading to wear. Together, these approaches can support a more comprehensive assessment of implant performance during validation.

Regardless of the selected sensing strategy, several implementation constraints must be addressed before integration into the final device. All materials, conductive additives and encapsulation solutions must be compatible with implantable applications and long-term exposure to the physiological environment. At the same time, sensor integration should not significantly affect the tribological behaviour of the UHMWPE insert, the mechanical response of the tibial tray or the fixation of the implant components. From the electronics perspective, the sensing elements must operate within the input ranges, power budget and channel availability of the project ASIC. Finally, both sensing routes require extensive validation under representative loading, abrasion and wet-environment conditions before progressing to integrated prototype testing.

5.3 Direct printed scratch sensor

The direct sensor is based on conductive paths deposited on the area of the polyethylene insert contacted by the femoral condyles. Progressive wear deforms, thins or removes portions of the printed pattern, increasing resistance or interrupting continuity. A multi-zone geometry can distinguish wear in different condylar regions.

5.3.1 Printing process and prototype geometry

Aerosol Jet Printing was selected for early prototypes because it is a non-contact additive process capable of depositing functional inks on curved or non-planar surfaces. In the selected workflow, CAD layouts are converted into printer paths, the ink is atomized and focused by gas streams, and the material is deposited on the UHMWPE insert without requiring masks or photolithography. Drying and curing are then required to remove solvents and consolidate the conductive path.

The initial demonstrators used serpentine and pad geometries representative of local resistive wear indicators. AJP parameters were tuned around wide-nozzle operation and low substrate temperature to avoid damaging the polyethylene. After deposition, samples were dried and metallic inks were consolidated by photonic curing using PulseForge technology, which can heat thin films rapidly while limiting thermal load to the polymer substrate.

Aspect	Condensed implementation note
Printing technology	AJP, wide nozzle, pneumatic atomization, 1-5 mm standoff distance.
Inks screened	Silver nanoparticle inks, PEDOT:PSS formulations, platinum ink, H20E conductive epoxy/paste.
Post-processing	Oven drying; photonic curing for metallic inks; lower-temperature treatment for polymeric inks.
Target output	Local change in resistance/continuity as wear increases across the condylar contact area.

AJP remains attractive because it allows rapid layout iteration and deposition on three-dimensional parts. Its main limitations for this use case are ink viscosity/process stability, adhesion on low-surface-energy UHMWPE, and the need to minimize cured-film thickness so that the sensor does not disturb tribology.

Funded by:

Schweizerische Eidgenossenschaft
Confédération suisse
Confederazione Svizzera
Confederaziun svizra

Funded by
the European Union

The SmILE project has received funding from the European Union's Horizon Europe programme and the Swiss State Secretariat for Education, Research and Innovation (SERI).

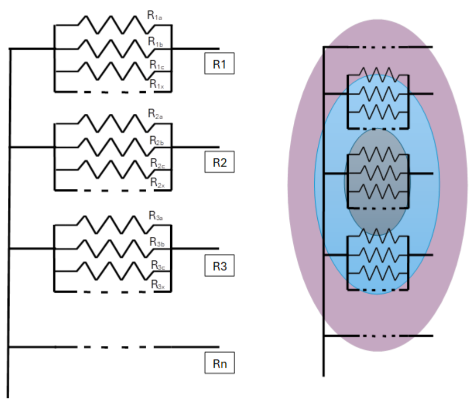

Resistive wear-sensor concept

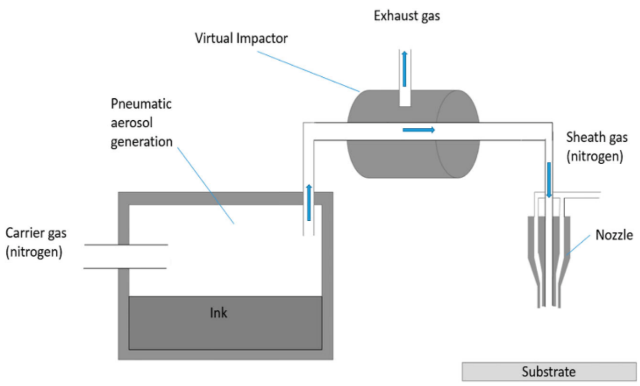

Aerosol jet printing principle

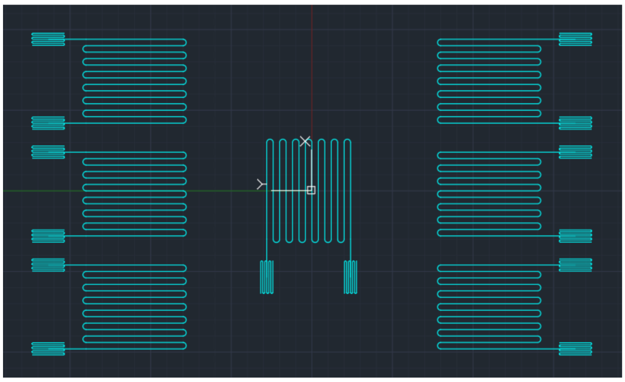

CAD layout printed traces

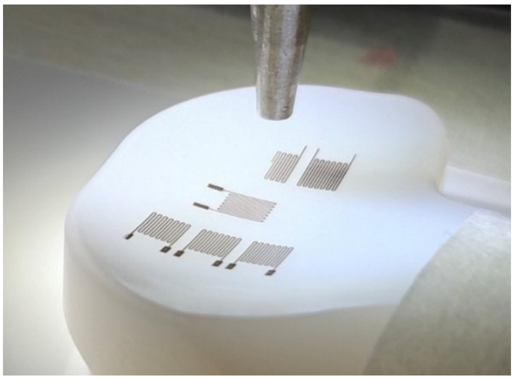

Printing on UHMWPE insert

Figure 24. Direct scratch-sensor concept, AJP process and representative printing on UHMWPE.

5.3.2 Ink screening and abrasion evidence

Initial microscope analyses compared silver inks from UTDOTS and GenesInk, PEDOT:PSS PH1000 formulations and platinum ink. Tribological screening was performed with a Tribotouch machine using hand-abrasion simulation at 2 Hz, 6 mm working distance and 1 N force, with increasing numbers of touches. The tests confirmed that abrasion progressively damages the printed traces, as expected from the sensing concept.

Material	Preliminary interpretation
GenesInk silver	Better retention than the UTDOTS silver sample, but trace discontinuity appeared after low-to-moderate cycle counts; traces were interrupted after repeated abrasion.
UTDOTS silver	Faster abrasion; near-complete material loss was observed after limited abrasion cycles.
PEDOT:PSS PH1000	Lower geometrical resolution than metallic inks, but slower visible abrasion; probable loss of functionality after high cycle counts must be verified electrically.
Platinum ink	Implant-relevant material, but early deposition/sintering produced high resistance or non-uniform films; process revision required.

Funded by:

Schweizerische Eidgenossenschaft
Confédération suisse
Confederazione Svizzera
Confederaziun svizra

Funded by the European Union

The SmILE project has received funding from the European Union's Horizon Europe programme and the Swiss State Secretariat for Education, Research and Innovation (SERI).

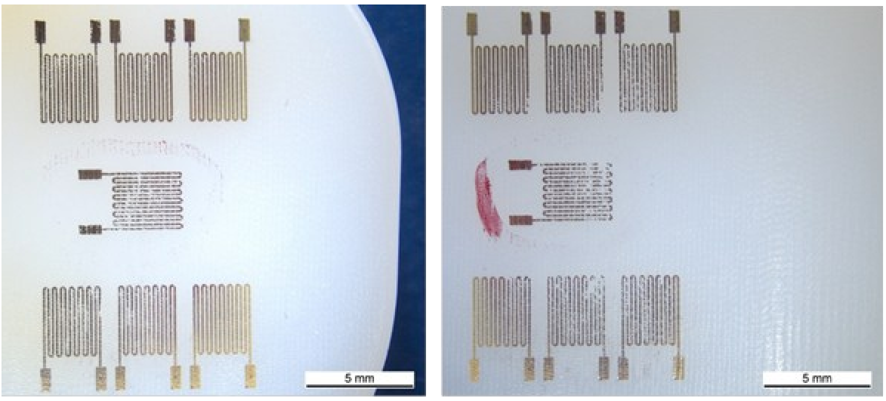

Genesink Ag after abrasion

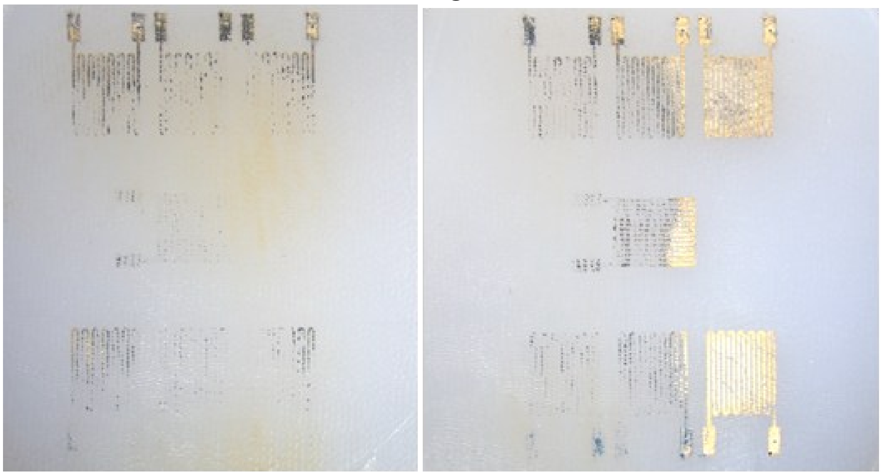

UTDOTS after abrasion

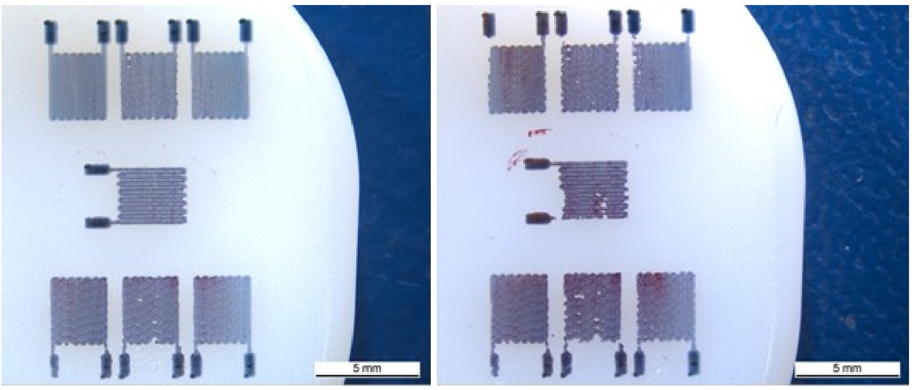

PEDOT:PSS after abrasion

Figure 25. Representative printed prototypes and abrasion outcomes for silver and PEDOT:PSS traces.

5.3.3 Preliminary Results

The preliminary experiments confirmed the feasibility of the direct printed sensing concept, demonstrating that abrasion produces detectable modifications of the conductive traces. At the current stage, however, the main limitations are related to process reliability rather than to the sensing principle itself. In particular, achieving stable adhesion on UHMWPE and uniform deposition of conductive materials remains the primary challenge, motivating a dedicated adhesion-promotion campaign.

Funded by:

Schweizerische Eidgenossenschaft
Confédération suisse
Confederazione Svizzera
Confederaziun svizra

Funded by the European Union

The SmILE project has received funding from the European Union's Horizon Europe programme and the Swiss State Secretariat for Education, Research and Innovation (SERI).

Different surface treatments and conductive materials were therefore investigated. Air-plasma activation increased the surface energy of UHMWPE but was not sufficient to ensure stable adhesion of PEDOT during tape peel-off tests, while platinum coatings showed only limited improvement. The addition of DMSO and PVP to PEDOT reduced the electrical resistance and produced homogeneous films immediately after deposition, although the coatings still exhibited insufficient adhesion without the use of a primer. The most promising results were obtained by introducing a thin TPU primer deposited from a THF solution prior to printing H20E. Under these conditions, scratch and tape tests indicated that the conductive layer remained attached to the substrate, with mechanical damage occurring within the material rather than at the interface. Nevertheless, selective deposition of $H_2$0E on curved UHMWPE inserts was still irregular and produced relatively thick conductive tracks (approximately 40–50 µm), highlighting the need for further optimisation of the deposition process.

Overall, the adhesion study demonstrated that aerosol jet printing can successfully produce conductive patterns on UHMWPE and that the printed traces respond to abrasive wear. Among the investigated solutions, the combination of a TPU primer and H20E currently provides the most encouraging preliminary results. However, several aspects still require further investigation before implant-level integration, including thickness control, deposition repeatability on curved surfaces, long-term tribological stability, electrical continuity during abrasion, and the selection of conductive materials compatible with long-term exposure to the physiological environment.

At the current stage of the project, the direct scratch sensor should therefore be regarded as a low-TRL sensing approach that has successfully demonstrated proof of concept but still requires significant process refinement before validation in integrated implant prototypes.

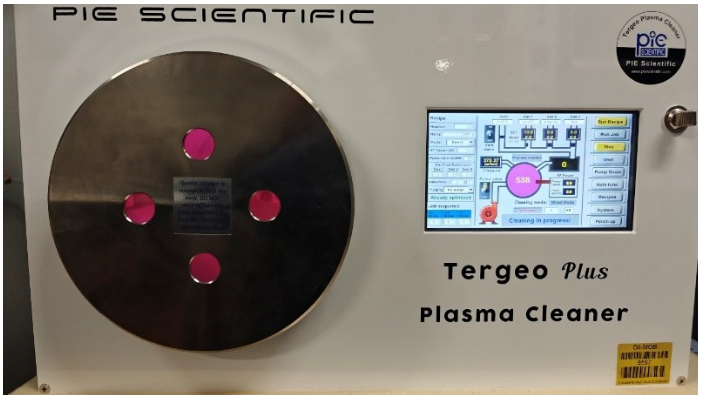

Plasma cleaning setup

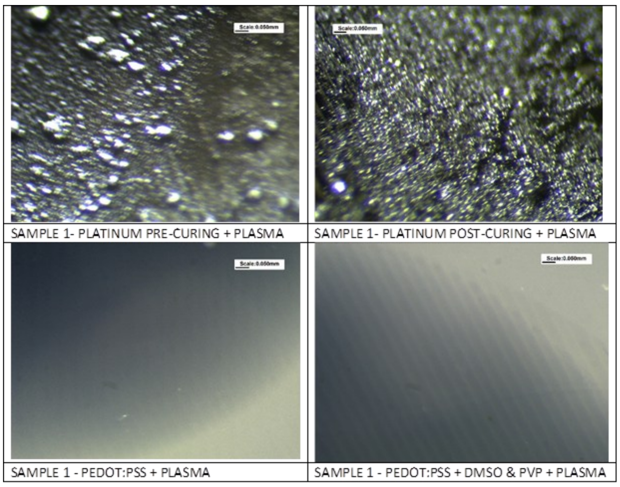

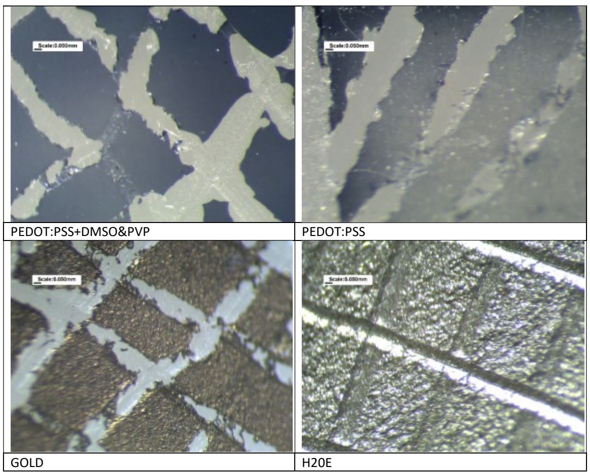

Plasma: Pt and PEDOT microscope views

Plasma peel-off results

Figure 26. Adhesion-promotion campaign: plasma and peel-off results.

Funded by:

Schweizerische Eidgenossenschaft
Confédération suisse
Confederazione Svizzera
Confederaziun svizra

Funded by the European Union

The SmILE project has received funding from the European Union's Horizon Europe programme and the Swiss State Secretariat for Education, Research and Innovation (SERI).

5.4 Indirect force + IMU sensing route

The second route monitors the mechanical causes of wear rather than surface material loss itself. Total knee implants may experience loads up to approximately three times body weight during daily activities, with non-uniform medial-lateral load distribution and moving contact points [1]. These variables interact with sliding, rolling and gliding at the metal-UHMWPE interface and are relevant drivers of wear [2].

The proposed system combines an IMU for joint kinematics with a force-sensing layer embedded between the polyethylene insert and the tibial tray. Kinematics alone can identify abnormal motion but cannot determine whether motion occurs under damaging load. Force alone can identify load distribution but lacks flexion/rotation context. Their combination enables a clinically interpretable mechanical state of the tibiofemoral joint.

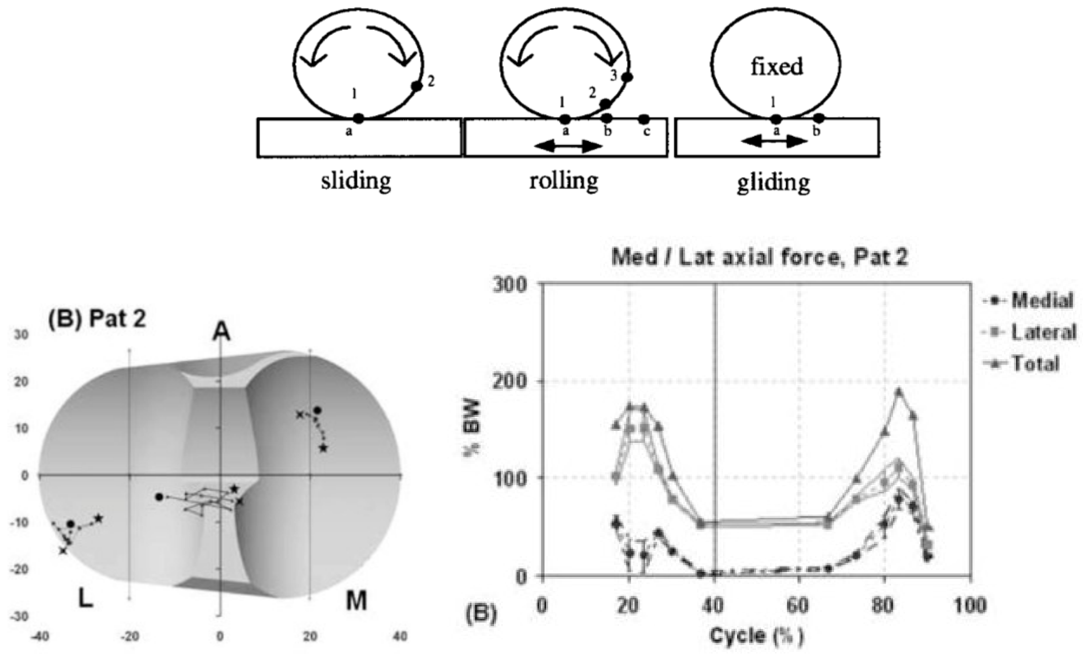

Figure 27. Literature-motivated wear mechanisms and examples of force/CoP variability.

Measurable parameter	Clinical / technical relevance	Sensors
Total axial force	Wear and loosening risk; direct with 1-2+ sensors if area coverage is adequate.	1-2
Medial-lateral load balance	Alignment and wear-distribution marker; compares load under the two condyles.	2-6
Condylar lift-off	Instability and asymmetric wear; detected when one condyle is unloaded.	2+
A-P contact migration / CoP shift	Proxy for femoral rollback and edge loading; requires spatial distribution.	6
Load rate and impacts	Fatigue and bone-remodelling stimulus; requires sufficient sampling and sensor time response.	1-6 + IMU
Cycle-to-cycle symmetry	Possible indicator of settling, creep or progressive soft-tissue imbalance.	1-6

Funded by:

Schweizerische Eidgenossenschaft
Confédération suisse
Confederazione Svizzera
Confederaziun svizra

Funded by the European Union

The SmILE project has received funding from the European Union's Horizon Europe programme and the Swiss State Secretariat for Education, Research and Innovation (SERI).

5.4.1 Force-sensing implementation and ASIC compatibility

Force-sensing resistors were selected as the most practical near-term force layer. Their resistance decreases under compressive pressure through a percolation mechanism in a polymer composite. For knee applications, the decisive specification is pressure range: local insert pressures may reach tens of MPa in literature and finite-element studies, so low-range FSRs are useful for feasibility but high-range commercial sensors or custom FSRs are required for final integration.

Sensor option	Role in the project
Tekscan A-401	High-TRL, single large-area element; candidate for one sensor per condyle or total-force measurement.
Tekscan A-301	High-TRL smaller element; candidate for multi-sensor arrays with at least three sensors per condyle.
Ohmite FSR05	Low-cost preliminary sensor used for feasibility tests, calibration and CoP demonstration.
Custom FSR / array	Potential final route if geometry, saturation pressure, thickness or ASIC interface need tailoring.

ASIC integration must use available resistive readout channels. The strain-gauge channel can be adapted with a resistive network, while the temperature channel appears particularly suitable because it is already designed for a broad resistance range. A series resistor can keep the FSR plus auxiliary resistance within front-end specifications. The remaining design questions are the number of available channels, flex-PCB space for networks, exact front-end range and achievable data rate, with at least 100 Hz desirable for impact/loading-rate information.

Funded by:

Schweizerische Eidgenossenschaft
Confédération suisse
Confederazione Svizzera
Confederaziun svizra

Funded by the European Union

The SmILE project has received funding from the European Union's Horizon Europe programme and the Swiss State Secretariat for Education, Research and Innovation (SERI).

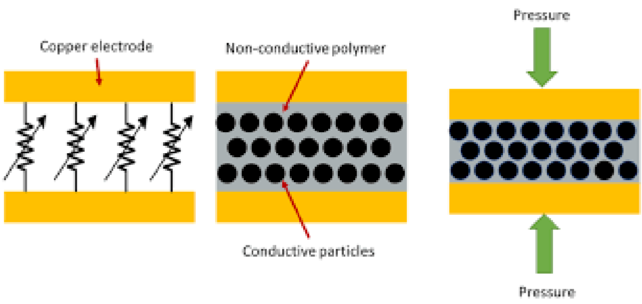

FSR working principle

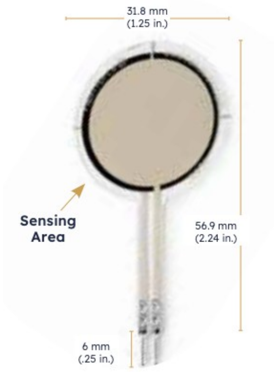

Tekscan A-401 option

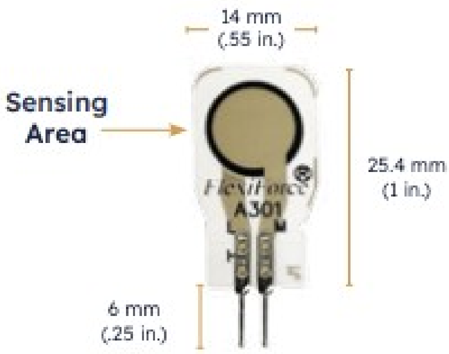

Tekscan A-301 option

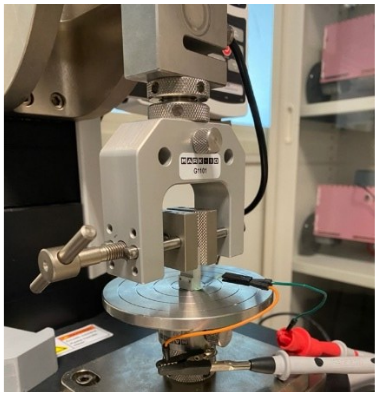

UTM calibration setup

Figure 28. FSR working principle, high-TRL Tekscan options and the preliminary calibration setup.

Design point	**Implementation note**
Minimum useful array	Two sensors, one per condyle, for total force split and condylar lift-off detection.
Preferred array	Six sensors or more, at least three per condyle, for medial-lateral balance and A-P CoP migration.
Mechanical integration	Sensors placed on the tibial tray and covered with a thin compliant layer or epoxy/silicone to transmit pressure while protecting the sensor.

5.4.2 Preliminary FSR calibration and TKA tests

Preliminary tests used Ohmite FSR05 sensors to assess feasibility. A Mark-10 ESM1500 UTM applied cyclic compression while a Keysight 6.5-digit DMM measured resistance. The calibration imposed 100 loading cycles at approximately 30 MPa using an indenter with the same size as the sensor. A two-term exponential model fitted the resistance-pressure curve with R2 = 0.99 and RMSE = 83.76 ohm.

A second test placed five FSR05 sensors between the polyethylene tibial insert and the titanium tibial tray in a TKA assembly. The UTM compressed the femoral component onto the insert/tray stack up to about 3.8 kN, representative of physiological tibiofemoral forces during daily activities. Resistance signals were filtered for dropouts and open-circuit values, and the calibrated pressure was recovered through lookup-table inversion of the fitted model.

Funded by:

Schweizerische Eidgenossenschaft
Confédération suisse
Confederazione Svizzera
Confederaziun svizra

Funded by
the European Union

The SmILE project has received funding from the European Union's Horizon Europe programme and the Swiss State Secretariat for Education, Research and Innovation (SERI).

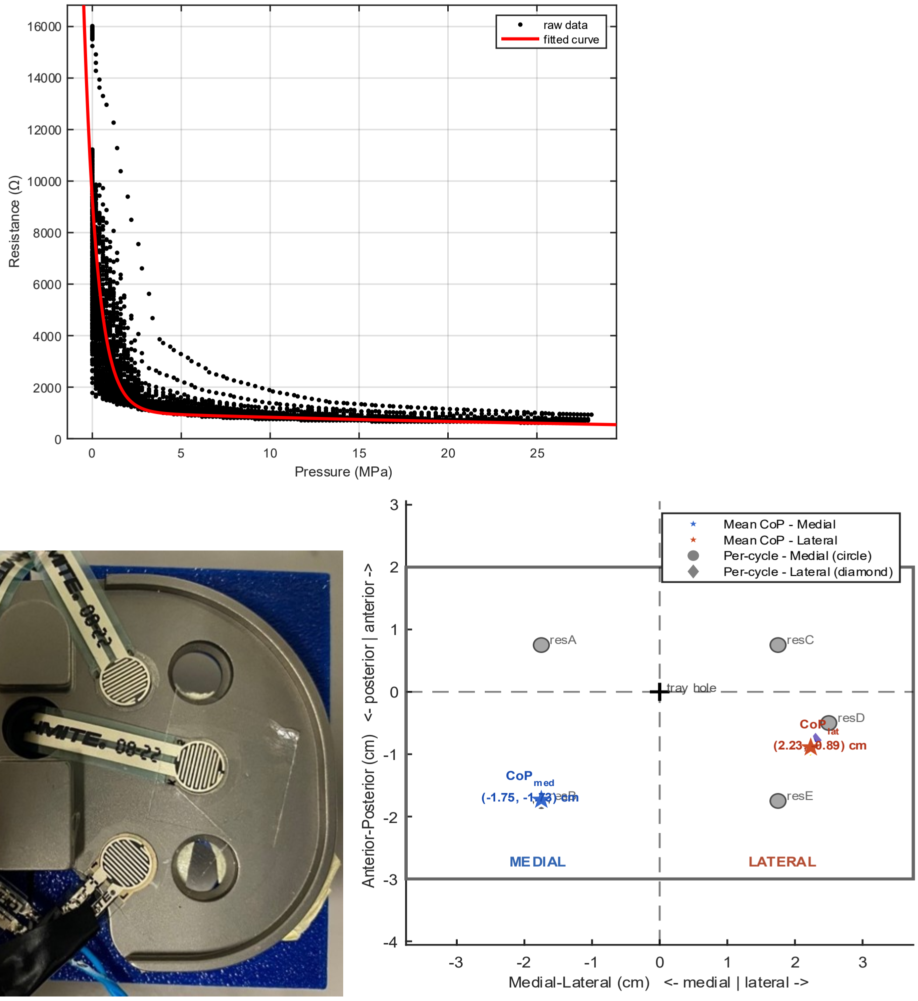

Figure 29. Calibration, five-FSR prototype, centre-of-pressure output.

Result	Interpretation
Calibration	Exponential pressure-resistance relation fitted successfully; confirms need for individual or batch calibration before quantitative use.
Pressure distribution	Five sensors provided sensor-wise peak-pressure estimates and repeatability over repeated compression cycles.
Centre of pressure	CoP was computed as the force-weighted centroid; robust to uniform gain error but sensitive to inter-sensor variability.
Limitations	FSR05 is a feasibility sensor, not final-range hardware; contact area, encapsulation, hysteresis and long-term drift must be quantified.

The tests demonstrate that a force-sensing layer can provide the data products required by the indirect route: total load trends, spatial distribution and CoP. Final validation must repeat the same logic with sensors matched to the target pressure range and integrated in a protected implant-compatible stack.

5.4.3 Official sensors calibration and preliminary TKA tests

The validation repeated the same logic with Tekscan® A301sensors, which pressure range matches with implant's behavior. The calibration was performed using a different approach: a stair of increasing pressure setpoints was applied to the sensor, with each value hold for 1 minute approximately. Resistance values measured with DMM were then analyzed in conductance. Each conductance value

Funded by:

Schweizerische Eidgenossenschaft
Confédération suisse
Confederazione Svizzera
Confederaziun svizra

Funded by the European Union

The SmILE project has received funding from the European Union's Horizon Europe programme and the Swiss State Secretariat for Education, Research and Innovation (SERI).

was taken by averaging the last 100 samples at plateau (~20 seconds). The result was a linear relationship between conductance and applied pressure from the UTM, as illustrated in Figure 30.

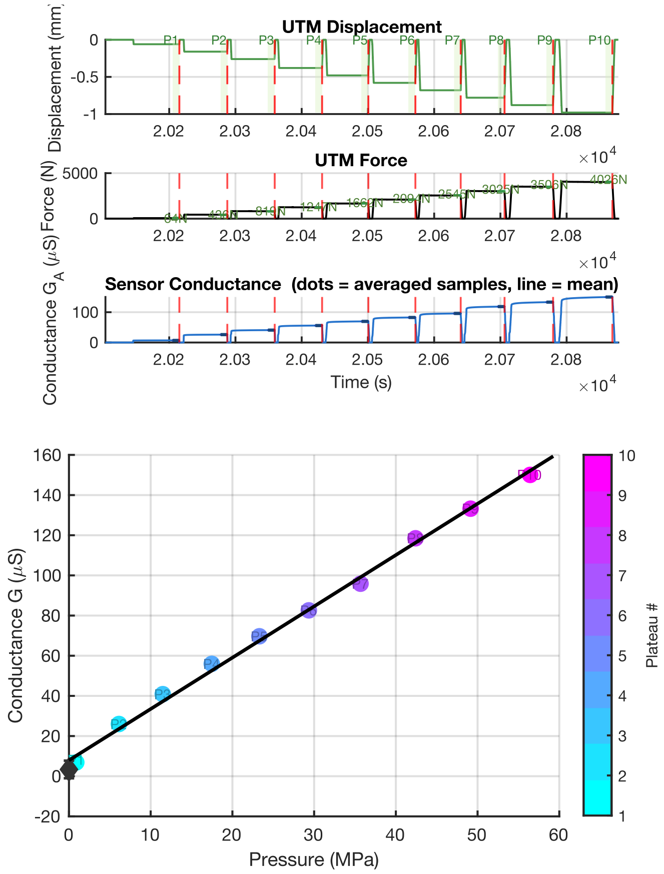

Figure 30. A301 calibration results: conductance vs pressure applied

In a second test, two A301 sensors were placed at the interface between inlay and tibia tray, one under each condyle. Using the UTM, axial forces were applied by the femoral component onto the inlay/tray stack. A history of sets 10 cycles of increasing by each set was applied: fist at 500 N, 1 kN, 2 kN and 3kN. Pressure was calculated inverting the calibration model. Results in Figure 31, show that sensors measure a balanced pressure distribution under each condyle as the setup would suggest. The maximum pressure is approximately 25 MPa. Sensitivity at low loads is to be improved; the cause is to be addressed to sensor contacts thickness produced in this prototype.

Funded by:

Schweizerische Eidgenossenschaft
Confédération suisse
Confederazione Svizzera
Confederaziun svizra

Funded by
the European Union

The SmILE project has received funding from the European Union's Horizon Europe programme and the Swiss State Secretariat for Education, Research and Innovation (SERI).

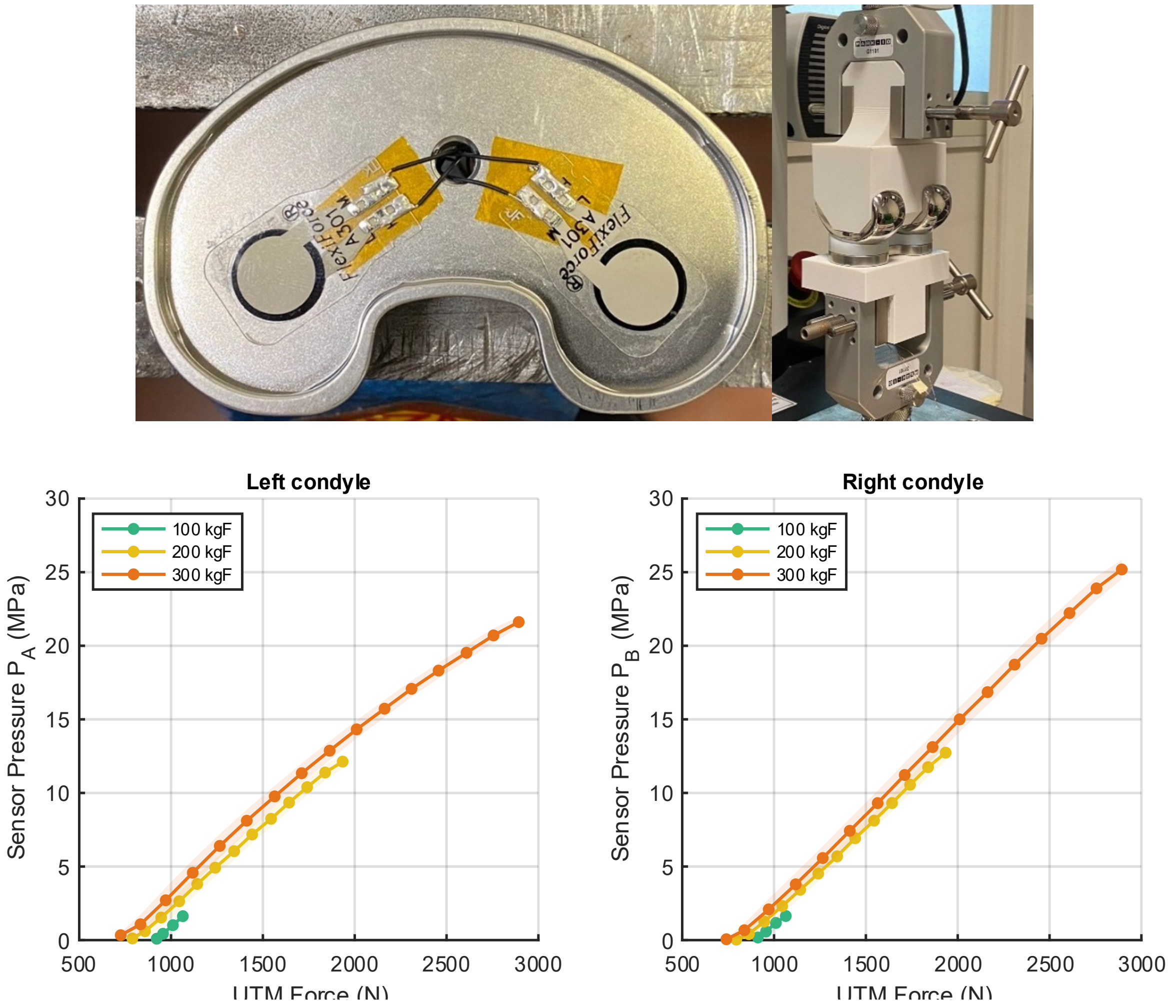

Figure 31. FSR positioning on tibia tray, test setup and TKA test results

5.5 Conclusions and next steps

The current activities identified two promising sensing strategies with different levels of technological maturity. The direct printed scratch sensor demonstrated its capability to detect local surface degradation, as confirmed by abrasion-induced damage to the conductive traces. However, further development is required to improve adhesion on UHMWPE, reduce and control the deposited layer thickness, and identify suitable conductive materials that can remain safely exposed during operation. Future work will therefore focus on refining the deposition process, improving repeatability on curved implant surfaces, and evaluating the electrical response during abrasion together with the effects of different surface pretreatments and adhesion promoters.

The indirect sensing approach, based on the combination of force sensing resistors (FSRs) and inertial measurements, appears closer to practical implementation and integration with the project ASIC. The next development phase will address sensor packaging and fixation on the insert, protective encapsulation using silicone or epoxy materials, calibration of the sensing channels, and verification of the electrical interface. Dedicated durability tests, including at least 10^4 loading cycles under representative physiological conditions, will be performed to assess long-term mechanical and electrical stability. The acquired data will be used to derive clinically relevant parameters, including total joint force, medial-lateral load distribution, lift-off events, anterior-posterior centre-of-pressure migration, loading rate and gait cycle symmetry. These measurements will also provide the input variables for the computational wear estimation models developed in the subsequent validation tasks.

Funded by:

Schweizerische Eidgenossenschaft
Confédération suisse
Confederazione Svizzera
Confederaziun svizra

Funded by the European Union

The SmILE project has received funding from the European Union's Horizon Europe programme and the Swiss State Secretariat for Education, Research and Innovation (SERI).

Considering the current maturity of both approaches, the FSR + IMU solution is recommended as the primary sensing strategy for short-term system integration and quantitative load monitoring. In parallel, development of the direct scratch sensor should continue as a lower-TRL activity, with progression toward system integration depending on the successful demonstration of reliable adhesion, stable electrical response during abrasion, and negligible influence on the tribological behaviour of the implant.

Funded by:

Schweizerische Eidgenossenschaft
Confédération suisse
Confederazione Svizzera
Confederaziun svizra

Funded by
the European Union

The SmILE project has received funding from the European Union's Horizon Europe programme and the Swiss State Secretariat for Education, Research and Innovation (SERI).

6 Drug release system (mesoporous silica particles)

6.1 Introduction

Work package 4.2.6 addresses the chemical functionalization of SmILE implant supports with a therapeutic payload through an electro-labile linker. The aim is to create a surface-bound drug reservoir that remains stable under non-stimulated conditions and can be released locally when the implant electronics apply an electrical stimulus.

For the current implementation, dexamethasone was selected as the model therapeutic molecule because its hydroxyl functionality enables derivatization while preserving a compact molecular structure suitable for surface anchoring. The synthetic work focused on preparing a dexamethasone-linker-anchor intermediate compatible with subsequent immobilization on the target supports.

The route developed to date establishes the key chemical steps required for surface attachment: linker activation, coupling to dexamethasone, introduction or preservation of the surface anchoring group, and purification/characterization of the final conjugate prior to support functionalization. The deliverable, therefore, documents the design criteria, the synthetic pathway, the preliminary support-functionalization workflow, and the remaining validation steps.

The next actions are to complete quantitative characterization of the intermediate and functionalized supports, determine surface loading, verify stability in relevant media, and demonstrate electrically triggered release under controlled stimulation conditions.

6.2 Scope and design rationale

The SmILE concept integrates sensing, actuation, and local therapeutic response within smart implantable systems. In this context, the functionalization work package provides the chemical interface between the support material and a releasable drug. The specific objective is not only to attach the molecule, but to attach it through a bond or linker architecture that can respond to an externally applied electrical signal.

The supports are considered the implant-facing substrates provided within the consortium. Since the final support chemistry may vary depending on the selected implant component and coating, the route has been designed around a modular conjugate: one end carries dexamethasone, the central unit contains the electro-labile motif, and the other end contains the anchoring functionality required for immobilization.

Design element	Selected approach	Role in WP4.2.6
Therapeutic payload	Dexamethasone (DEX)	Compact drug molecule with derivatizable hydroxyl group; relevant for local modulation of inflammation around implant interfaces.
Responsive element	Electro-labile linker	Designed to remain stable during handling and incubation, while undergoing cleavage or bond scission upon electrical stimulation.
Surface anchoring group	Support-compatible terminal function	Allows covalent or high-affinity immobilization on the selected SmILE supports after surface activation.
Support interface	Implant support/coating	Provides the solid phase that will carry the electro-responsive drug reservoir.
Readout	Released DEX or proxy molecule	Quantification by HPLC/UV, LC-MS, or another agreed analytical method before and after stimulation.

Funded by:

Schweizerische Eidgenossenschaft
Confédération suisse
Confederazione Svizzera
Confederaziun svizra

Funded by the European Union

The SmILE project has received funding from the European Union's Horizon Europe programme and the Swiss State Secretariat for Education, Research and Innovation (SERI).

6.2.1 Key implementation constraints

Constraint	Implication
Implant compatibility	The chemistry must avoid harsh residual reagents and must be compatible with final cleaning/sterilization strategies.
Electrical actuation	The linker should respond under potentials compatible with the electronic module and without damaging the support.
Surface stability	The drug conjugate should withstand washing and non-stimulated incubation without premature release.
Analytical traceability	Each step requires structural or surface evidence to support progression to the next stage.
Scalability	The route should remain executable on small support pieces and later on representative implant geometries.

6.3 Electro-labile linker and surface-anchoring strategy

The functionalization strategy follows a modular design in which the electro-labile linker is placed between dexamethasone and the surface anchoring group. This configuration ensures that the drug is retained at the support interface until the electrical stimulus promotes cleavage of the labile bond. The final molecular architecture can be summarized as:

Support - anchoring group - electro-labile linker - dexamethasone

The exact linker identity, anchoring group, and cleavage mechanism should be completed with the final consortium-approved nomenclature. The present draft keeps the wording intentionally general so that the document remains valid for the final support chemistry while still documenting the progress of the synthetic route (Figure 32).

Route option	Description	Advantage	Risk
Anchoring-first route	The support is first functionalized with the linker, then coupled to dexamethasone.	Fewer soluble intermediates; direct surface construction.	Surface reactions can be harder to quantify and purify.
Drug-conjugate route	The DEX-linker-anchor conjugate is synthesized and purified in solution, then immobilized on the support.	Better structural control before immobilization; easier NMR/HPLC characterization.	Requires the final conjugate to remain soluble and reactive enough for support attachment.
Hybrid route	A partially protected linker is attached to DEX, then activated for support coupling.	Balances solution-phase control and surface flexibility.	Requires careful protecting-group and activation sequence.

For the current work, the drug-conjugate route is recommended as the primary reporting path because it allows the chemical identity of the dexamethasone-linker-anchor intermediate to be demonstrated before surface immobilization.

Funded by:

Schweizerische Eidgenossenschaft
Confédération suisse
Confederazione Svizzera
Confederaziun svizra

Funded by the European Union

The SmILE project has received funding from the European Union's Horizon Europe programme and the Swiss State Secretariat for Education, Research and Innovation (SERI).

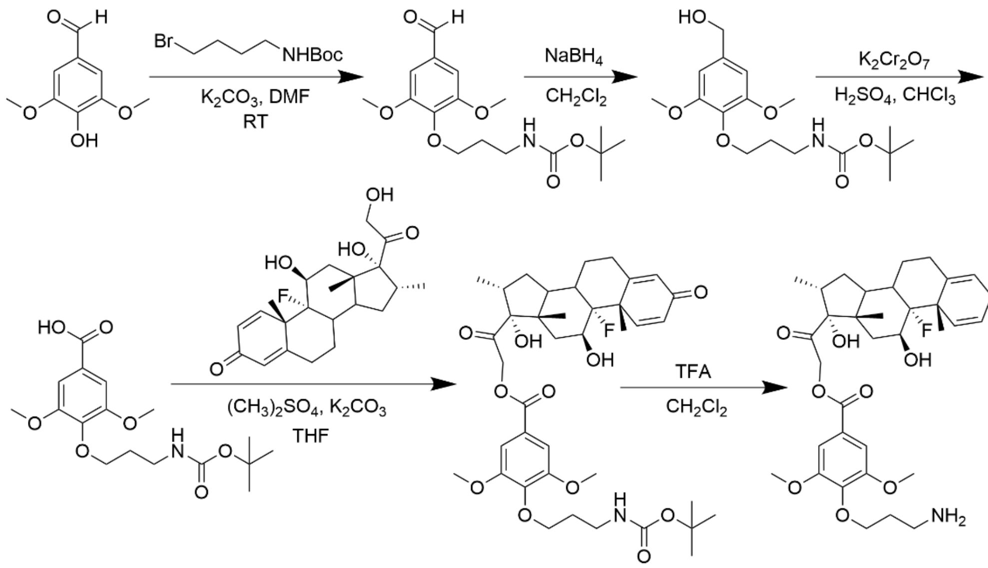

Figure 32. Electro-responsive functionalization concept and proposed molecular architecture.

6.4 Synthetic route towards dexamethasone-linker-anchor conjugate

The synthetic route performed within WP4.2.6 aimed to prepare a dexamethasone derivative containing both the electro-labile linker and the terminal anchoring function needed for support immobilization. The route is reported below as an editable scheme so that the exact reagents, yields, and compound codes can be inserted once the final laboratory notebook entries are consolidated.

Step	Purpose	Starting material(s)	Product	Conditions to complete	Evidence
1	Preparation / activation of electro-labile linker	Electro-labile linker precursor + activating reagent	Activated linker intermediate	[Solvent, temperature, time, atmosphere]	[Yield / conversion]
2	Coupling to dexamethasone	Dexamethasone + activated linker	DEX-linker intermediate	[Base/catalyst, solvent, purification]	[Yield / purity]
3	Introduction or deprotection of anchoring group	DEX-linker intermediate	DEX-linker-anchor conjugate	[Deprotection or coupling conditions]	[Yield / purity]
4	Purification and analytical confirmation	Crude conjugate	Purified DEX-linker-anchor	Chromatography / precipitation / dialysis as applicable	[HPLC purity, NMR, MS]
5	Support functionalization	Activated support + conjugate	DEX-functionalized support	Incubation, washing and drying conditions	[Surface loading]

The key synthetic milestone for this deliverable is the formation of the DEX-linker-anchor conjugate. Evidence should include at least one soluble-phase analytical method, ideally ^{1}H NMR and LC-MS or HPLC, plus chromatographic purity if available. Surface immobilization should then be supported by techniques sensitive to the support interface, such as XPS, FTIR/ATR, contact-angle measurements, fluorescence/UV quantification if a chromophore is present, and release analysis after cleavage.

Funded by:

Schweizerische Eidgenossenschaft
Confédération suisse
Confederazione Svizzera
Confederaziun svizra

Funded by the European Union

The SmILE project has received funding from the European Union's Horizon Europe programme and the Swiss State Secretariat for Education, Research and Innovation (SERI).

6.4.1 Preliminary interpretation of the synthetic work

Status item	Concise conclusion
Completed	Synthetic route for introducing the electro-labile linker between dexamethasone and the anchoring group has been carried out.
To complete	Insert compound codes, isolated amounts, yields, reaction monitoring and purification details.
Main evidence required	NMR assignment of diagnostic linker/DEX signals; MS confirmation of expected mass; HPLC purity or chromatographic profile.
Critical point	Confirm that the functional group used for dexamethasone derivatization does not prevent the intended release or analytical detection of DEX.
Deliverable interpretation	The route establishes the feasibility of generating an electro-responsive DEX derivative for subsequent support immobilization.

6.5 Functionalization of implant supports

The functionalization workflow translates the soluble DEX-linker-anchor conjugate onto the selected SmILE supports. The process is divided into support pretreatment, surface activation, conjugate immobilization, washing, and post-functionalization characterization. The exact protocol should be adapted to the chemistry of the final support surface, but the general sequence remains applicable across representative implant support pieces.

Stage	Operation	Purpose	Recommended evidence
1. Support pretreatment	Cleaning and surface activation	Remove organic residues and generate reactive surface groups.	Solvent wash, plasma, chemical activation or consortium-approved pretreatment.
2. Immobilization	Incubation with DEX-linker-anchor conjugate	Attach the electro-responsive drug conjugate to the support.	Concentration, solvent, pH, time, and temperature to be specified.
3. Washing	Sequential washing steps	Remove non-covalently adsorbed drug and residual reagents.	Monitor wash fractions for DEX signal.
4. Drying / conditioning	Controlled drying or equilibration	Stabilize the functionalized surface before testing.	Avoid conditions that trigger premature cleavage.
5. Baseline characterization	Surface and release controls	Confirm attachment and establish non-stimulated release background.	XPS/FTIR/contact angle/loading assay.

6.5.1 Controls required for support validation

Control	Purpose
Bare support	Confirms that the support itself does not release interfering species in the analytical method.
Support + linker without DEX	Distinguishes linker/surface signals from drug-specific signals.
Support + physically adsorbed DEX	Assesses the contribution of non-covalent adsorption and washing efficiency.
Functionalized support without electrical stimulus	Measures passive release / hydrolytic leakage under storage or incubation.
Functionalized support with electrical stimulus	Demonstrates triggered release and defines the stimulation window.

Funded by:

Schweizerische Eidgenossenschaft
Confédération suisse
Confederazione Svizzera
Confederaziun svizra

Funded by the European Union

The SmILE project has received funding from the European Union's Horizon Europe programme and the Swiss State Secretariat for Education, Research and Innovation (SERI).

6.6 Characterization and release validation plan

The validation plan should demonstrate three linked outcomes: the conjugate was synthesized, the conjugate was immobilized on the support, and the immobilized drug can be released preferentially after electrical stimulation. The table below summarizes the proposed evidence package.

Validation target	Recommended method(s)	Acceptance evidence
Soluble conjugate identity	$^{1}H/^{13}C$ NMR, LC-MS or HRMS, HPLC	Expected mass, diagnostic DEX and linker signals; acceptable purity.
Support functionalization	XPS, FTIR/ATR, contact angle, elemental analysis if applicable	Appearance of linker/drug-related surface signals compared with bare support.
Drug loading	UV/HPLC quantification by depletion, extraction or release	Estimated amount of DEX attached per support area or mass.
Passive stability	Incubation in PBS or a relevant medium without stimulus	Low background release over the planned test window.
Electro-triggered release	Controlled potential/current stimulation + HPLC/UV analysis	Higher DEX release after stimulation compared with no-stimulus control.
Post-release surface status	XPS/FTIR/contact angle and microscopy	Evidence of cleavage/reduction in drug-related surface signal without severe support damage.

6.7 Proposed electrically triggered release experiment

Functionalized support should be placed in a defined volume of release medium and connected to the electrical stimulation setup. Baseline aliquots should be collected before stimulation to quantify passive release. The electrical stimulus should then be applied under a defined potential/current, duration and number of pulses. Aliquots collected after stimulation should be analysed using the selected DEX quantification method and compared with unstimulated controls processed in parallel.

Parameter	Draft setting	Comment
Medium	PBS or consortium-agreed physiological medium	Record pH, ionic strength and volume.
Electrical stimulus	[Potential/current], [duration], [pulse profile]	Must be compatible with support and electronic module.
Sampling	Pre-stimulus, immediately post-stimulus, delayed time points	Allows kinetic profile and background correction.
Quantification	HPLC/UV or LC-MS	Use calibration curve of DEX and relevant conjugate fragments.
Controls	Bare support, adsorbed DEX control, no-stimulus functionalized support	Required to demonstrate triggered rather than passive release.

Funded by:

Schweizerische Eidgenossenschaft
Confédération suisse
Confederazione Svizzera
Confederaziun svizra

Funded by the European Union

The SmILE project has received funding from the European Union's Horizon Europe programme and the Swiss State Secretariat for Education, Research and Innovation (SERI).

6.8 Conclusions and next actions

The work performed so far supports the feasibility of the chemical route for anchoring dexamethasone to SmILE supports through an electro-labile linker. The present maturity is suitable for a deliverable reporting synthetic progress and the planned validation route, while additional data are required before claiming a fully validated electrically triggered release system.

Status item	Concise conclusion
Validated so far	A synthetic route towards dexamethasone anchoring through an electro-labile linker has been carried out.
Partially completed	Support functionalization workflow is defined; final support-specific conditions and loading values must be inserted.
Not yet fully solved	Quantitative release under electrical stimulation; long-term stability; final biocompatibility/sterilization compatibility.
Main technical risk	Premature hydrolysis or insufficient cleavage selectivity between passive incubation and stimulated release.
Mitigation	Compare no-stimulus and stimulated samples, optimize linker chemistry and stimulation window, and quantify all wash/release fractions.

Action area	Next step	Timing
Synthetic documentation	Insert final reaction scheme, compound codes, yields, purification and analytical spectra.	Immediate
Support functionalization	Finalize surface pretreatment and immobilization protocol for the selected support material.	Short term
Loading quantification	Determine DEX loading per surface area and washing efficiency.	Short term
Stability test	Measure passive release in the relevant medium over the agreed time window.	Short term
Electrical release test	Apply controlled stimulus and quantify released DEX versus unstimulated controls.	Next validation step
Integration feedback	Align stimulation conditions with the electronic/actuator constraints of WP4.	Parallel

WP4.2.6 has advanced the chemical basis for electro-responsive drug functionalization of SmILE implant supports. Dexamethasone was selected as the therapeutic payload, and a synthetic route has been performed to enable its anchoring through an electro-labile linker. This route provides the modular chemical platform required to connect the drug, the responsive cleavage unit, and the support-compatible anchoring group.

The deliverable confirms that the task has moved from design rationale to synthetic implementation. The main remaining work is analytical consolidation: completing the structural evidence for the soluble conjugate, confirming successful immobilization on the support, quantifying surface loading, and demonstrating increased dexamethasone release under electrical stimulation relative to non-stimulated controls.

For subsequent SmILE integration, the functionalized support should be evaluated alongside the electronic stimulation parameters to identify a release window that is chemically efficient, electronically feasible, and compatible with implant-relevant conditions.

Funded by:

Schweizerische Eidgenossenschaft
Confédération suisse
Confederazione Svizzera
Confederaziun svizra

Funded by the European Union

The SmILE project has received funding from the European Union's Horizon Europe programme and the Swiss State Secretariat for Education, Research and Innovation (SERI).

7 Smart activity monitoring (IMU + preprocessing)

7.1 Summary

Based on the partners' requirements, the sensor types and models were selected. Based on the basic sensing principles, the algorithmic possibilities were evaluated to derive the required parameters.
One of the key required parameters is the angle of the joint that the endoprosthesis replaces or mounts to. For this, different sensing principles were evaluated. Based on constraints given by the application and medical certification, as well as use-case-specific requirements, a primary sensing principle was determined. A test setup was built to benchmark the solution. This setup was used to establish a baseline using currently commercially available sensor angle functionality. To meet the requirements of the use case, a new algorithm was initiated that is better suited to provide the joint angle in dynamic cases.
The solution derived based on two IMUs requires further evaluation, but is deemed a good fit for the developed smart implant device, especially due to the technology readiness of the basic sensor and the initial results. However, since it cannot fulfil the requirement of detecting translational movements with the required resolution and accuracy, another solution based on a different sensing principle will be evaluated at a research level.

7.2 Introduction

Multiple features were requested by the partners in WP5 for the different implants. Commonly requested functionalities included smart features such as step detection and counting, as well as range-of-motion and subsequent angle detection for joint endoprosthesis devices.
BST focused on comparing existing algorithms for calculating joint angles based on quaternions derived from IMU data. In addition, BST analysed the results of a newly initiated algorithm intended to improve the performance of specific joint angle detection.
As no experimental data from the final implant platform or clinical trials was available at this stage, preliminary investigations were conducted by UROS using a representative experimental setup. The purpose of these investigations was to identify potential limitations and challenges associated with IMU-based angular estimation for defined rotational axes.

7.3 Bosch Sensortec Contribution

7.3.1 Movement Features

From WP5, the requirement was placed on the electronics to detect steps and any/significant motion events. Significant motion events are especially relevant for waking up the electronics. Furthermore, step detection is crucial for acquiring additional data at the right time, for example load events while the person is applying force to the device by taking a step. In addition, activity can also be tracked in this way and can be used as a healing parameter.
To determine these parameters and provide the option to implement algorithms such as fall/shock detection later, a smart IMU, namely the BHI380, was chosen. This IMU features a gyroscope, accelerometer, and microcontroller in a standard-sized IMU package.
Therefore, algorithms can run directly on the IMU without the need to wake up the host MCU, thereby saving power. Functions such as significant motion and step detection are implemented on the IMU itself, using only the accelerometer in a power-optimized manner, and can run with power draws in the order of some tens of µA.

7.3.2 Angle Determination Sensing Principles

To determine the movement range and evaluate the healing process, as well as the health of the implant, it is crucial to determine the angle of the joint after the implant has been positioned inside the body. For this, multiple sensor principles can be used. Depending on the implant, the partners are interested in obtaining rotational and translational movement data.

Funded by:

Schweizerische Eidgenossenschaft
Confédération suisse
Confederazione Svizzera
Confederaziun svizra

Funded by
the European Union

The SmILE project has received funding from the European Union's Horizon Europe programme and the Swiss State Secretariat for Education, Research and Innovation (SERI).

Magnetometer-based solution

The first considered solution is based on a magnetometer in the active part of the implant and a magnet in the other part of the implant. This solution would have had the benefit of requiring only one active implant electronic in one part of the implant, while still being able to detect three-dimensional rotational joint angles. In the proposed solution, a Tunnel Magneto Resistive (TMR) sensor would have been applied on one side of the implant. This side would also house the other sensors and electronics. The other side of the implant, which moves relative to the first, would have been entirely passive, with a permanent magnet or magnetic structure disposed in it that can be sensed by the TMR sensor. Based on the magnetic field strength measured across its three axes, the TMR sensor would therefore be able to determine how the magnet is oriented and, consequently, the relative angle between the two implant parts. This system could have been extended to multiple TMR sensors and magnets to gain information regarding the translational positions of the implant parts forming the joint. Since magnetic encoders are state of the art and initial tests verified the feasibility of detecting the orientation of the magnet, we have high functional confidence in this solution. However, the solution was not further developed due to concerns regarding the certification effort for endoprosthesis parts including magnets. Furthermore, the requirement for MRI compliance made this solution infeasible due to the high magnetic field strengths expected during the MRI process. The expected field strengths greater than 5 Tesla far exceed the maximum range of currently available TMR sensors with the required resolution and sensitivity necessary to achieve the required joint angle and position functionality. When exceeding the range this far, it was concluded in the evaluation that the TMR bridge itself would suffer irreversible damage, which was not acceptable for the solution.

Multi-IMU-based solution

The other proposed solution was to leverage the IMU, which had already been selected for power saving and smart features such as step and significant motion detection. Since it features an MCU, additional algorithms such as Game Rotation Vector calculation from the IMU data can run on the device itself.

For angle detection, a single IMU can be used to reference the orientation of the IMU and therefore the implant part relative to the Earth's gravitational vector. Since, depending on the pose, the human body can be positioned arbitrarily relative to the Earth's gravitational vector, ambiguities and uncertainties arise that were not acceptable. Therefore, it was proposed to apply a second implant electronic on the second implant part to determine the joint angles without ambiguity relative to each other based on the two IMU values. This solution was chosen for joint angle detection with the developed electronics in the endoprosthesis. As an alternative to a second implant electronic, a local wearable could also be used on the outside of the body part whenever joint angle data should be recorded. However, this is less optimal regarding user experience. Therefore, the project aims to integrate two separate electronics equipped with one IMU each at the two different joint-forming parts for all use cases this is feasible for.

It was accepted that translational movements, especially in the knee use case, in the specified range (5 mm) cannot be sensed by this solution. However, for joint angle calculation, this solution best fits the timeline for the implant electronics, since there is high confidence in achieving the required angular resolution for the use cases. This is especially true because a basis already exists in the form of commercially available solutions for calculating Game Rotation Vectors (GRV) inside the IMU. However, this algorithm is optimized for different devices and use cases. It is not optimized to calculate relative angles between multiple IMUs in dynamic scenarios, such as swinging the leg while walking.

To determine the performance of the developed solution, a test setup was implemented based on a robotic arm, providing ground-truth joint angle data from its built-in encoders. This allows us to benchmark the commercially available solution adapted to the joint angle detection use case. To capture the IMU data, the smart connected sensor devices from BST were used. The same devices

Funded by:

Schweizerische Eidgenossenschaft
Confédération suisse
Confederazione Svizzera
Confederaziun svizra

Funded by the European Union

The SmILE project has received funding from the European Union's Horizon Europe programme and the Swiss State Secretariat for Education, Research and Innovation (SERI).

were also made available to multiple partners for movement analysis studies. Furthermore, they are used as well as a platform to enable development of the data stream for the later electronics.

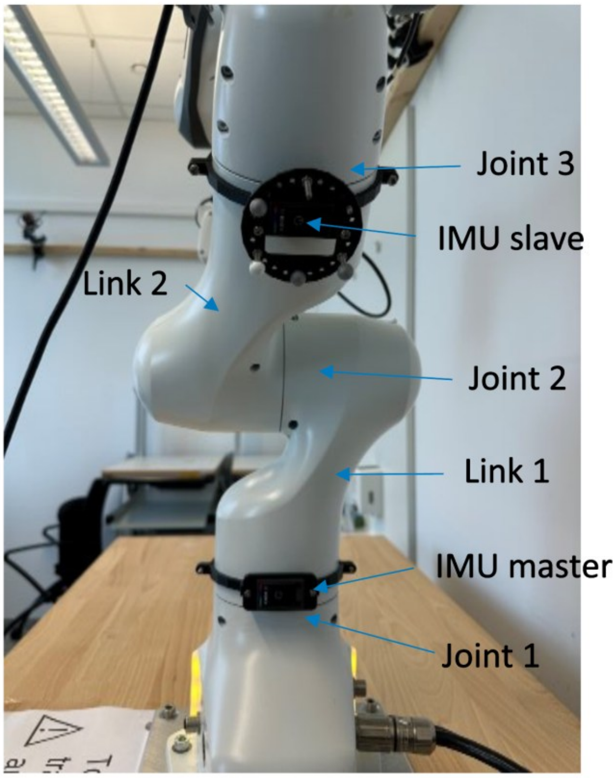

Figure 33. Robotic arm with mounted smart connected sensor devices, which include the IMUs and stream the data to the host.

Two IMUs were mounted to a robot arm. In the tests so far, the two IMUs are mounted on links at both ends of a joint. This is done to simplify the problem in the initial development phase. For the next step, multiple joints will be incorporated between the IMUs. In this way, a more multidimensional rotation can be realized, which more closely resembles, for example, the human knee with multiple rotational degrees of freedom. The data was streamed to the host PC via Bluetooth. For time synchronization of the sensor and robotic system, a defined movement pattern was used to align both time bases.

7.4 University of Rostock Contribution

7.4.1 Motivation

The objective of this subtask within Work Package 4 was to develop and evaluate energy-efficient active monitoring algorithms for assessing patients' rehabilitation status using smart implants. In addition, monitoring the condition and functional behaviour of the implant after surgery is considered highly relevant for future medical applications. To achieve this, the use of inertial measurement units (IMUs) was investigated as a means of estimating the patient's actual range of motion.
As no experimental data from the final implant platform or clinical trials was available at this stage, preliminary investigations were conducted using a representative experimental setup. The purpose of these investigations was to identify potential limitations and challenges associated with IMU-based angular estimation for defined rotational axes. The following sections present the methodology, findings, and key observations obtained during these initial experiments.

Funded by:

Schweizerische Eidgenossenschaft
Confédération suisse
Confederazione Svizzera
Confederaziun svizra

Funded by the European Union

The SmILE project has received funding from the European Union's Horizon Europe programme and the Swiss State Secretariat for Education, Research and Innovation (SERI).

7.4.2 Experimental Setup

The experimental setup was based on a UR5e robot by Universal Robots. This device provides 6 degrees of freedom corresponding to its rotational axes. The IMUs were mounted on the upper and middle limbs of the robot, enabling unrestricted motion in all three spatial dimensions and allowing the relative orientation between the sensors to be fully evaluated.

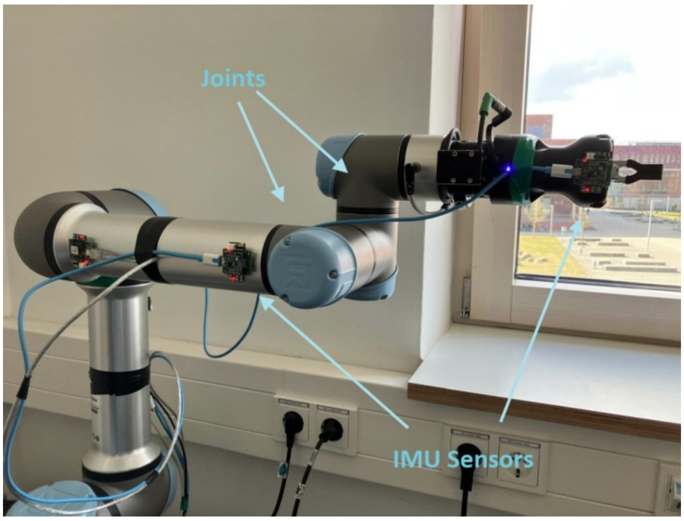

Figure 34. Experimental Setup UROS

To emulate the intended hardware platform of the SmILE implants as closely as possible, a Bosch Application Board 3.1 equipped with a Bosch BHI360 shuttle board was used. The BHI360 offers specifications comparable to the BHI380, while the application board is based on the Nordic nRF52840 microcontroller. Consequently, the collected sensor data is considered representative of the final implant platform.

To minimise synchronisation errors and packet losses, communication between the host and sensor nodes was implemented via the UART interface of the sensor platforms. The orientation vector (9-DoF) was generated using the BHI360 sensor in combination with a BMM150 magnetometer. Orientation data was represented as quaternions and sampled at an output data rate (ODR) of 100 Hz. Each sensor board transmitted its recorded samples to a dedicated host platform.

The ground truth reference signal was obtained directly from the robot controller. This reference data included the rotational joint angles, timestamps, and additional metadata describing the robot's operating mode. In these initial experiments only a rotation in one-dimension was performed and evaluated.

Funded by:

Schweizerische Eidgenossenschaft
Confédération suisse
Confederazione Svizzera
Confederaziun svizra

Funded by the European Union

The SmILE project has received funding from the European Union's Horizon Europe programme and the Swiss State Secretariat for Education, Research and Innovation (SERI).

7.4.3 Limitations and Restrictions

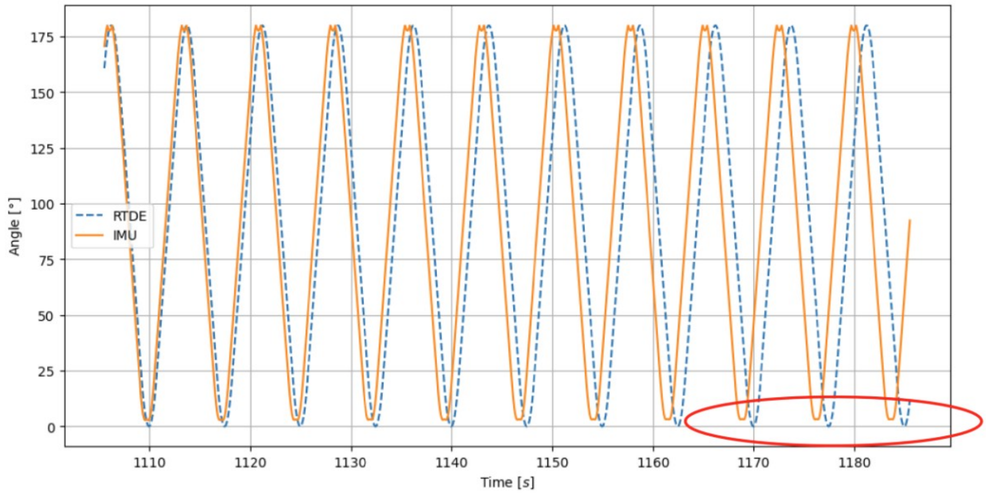

Figure 35. Computed Angles using IMUs vs Ground Truth Data Captured by UR5 Robot (RTDE)

To get an initial overview of the limitations and possible issues, preliminary investigations were conducted.
The figure above illustrates the primary issues encountered when working with IMU-derived angular measurements. The dashed blue curve represents the ground truth signal acquired from the robot system, whereas the orange curve corresponds to the angular estimation obtained from the IMUs. Only one joint of the robot was rotated in this initial trials.
As highlighted by the red ellipse, a noticeable sensor drift can be observed over time. In addition, the signals from the robot and the IMUs are not perfectly synchronised, resulting in a progressive temporal offset between the measured and reference signals. These effects significantly influence the assesability of the accuracy of the angular estimation and therefore must be addressed before reliable asses the accuracy of the proposed approaches.

7.4.4 Synchronisation Approach

To obtain comparable and reliable insights into the accuracy of the IMU-derived angular measurements, all involved devices had to be synchronised. Various approaches exist for synchronising devices in both wired and wireless systems. However, due to the constraints of the experimental setup particularly the absence of a dedicated central clock shared among all devices a kinematic synchronisation approach was selected.
The proposed method is based on executing a deterministic motion routine to compensate for temporal offsets between the individual devices and to establish a common time reference. For this purpose, the generated kinematic time series must exhibit favourable autocorrelation properties. Autocorrelation describes the process of shifting a signal over itself and calculating a similarity measure for each shift value. For synchronisation applications, the autocorrelation function should ideally exhibit a narrow and distinct peak together with low sidelobe amplitudes, enabling accurate detection of temporal alignment.
Sequences that fulfil these requirements are known as Barker codes. Such sequences are widely used in radar systems and other high-frequency technologies due to their excellent correlation properties.

Funded by:

Schweizerische Eidgenossenschaft
Confédération suisse
Confederazione Svizzera
Confederaziun svizra

Funded by the European Union

The SmILE project has received funding from the European Union's Horizon Europe programme and the Swiss State Secretariat for Education, Research and Innovation (SERI).

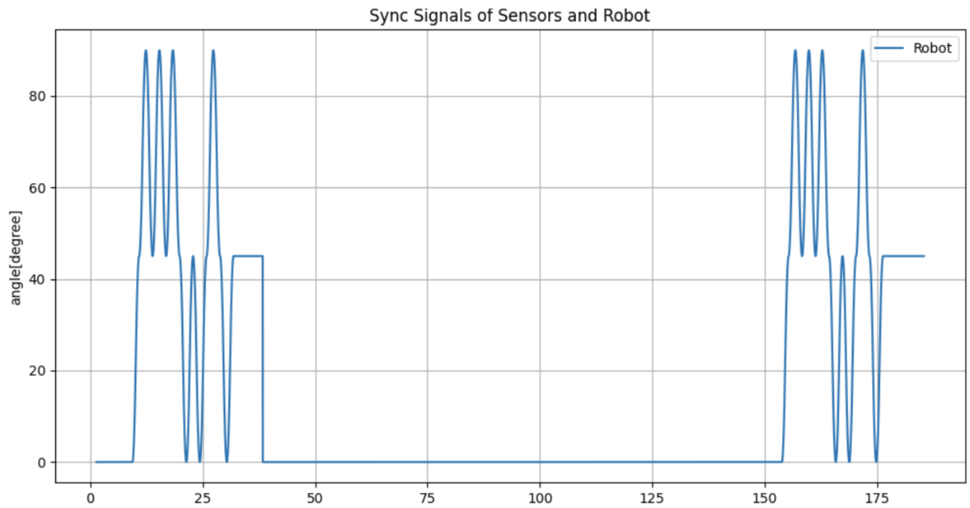

Figure 36. Barker-Code Used for Synchronization Before and After Actual Measurement

The figure above illustrates the Barker-code sequence used in this work, consisting of seven elements. A Barker code contains only the values −1 and +1. In the presented setup, the sequence was encoded into the robot arm's range of motion and executed both at the beginning and at the end of each trial. The value +1 was represented by a joint angle of 90°, whereas the value −1 corresponded to an angle of 0°. This motion-based encoding enabled the synchronisation sequence to be detected reliably within both the robot reference data and the data derived from the IMUs.

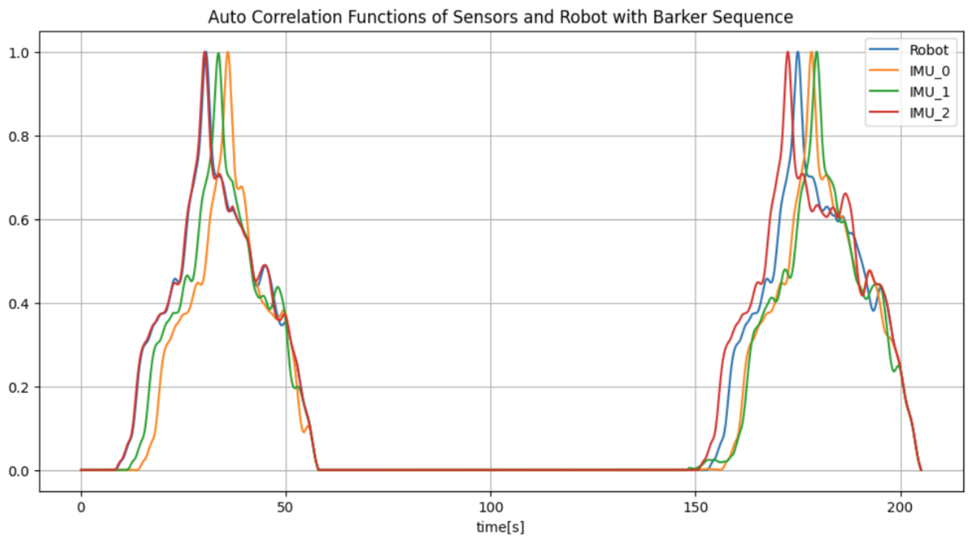

Figure 37. Autocorrelation Functions of Different Sensors and Robot Data obtained from Barker Codes

The autocorrelation sequences illustrated in the figure above demonstrate the effectiveness of the Barker-code-based approach for synchronization purposes. The curves represent the autocorrelation coefficients as a function of time. A pronounced peak is consistently observable across all sensor signals as well as the ground truth reference, indicating reliable temporal alignment characteristics inherent to the applied method.

In addition, systematic temporal offsets between the sensor signals are evident, which arise due to discrepancies in the respective clock systems. These time biases can be directly inferred from the shifts observed in the autocorrelation functions. To compensate for these discrepancies, all signals are resampled using scaling factors derived from the parameters estimated via the autocorrelation analysis. This resampling process effectively aligns the signals onto a unified time base, thereby mitigating the impact of clock-induced timing variations.

Funded by:

Schweizerische Eidgenossenschaft
Confédération suisse
Confederazione Svizzera
Confederaziun svizra

Funded by the European Union

The SmILE project has received funding from the European Union's Horizon Europe programme and the Swiss State Secretariat for Education, Research and Innovation (SERI).

The final outcome of the synchronization procedure is presented in the figure below. This figure illustrates the absolute error between the ground truth and the angles estimated from the IMU measurements.

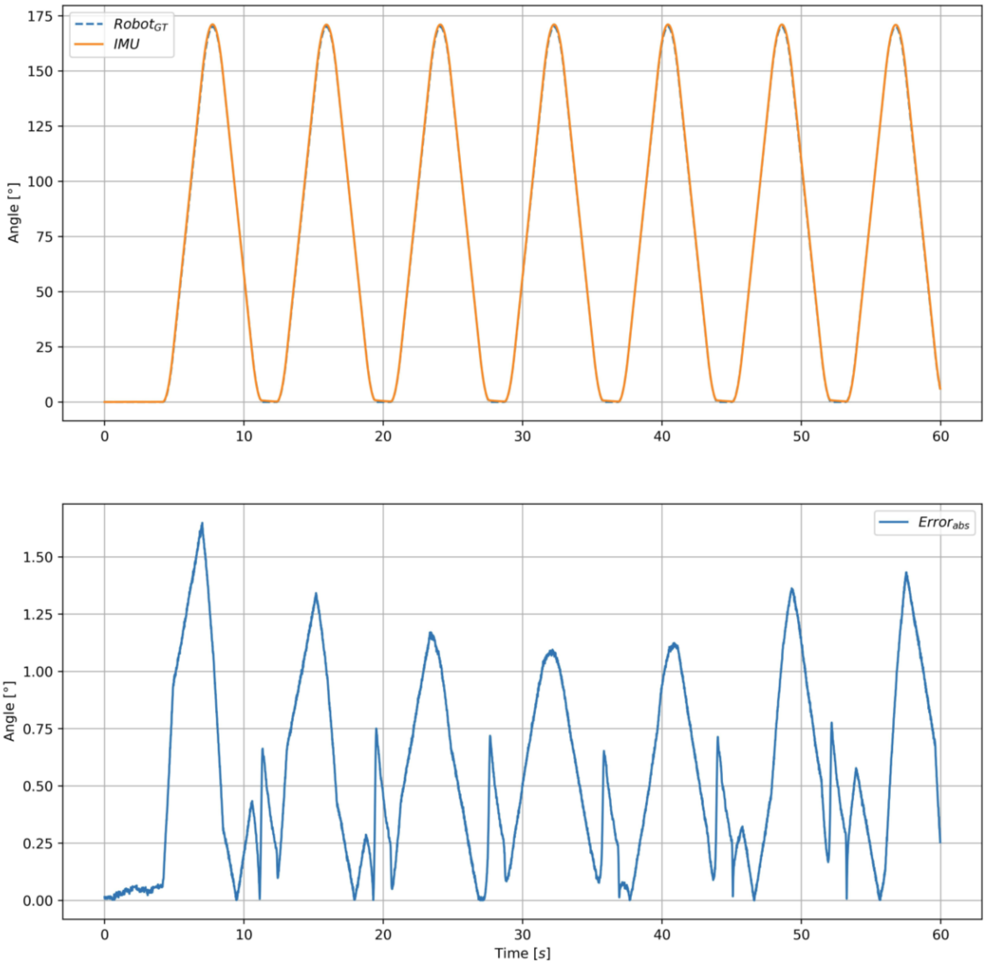

Figure 38. Top: Computed Angles using IMU Data vs Ground Truth from Robot after Resampling and Synchronization Bottom: Remaining Absolut Error between Ground Truth and Estimated Angles

7.4.5 Outlook

The preliminary investigations demonstrated the feasibility of using IMU-based sensing for monitoring implant movement and rehabilitation status within the SmILE project. By employing a UR5e robotic platform and Bosch-based sensor hardware comparable to the intended implant system, important insights into the practical challenges of angular estimation were obtained. The experiments highlighted two major limitations of IMU-based measurements: sensor drift and time synchronisation inaccuracies between devices and the ground truth system.

To address the synchronisation issue, a kinematic synchronisation approach based on Barker-Code sequences was developed and evaluated. The autocorrelation analysis confirmed that the proposed method provides reliable peak detection and enables the estimation of temporal offsets between devices. By applying resampling techniques with parameters derived from the autocorrelation functions, the synchronisation accuracy between IMU signals and robot reference data was significantly improved.

Overall, the conducted experiments provide a solid foundation for further development of energy-efficient active monitoring algorithms for smart implants and validate the potential of IMU-based motion tracking in realistic rehabilitation scenarios, when real-world data of trails is available. In the subsequent project phase, URO will collaborate with UMR and test the sensor performance by sticking

The SmILE project has received funding from the European Union's Horizon Europe programme and the Swiss State Secretariat for Education, Research and Innovation (SERI).

them onto the joint endoprosthesis under the VIVO joint simulator, in order to obtain more realistic joint kinematic data and compare the measured signals with the ground truth data.

7.6 Conclusions and next steps

The implementation of the planned IMU will enable the implant to track steps and wake up with a high battery efficiency. The MCU which is part of the selected IMU allows to efficiently run further algorithms when they are developed and ready to be deployed.
Besides this the implementation of a secondary IMU on the secondary implant part is promising in regards to the achieved performance for one dimensional joints. There is a high confidence that this principle can be used in an actual implant as well as that it can achieve the required angular performance. Due to this it was decided to utilize this sensing principle in the final unified implant electronics developed in SmILE.

Funded by:

Schweizerische Eidgenossenschaft
Confédération suisse
Confederazione Svizzera
Confederaziun svizra

Funded by
the European Union

The SmILE project has received funding from the European Union's Horizon Europe programme and the Swiss State Secretariat for Education, Research and Innovation (SERI).

8 Smart actuators (SMA)

8.1 Introduction

This document reports on the development of an adaptive tibial plate system incorporating SMA-based actuation to achieve controlled modulation of structural stiffness. The common design target is a compact implant-compatible actuator mechanism capable of adjustable interfragmentary stiffness, mechanically integrated within a tibial plate envelope of 10.5 × 16 × 175 mm, and actuated by SMA wire bundles operating within structurally acceptable load ranges.
The stiffness modulation mechanism is based on a three-component system consisting of a movable pin, a polymer element, and a polymer holder. Insertion and retraction of the pin controls the polymer's resistance to deformation and results in at least two distinct states of stiffness. Experimental characterization confirmed that the soft-state mechanical resistance is tunable through polymer selection: silicone (Shore A 40), TPU (Shore A 80) and TPU (Shore A 95) were evaluated, with force–displacement behavior measured on a dedicated test bench. Pin reaction forces were found to be mitigable by ensuring sufficient pin penetration depth relative to polymer depth.
SMA actuator integration required the development of a reliable clamping and connection mechanism providing both force transmission and electrical insulation. Early PEEK-based clamp geometries achieved a maximum clamping force of 12 N, which was insufficient for reliable actuation. Machined aluminum clamps demonstrated the most promising performance, reaching 50 N. Electrical insulation remains a critical open challenge; measures investigated include Kapton tape wrapping and microfabricated insulating sleeves. Additively manufactured connector concepts and a transverse locking pin approach are currently under development as parallel solution paths.
Numerical simulations under axial loading (1500 N) confirmed structural integrity with stress levels below the material yield strength of 400 MPa. Four-point bending simulations and experiments are planned for the subsequent phase to fully characterize implant stiffness behavior.
The self-sensing capability of the SMA components is targeted for actuator state monitoring rather than direct fracture gap measurement. The feasibility of inferring pin position from SMA electrical resistance and power signals via a recurrent neural network was demonstrated in a simplified experimental setup, achieving a displacement prediction RMSE of 0.0247 mm (0.63% of full range) in real-time on an embedded microcontroller. Adaptation of this methodology to the present system is planned as a key next step.
The recommended path forward is to resolve the electrical insulation challenge in the clamping mechanism — prioritizing the aluminum clamp or locking pin connector concept — while advancing four-point bending validation and initiating the integration of the self-sensing pipeline into the full implant system.

8.2 Active Tibial Plate with Integrated SMA Actuator System

A novel active tibial plate concept incorporating an integrated shape memory alloy (SMA) actuator mechanism was developed. The proposed system enables adjustable implant stiffness, thereby allowing controlled interfragmentary motion, which is intended to promote bone healing and growth stimulation. The implant features a height of 10.5 mm, a width of 16 mm, and a length of 175 mm (see Figure 39).

Funded by:

Schweizerische Eidgenossenschaft
Confédération suisse
Confederazione Svizzera
Confederaziun svizra

Funded by the European Union

The SmILE project has received funding from the European Union's Horizon Europe programme and the Swiss State Secretariat for Education, Research and Innovation (SERI).

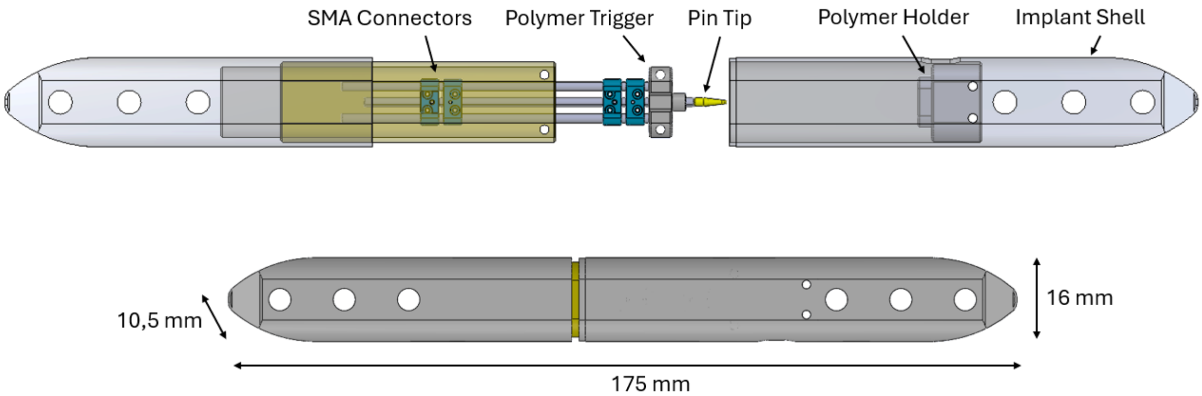

Figure 39: CAD model and dimensional overview of the SMA-actuated implant prototype, showing the SMA connectors, polymer trigger, pin tip, polymer holder, and implant shell.

The design incorporates two antagonistic SMA bundles attached to the SMA connectors. The connectors transmit the actuation forces of the SMA elements to the guiding rods, and ultimately to the pin tip, allowing precise inward and outward displacement of the pin tip. The corresponding stiffness modulation mechanism and its effects on implant behavior are described in the subsequent section.
Numerical simulations were conducted under axial loading conditions to evaluate the mechanical response and structural integrity of the implant (see Figure 40). The current design was selected to ensure that the material yield strength of 400 MPa is not exceeded while maintaining an appropriate safety factor. An axial load of 1500 N was applied to assess stress distribution throughout the implant system. Further investigations, including four-point bending simulations and experiments, are planned for the subsequent phase to characterize the bending performance and stiffness behavior of the design.

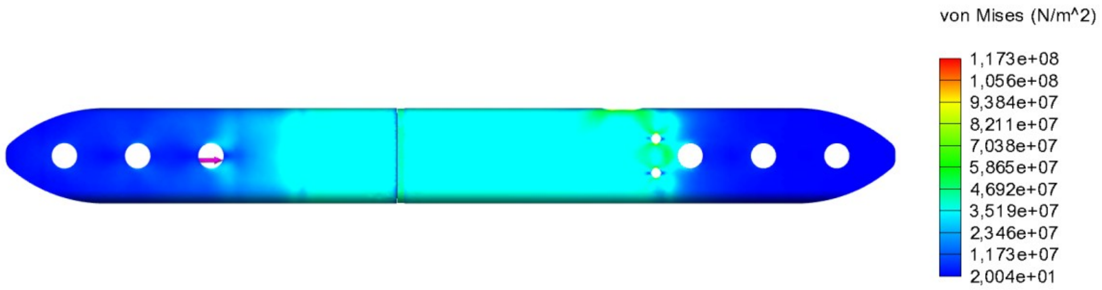

Figure 40: Finite element analysis (FEA) results of the implant structure showing the von Mises stress distribution under mechanical loading conditions.

8.3 Stiffness Modulation Mechanism

Stiffness modulation is achieved through a three-component mechanical mechanism consisting of a movable pin, a polymer element, and a polymer holder (see Figure 41). When the pin is inserted into the polymer element, the holder suppresses deformation due to the material's incompressibility, resulting in a stiff implant configuration. Retracting the pin creates a cavity within the polymer element, enabling its deformation and thereby reducing overall implant stiffness.

Funded by:

Schweizerische Eidgenossenschaft
Confédération suisse
Confederazione Svizzera
Confederaziun svizra

Funded by the European Union

The SmILE project has received funding from the European Union's Horizon Europe programme and the Swiss State Secretariat for Education, Research and Innovation (SERI).

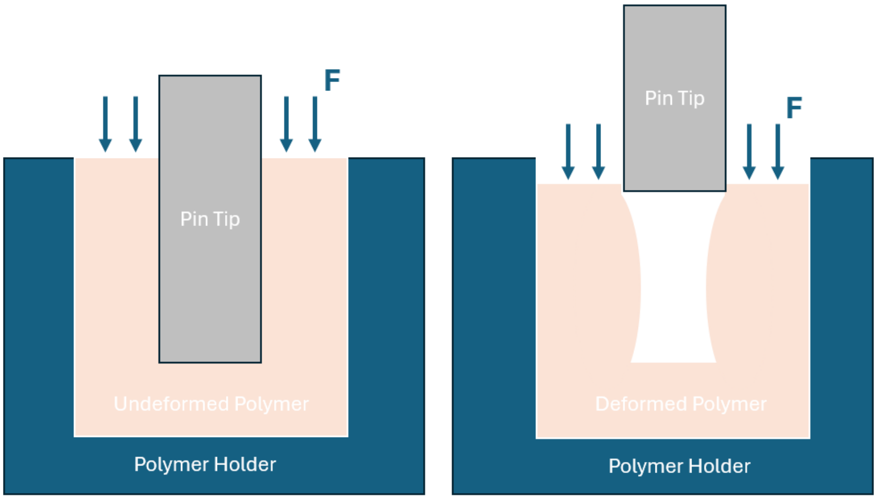

Figure 41: Schematic illustration of the experimental setup used to investigate the mechanical behavior of the polymer implant. The left side shows the undeformed polymer state, while the right side depicts the deformed polymer under axial loading.

To characterize this softening behaviour, a dedicated test bench was designed and constructed to investigate the mechanism independently from the full implant system. The test stand consists of a motor (1) driving the polymer trigger, two load cells (2, 4) measuring the compression force acting on the polymer and the reaction force exerted on the pin (5), an adapter (3), and the polymer holder with the polymer element (6) (see Figure 47). Experimental series were conducted using different polymer materials and varying pin taper geometries to evaluate their influence on the mechanical response.

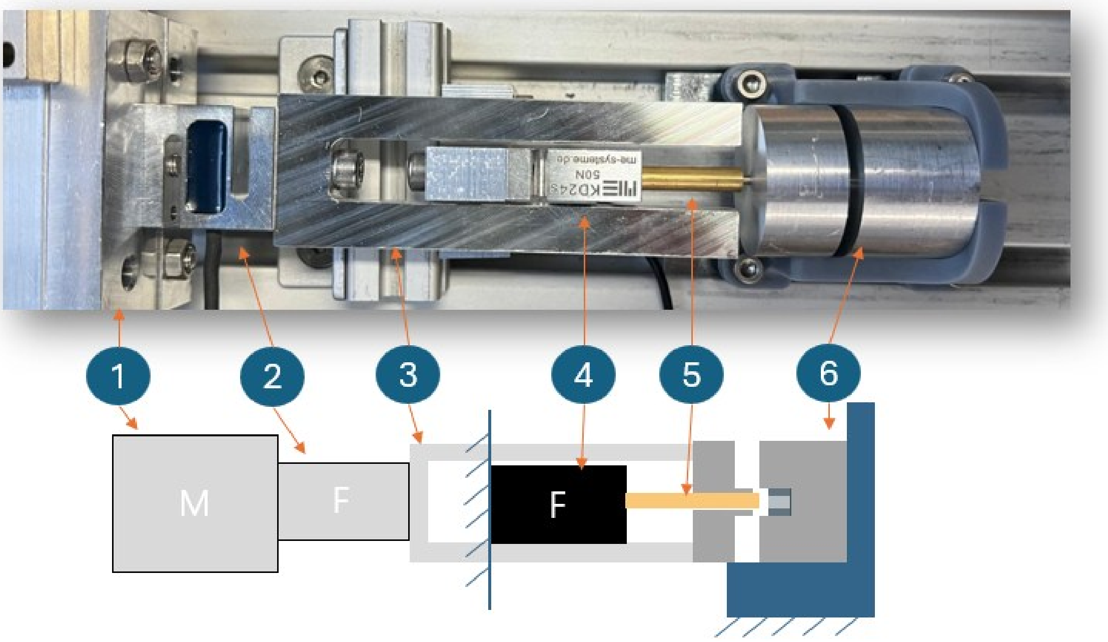

Figure 42: Experimental test bench for characterizing the force-displacement response of the implant system. The numbered components include (1) the motor, (2) the load cell, (3) the adapter, (4) the polymer holder, (5) the pin, and (6) the investigated polymer.

The force–displacement characteristics were evaluated for three polymer materials: silicone with a Shore A hardness of 40, TPU with a Shore A hardness of 80, and TPU with a Shore A hardness of 95 (see Figure 48). The results demonstrate that the mechanical resistance of the implant in its compliant state can be adjusted through appropriate polymer selection. Additionally, the reaction force exerted

Funded by:

Schweizerische Eidgenossenschaft
Confédération suisse
Confederazione Svizzera
Confederaziun svizra

Funded by
the European Union

The SmILE project has received funding from the European Union's Horizon Europe programme and the Swiss State Secretariat for Education, Research and Innovation (SERI).

on the pin was found to be mitigable by ensuring that the pin penetration depth exceeds the depth of the polymer element.

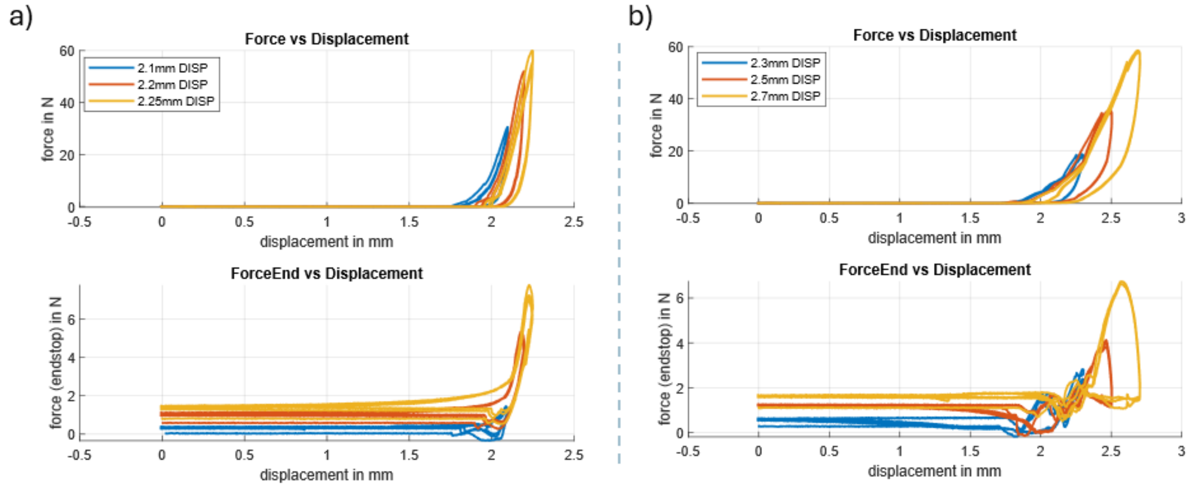

Figure 43: Force-displacement behavior of two polymer materials under different deformation conditions: (a) silicone with a Shore A hardness of 40 and (b) TPU with a Shore A hardness of 95. The upper plots show the compression force required to deform the polymer element, while the lower plots present the resulting reaction force exerted by the polymer on the pin.

8.4 SMA Actuator Integration and Force Transmission

SMA actuators were integrated to drive the movable pin and thereby trigger the stiffness transition. Simulations of the clamping and connection mechanism were performed and subsequently validated experimentally. Several design iterations were developed (Figure 44) with the objective of increasing the clamping force acting on the pin rods — a prerequisite for reliable force transmission from the SMA wire to the mechanism. Beyond sufficient clamping force, all components were required to provide electrical insulation to prevent short-circuiting through the pin–rod assembly.

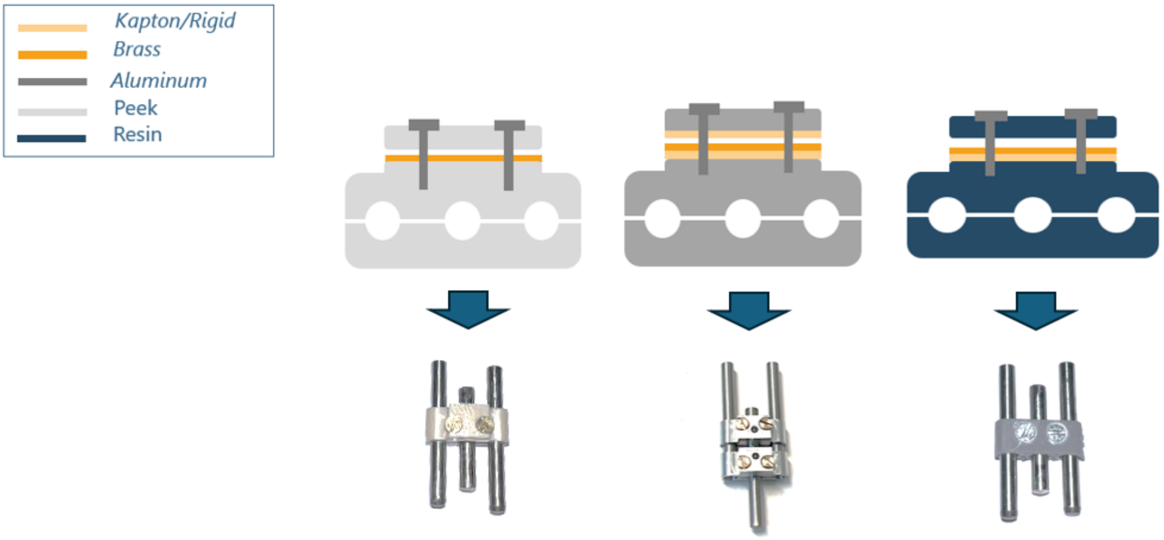

Figure 44: Evolution of the implant clamping concept from initial PEEK-based designs to the optimized aluminium clamp.

Validation experiments revealed that the clamping force achieved in early iterations was insufficient for reliable actuation. Subsequent investigations included material substitutions from PEEK to resin-based components and, ultimately, machined aluminum clamps. To quantify the improvement,

Funded by:

Schweizerische Eidgenossenschaft
Confédération suisse
Confederazione Svizzera
Confederaziun svizra

Funded by the European Union

The SmILE project has received funding from the European Union's Horizon Europe programme and the Swiss State Secretariat for Education, Research and Innovation (SERI).

clamping forces were measured on a standardized test bench. The maximum clamping force achieved with the PEEK geometry was 12 N, while the optimized aluminum variant reached 50 N (see Figure 50).

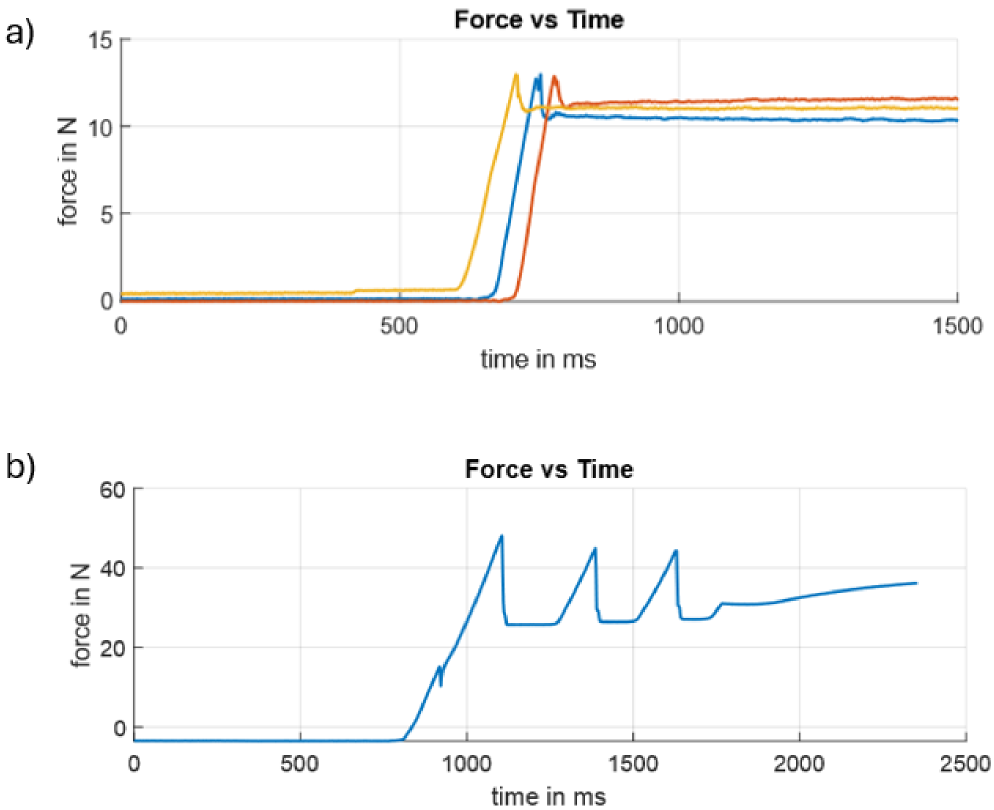

Figure 45: Validation results of the clamping force measurements. (a) Initial PEEK-based clamp configuration reaching a maximum clamping force of approx. 12 N. (b) Optimized aluminum clamp design achieving forces up to 50 N.

However, electrical insulation remained a critical challenge throughout. Insulation measures included Kapton tape wrapping and microfabricated insulating sleeves (see Figure 46); any direct contact between the SMA wires and metallic connectors — whether through the connector body or the clamping screws — leads to a short circuit.

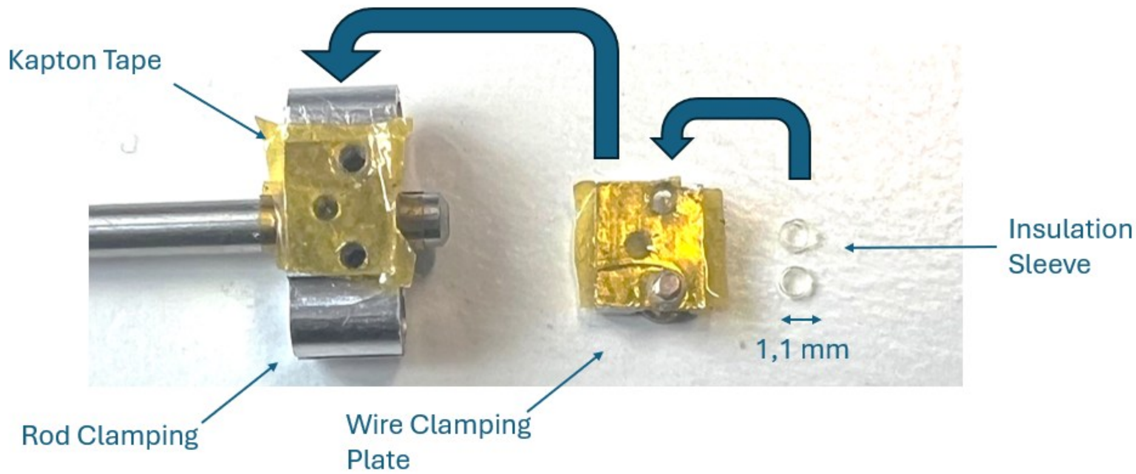

Figure 46: Electrical insulation concept for the SMA-clamp. Insulation measures included Kapton tape wrapping and a microfabricated insulation sleeve to prevent electrical short circuits between SMA wires, aluminum connectors, and clamping components.

Funded by:

Schweizerische Eidgenossenschaft
Confédération suisse
Confederazione Svizzera
Confederaziun svizra

Funded by the European Union

The SmILE project has received funding from the European Union's Horizon Europe programme and the Swiss State Secretariat for Education, Research and Innovation (SERI).

In parallel, additively manufactured SMA connector concepts were pursued to address the combined requirements of clamping performance and electrical insulation. A further novel connection approach is currently under investigation, in which transverse locking pins are used to prevent slipping rather than relying on direct clamping onto the actuator rods.

8.5 Self-Sensing for Actuator State Monitoring

Beyond their actuating function, the SMA components are leveraged for self-sensing — exploiting the well-characterized relationship between electrical resistance and the thermomechanical state of the alloy. It should be noted that the current system targets stiffness modulation rather than axis correction; accordingly, self-sensing is employed here not to measure fracture gap geometry directly, but to monitor the operational state of the stiffness actuator itself — specifically, to infer the position of the movable pin and thereby verify whether the intended stiffness transition has been successfully executed.

The highly nonlinear and hysteretic relationship between SMA resistance and actuator displacement, arising from the complex coupling of phase transformation, temperature, and mechanical load, makes direct model-based inference unreliable, as illustrated by the resistance–displacement and power–displacement characteristics shown below.

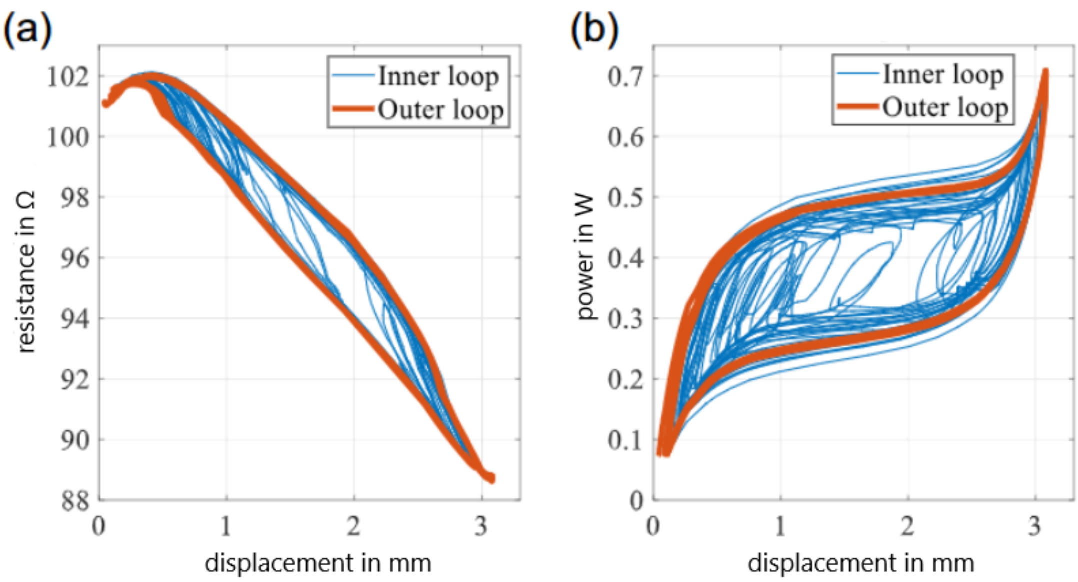

Figure 47: Correlation between: (a) resistance and displacement and (b) power and displacement for inner and outer SMA loops during actuator motion.

The feasibility of a neural network-based self-sensing approach was demonstrated in a simplified experimental setup. By combining electrical resistance and electrical power as inputs, a recurrent neural network was shown to accurately predict SMA actuator displacement in real time on a microcontroller-based embedded system (see Figure 47), achieving a root mean square error of 0.0247 mm — corresponding to 0.63% of the maximum displacement range. Generalizability was confirmed across multiple SMA wire actuators of varying geometry and material properties. Adapting this methodology to the present stiffness actuator system represents a key next step, enabling continuous inference of pin position from the SMA wire signals alone and providing real-time confirmation of the stiffness state without the need for an additional displacement sensor.

Funded by:

Schweizerische Eidgenossenschaft
Confédération suisse
Confederazione Svizzera
Confederaziun svizra

Funded by the European Union

The SmILE project has received funding from the European Union's Horizon Europe programme and the Swiss State Secretariat for Education, Research and Innovation (SERI).

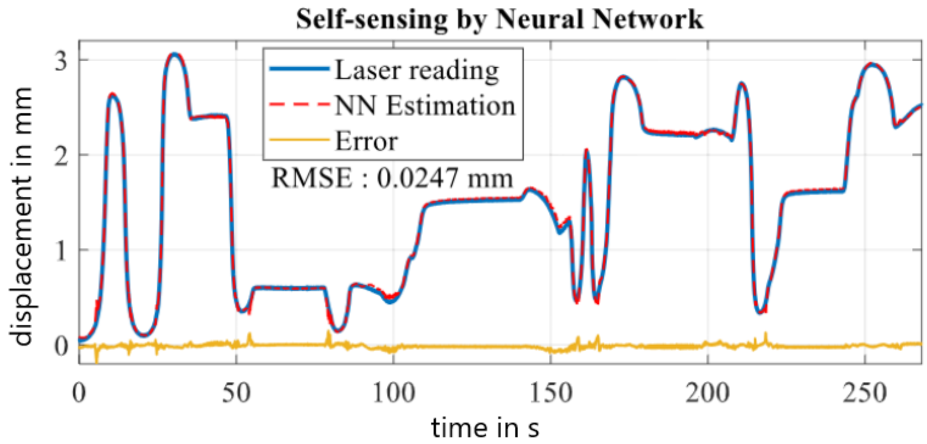

Figure 48: Neural network-based self-sensing performance for displacement estimation of the SMA actuator.

8.6 Conclusion and Next Steps

An active tibial plate concept incorporating an SMA-based stiffness modulation mechanism was developed and further refined during the reporting period. The implant design was reduced to a compact geometry suitable for implantation while maintaining the required functionality of the actuator and stiffness modulation system. Numerical simulations under axial loading conditions were performed to evaluate the structural integrity of the design and to verify that the expected stress levels remain below the material limits.

Experimental investigations of the stiffness modulation mechanism demonstrated that the force–displacement characteristics of the compliant implant state can be adjusted through appropriate polymer selection. In parallel, several SMA connector and clamping concepts were evaluated, resulting in a substantial increase in force transmission capability compared to the initial designs. The conducted investigations also highlighted the importance of reliable electrical insulation for actuator integration into the implant system.

Furthermore, the applicability of a neural-network-based self-sensing approach for monitoring the actuator state was assessed. The transfer of this methodology to the SMA stiffness modulation system is considered a relevant next step. Experimental validation of the complete implant design under four-point bending conditions will be performed in the next project phase once the manufactured implant components become available.

The following activities are identified for the subsequent development phase:

Four-point bending characterization — Bending simulations and experiments are to be carried out on the current implant design to assess stiffness behavior and validate the numerical model against experimental data. This requires procurement of manufactured implant components from the fabrication partner.

Polymer characterization and selection — Further polymer studies are to be conducted in coordination with the clinical and biomechanical team to define the target force–displacement characteristic for the soft implant state. Material candidates are to be evaluated against this specification to identify the polymer best suited for integration into the final design.

Clamping and connector development — Experimental validation of additively manufactured clamp concepts is to be conducted, with particular focus on print resolution and dimensional accuracy at the 2 mm rod interface. In parallel, the aluminum clamp design is to be further refined to resolve the remaining electrical insulation challenge, evaluating Kapton-based and sleeve-based insulation strategies under representative clamping loads.

Self-sensing integration — The neural network-based self-sensing approach, validated in a simplified SMA wire setup, is to be adapted to the stiffness actuator system. This includes acquiring resistance and power characterization data under representative actuation conditions and retraining the model accordingly.

Funded by:

Schweizerische Eidgenossenschaft
Confédération suisse
Confederazione Svizzera
Confederaziun svizra

Funded by the European Union

The SmILE project has received funding from the European Union's Horizon Europe programme and the Swiss State Secretariat for Education, Research and Innovation (SERI).

9 References

[1] K. M. Varadarajan, A. L. Moynihan, D. D'Lima, C. W. Colwell, and G. Li, "In vivo contact kinematics and contact forces of the knee after total knee arthroplasty during dynamic weight-bearing activities," J. Biomech., vol. 41, no. 10, pp. 2159–2168, Jul. 2008, doi: 10.1016/j.jbiomech.2008.04.021.

[2] T. M. McGloughlin and A. G. Kavanagh, "Wear of ultra-high molecular weight polyethylene (UHMWPE) in total knee prostheses: A review of key influences," Proc. Inst. Mech. Eng. H, vol. 214, no. 4, pp. 349–359, 2000, doi: 10.1243/0954411001535390.

[3] R. Wadhwa, C. F. Lagenaur, and X. T. Cui, "Electrochemically controlled release of dexamethasone from conducting polymer polypyrrole coated electrode," J. Control. Release, vol. 110, no. 3, pp. 531–541, Feb. 2006, doi: 10.1016/j.jconrel.2005.10.027.

[4] M. E. Alkahtani, M. Elbadawi, and A. W. Basit, "Electroactive Polymers for On-Demand Drug Release," Adv. Healthcare Mater., vol. 13, no. 5, Art. no. e2301759, Feb. 2024, doi: 10.1002/adhm.202301759.

[5] C. Boehler et al., "Actively controlled dexamethasone release from implanted microelectrodes," Biomaterials, vol. 129, pp. 176–187, May 2017, doi: 10.1016/j.biomaterials.2017.03.004.

[6] I. Arasaratnam and S. Haykin, "Cubature Kalman filters," IEEE Trans. Autom. Control, vol. 54, no. 6, pp. 1254–1269, Jun. 2009, doi: 10.1109/TAC.2009.2019803.

Funded by:

Schweizerische Eidgenossenschaft
Confédération suisse
Confederazione Svizzera
Confederaziun svizra

Funded by
the European Union

The SmILE project has received funding from the European Union's Horizon Europe programme and the Swiss State Secretariat for Education, Research and Innovation (SERI).